DEVELOPMENT AND CHARACTERIZATION OF METHYLENE BLUE OLEATE SALT-LOADED POLYMERIC NANOPARTICLES AS A TREATMENT FOR GLIOBLASTOMA

DISSERTATION

Presented to the Graduate Council of the

Graduate School of Biomedical Sciences

University of North Texas

Health Science Center at Fort Worth

in Partial Fulfillment of the Requirements

For the Degree of

DOCTOR OF PHILOSOPHY

By

Jessica M. Castañeda-Gill, B.S., M.S.

Fort Worth, Texas

November 2016

ACKNOWLEDGMENTS

The last several years have been a very interesting learning experience as a result of my graduate training at the University of North Texas Health Science Center. I would like to begin by thanking my mentor, Dr. Jamboor K. Vishwanatha, for giving me the opportunity to work and learn in his lab. I would also like to thank my advisory committee members Dr. Amalendu P. Ranjan, Dr. ShaoHua Yang, Dr. Andras Lacko, and Dr. Michael L. Smith for their guidance and support during my research journey.

I am greatly appreciative of the research funding I received from NIH grants R21CA194295 (National Cancer Institute) and T32AG020494 (National Institute on Aging), as well as to the Graduate School for the financial support of my training. I want to thank the Graduate School, the Department of Molecular and Medical Genetics, the Department of Molecular Biology and Immunology, and their administrative staff members whom have helped me along the way. I am also thankful to Dr. Yang, Dr. Gryczynski, and their staff and students at UNTHSC for allowing me to use their lab facilities, as well as Dr. Noelle Williams and her staff at UT Southwestern Medical Center's Preclinical Pharmacology Core Lab for their assistance in completing my proposed animal studies.

I also want to thank my lab mates for helping make the long hours and weekends, and constant frustrations manageable. I would like to acknowledge both past and current members of the lab that I have worked with during my time at UNTHSC including Dr. Amalendu Ranjan, Dr. Anindita Mukerjee, Dr. Pankaj Chaudhray, Dr. Smrithi Rajendiran, Dr. Marilyne Kpetemey, Dr.

Sayantan Maji, Andrew Gdowski, Lee Gibbs, and Timothy Van Treuren. You have no idea how grateful I am to have talked, joked, and worked with you during the last several years.

Last, but not least, I would like to thank my family, both near and far, for their constant love and support during my graduate career, as I know it has not been easy. To my parents, thank you for your love, support, inspiration, and encouragement throughout my entire life, demonstrating that I can do anything if I try hard enough. Thank you will never be enough. To my husband, who has dealt with me during every high and low of graduate school, thank you more than words can say. And lastly, to my baby boy, thank you for being you and showing me that anything is possible. I hope that you accomplish anything you dream of in the future, and know that you are loved.

TABLE OF CONTENTS

Page

LIST OF TABLES

CHAPTER II

LIST OF ILLUSTRATIONS

CHAPTER I

CHAPTER II

ABBREVIATIONS

ABC	ATP-binding cassette
AchE	Acetylcholine esterases
AD	Alzheimer's Disease
Apo	Apolipoprotein
ATP	Adenosine triphosphate
BBB	Blood-brain barrier
BCEC	Brain capillary endothelial cell
BCNU	bis-chloroethylnitrosourea
CCNU	N-(2-chloroethyl)-N'-cyclohexyl-N-nitrosourea
cGMP	cyclic guanosine monophosphate
CNS	Central nervous system
CRT	Conformal radiation
CT	Computed tomography
DNA	Deoxyribonucleic acid
EBRT	External beam radiation therapy
EGF/EGFR	Epidermal growth factor/receptor
ETC	Electron transport chain
GBM	Glioblastoma

HIF-1	Hypoxia-inducible factor 1
HNP	Hybrid nanoparticle
hTERT	human telomerase reverse transcriptase
IMRT	Intensity modulated radiotherapy
LDL	Low density lipoprotein
LMB	Leucomethylene blue
MAO A	Monoamine-oxidase A
MB	Methylene blue
MBOS	Methylene blue oleate salt
MBOSNP	Methylene blue oleate salt-loaded polymeric nanoparticle
MDR	Multi-drug resistant
Mdm2	Mouse/murine double minute 2
MRI	Magnetic resonance imaging
mtDNA	mitochondrial DNA
NADH	Nicotinamide adenine dinucleotide hydrogen
NADPH	Nicotinamide adenine dinucleotide phosphate
NF1	Neurofibromatosis-1
NOS	Nitric oxide synthase
NP	Nanoparticle
OXPHOS	Oxidative phosphorylation
PCA	Polycyanoacrylate
PCL	Polycaprolactone
PDGF/PDGFR	Platelet-derived growth factor/receptor

PDI	Polydispersity index
PDT	Photodynamic therapy
PEG	Polyethylene glycol
PET	Positron emission tomography
PF68	Pluronic F68
PGA	Polyglycolic acid
P-gp	P-glycoprotein
PI3K	Phosphoinositide 3-kinase
PK	Pharmacokinetic
PKM2	Pyruvate kinase M2 isoform
PLA	Polylactic acid
PLGA	Poly(lactic-co-glycolic acid)
PTEN	Phosphatase and tensin homolog
PVA	Polyvinyl alcohol
QD	Quantum dot
Rb	Retinoblastoma
RBC	Red blood cell
RES	Reticuloendothelial system
RNA	Ribonucleic acid
ROS	Reactive oxygen species
RSR	Relative survival rate
SLN	Solid lipid nanoparticle
TMZ	Temozolomide

VEGF/VEGFR	Vascular endothelial growth factor/receptor

CHAPTER I

INTRODUCTION

Glioblastoma

Statistics, Risk Factors and Diversities, Signs and Symptoms

Glioblastoma (GBM), formerly known as glioblastoma multiforme, is a type of primary human brain tumor within the category of glioma and subcategory astrocytoma due to its derivation from supportive glial cells called astrocytes; it accounts for over half of all glioma cases and approximately 15% of all primary human brain tumors, presenting the lowest five-year relative survival rate (RSR) of all central nervous system (CNS) cancers and ranking in the top 5 lowest RSRs for all cancer types, particularly with advancing age [1-4]. GBM, a rapidly developing grade IV brain cancer that originates from astrocytes located primarily within the supratentorial region of the cerebrum, is considered the most common and aggressive primary human brain tumor due to poor prognosis (15 months maximum post-diagnosis with treatment) and substandard five-year RSR (less than 5%) [3-8]. With that said, GBM primarily remains localized to the brain, with occassional occurrence in the brain stem, cerebellum, or spinal cord; however, extracranial metastasis is known to be very rare [6, 9-13]. While GBM can affect individuals of all ages, it occurs more frequently in adults, primarily middle-aged people between 45 and 65, with a gender disparity favoring men, as well as a slight racial discrepancy towards Caucasians [3, 7, 10, 14, 15].

While GBM has molecular subtypes, which will be discussed in detail in a later section, it is more commonly categorized as either primary or secondary GBM, according to its development and progression [7, 10, 11, 14, 16-19]. Primary GBM, which accounts for over 80-90% of all GBM cases, develops *de novo*, producing the most aggressive tumors due to their sudden growth [7, 14, 16-20]. This class of GBM tumors is 3 times more common in men than women and occurs more frequently in individuals over the age of 45, with an average age of occurrence of 64 and a peak incidence between 75 and 84 [6, 7, 11, 14-16, 21-27].

In contrast, secondary GBM arise from grade II and III astrocytomas that are genetically converted to the higher-grade IV GBM [7, 11, 14, 16, 20]. The term "secondary" when discussing GBM is different from the traditional use of the phrase, which refers to the metastasis of a tumor from its primary site of development. Throughout the remainder of this paper, reference to "secondary" tumors will denote secondary GBM, and not metastatic tumors. Thus, secondary GBM occurs at a higher rate in patients under the age of 45, the average age of secondary GBM diagnosis, have a gender disparity towards women, and tend to be more easily treated due to their differing pathogenic pathway [7, 11, 14-16, 20, 23-26, 28-33]. While the two subtypes appear identical histologically, they bear significant molecular differences, providing for potentially distinct therapy regimens [20]. The molecular aspects of and therapy options for GBM will be discussed in a subsequent section.

While no direct cause has been linked to GBM development, particularly in relation to inheritability, numerous environmental and genetic factors have been stated to increase risk including contact with ionizing radiation, which can result from treatment of a previous brain tumor particularly during childhood and adolescence; frequent, occupational contact with carcinogenic compounds and their by-products; recurrent exposure to tobacco smoke; and

several genetic conditions as previously stated [6, 7, 11, 14, 16, 27, 34-47]. Inversely, studies have shown that individuals with a past reaction to environmental allergens and/or occurrence of chicken pox have a reduced risk of GBM, following combination analysis of self-reports and genetic biomarkers [16, 27, 35, 48-59].

With that said, the development of a combination of symptoms is common during the progression of GBM as a result of intracranial pressure [2, 7, 35]. The most widespread sign is headaches, which occur in over half of patients ultimately diagnosed with GBM, and are distinguished from a traditional headache and/or migraine due to their gradual intensification in strength and occurrence, as well as localization corresponding to the tumor site [2, 7, 11, 14, 35]. Other symptoms generally associated with GBM include nausea and vomiting; seizures; cognitive loss; and behavioral changes, with tumor location-specific symptoms being unilateral weakness or loss of movement, language impairment, and tactile and visual deficits [2, 7, 11, 14, 35, 60, 61].

Pathology and Molecular Biology of Glioblastoma

Glioblastoma (GBM) and its glial cell lineage were originally characterized by German doctor, social scientist, and the father of modern pathology, Rudolf Virchow in 1863, with additional clinical development on the disease by Globus and Strauss in 1925 and Bailey and Cushing in 1926 [10, 62-65]. Originally referred to as spongioblastoma multiforme, it was Drs. Bailey and Cushing whom coined the name glioblastoma multiforme due to its cytological and histological heterogeneity [10, 64-67].

GBM is characterized by its mix of neoplastic and stromal tissues; nuclear variability in size, shape, and amount; increased mitotic activity; heightened level of necrosis and subsequent reduction in apoptosis; glomeruloid angiogenesis; and compromised tight junctions between

brain capillary endothelial cells of the blood-brain barrier (BBB) [10, 11, 14, 65, 67-74]. As stated, GBM is known to induce BBB breakdown and alterations, such as edema and increased intracranial pressure, through partly understood mechanisms [75-77]. These processes include downregulation of tight junction proteins, such as claudins; occludin; and agrin, and potentially involve the release and upregulation of soluble factors, such as proteases (matrix metalloproteinases, plasminogen activators, and cathepsin B); vascular endothelial growth factor (VEGF); and scatter factor/hepatocyte growth factor, to induce endothelial cell permeability at tight junctions [76, 78-87].

Due to GBM and its effect on the BBB, the normal immunological environment in the CNS is also drastically changed. While immune cells are present during the development and progression of GBM, their abilities are dampened due to the production and secretion of tumor-associated antigens and cytokines [11, 14, 88, 89]. In addition to the aforementioned alterations, other prominent GBM-induced immune changes include diminished antibody production by B cells, reduced T cell activities, and generation of immunosuppressive factors by neighboring immune cells [11, 14, 90-97].

A potential cause of the cellular robustness and evasiveness of GBM may be due to metabolic alternations and mitochondrial dysfunctions [98-102]. As previously stated, GBM utilizes aerobic glycolysis for adenosine triphosphate (ATP) production at a higher rather than oxidative phosphorylation (OXPHOS), demonstrating an apparent problem in proper mitochondrial function in a process referred to as the Warburg effect. In addition to this energetically unfavorable choice, both apoptotic pathways, but more so the intrinsic, exhibit dysfunction, further aiding the development and progression of GBM [99, 102-106]. However, while the selection of aerobic glycolysis over OXPHOS seems detrimental to GBM, studies have

shown that this bioenergetic switch occurs in order to increase tumor biomass via the redistribution of carbon skeletons for synthesis of nucleotides, amino acids, and fatty acids [100, 102, 103, 107].

With that said, these mitochondrial and metabolic changes are thought to result from the accumulation of mutations within both genomic and mitochondrial deoxyribonucleic acid (mtDNA), which feed a vicious cycle of additional mutations initiating further mitochondrial dysfunction and metabolic reprogramming [99, 100, 102, 103, 108-112]. Some of the areas affected include components of the glycolytic and OXPHOS pathways, oncogenes and tumor suppressors, and apoptosis [99, 100, 102, 103, 110, 111]. As previously mentioned, cancer cells, including GBM, depend on aerobic glycolysis for energy production, shunting the resultant pyruvate into lactate. The subsequent lactate is then exported from the cell to maintain its pH, which leads to an acidic microenvironment that aids GBM progression [99, 100, 103, 113-115]. The key enzyme involved in pyruvate production during glycolysis is pyruvate kinase, which exists as four isoforms with only one, PKM2, exhibiting high expression in cancer cells [100, 102, 116-119]. PKM2 occurs in an inactive dimeric form that prevents pyruvate sythesis, but in turn allows for the biosynthetic precursors needed for tumor biomass growth, and as an active tetramer that performs the characteristic pyruvate synthesis [100]. In GBM, PKM2 messenger ribonucleic acid (RNA) and protein expression levels are upregulated compared to lower-grade gliomas, demonstrating the molecule's role in the aggressive nature of the highest grade glioma [120]. Additionally, OXPHOS complexes have been shown to be negatively regulated in GBM, further reinforcing the utilization of aerobic glycolysis [103, 110, 111]. In several studies, issues within the OXPHOS pathway were described and determined to be due to either

deoxyribonucleic acid (DNA) mutations or protein down-regulation of Complexes I-IV [110, 111, 121, 122].

While complexes within the OXPHOS pathway are known to be directly modified in GBM, external factors, such as oncogenes and tumor suppressors, can be affected due to these resultant changes in metabolism, as well as alter these pathways via feedback loops [123]. During the disease progression, GBM is exposed to varying levels of oxygen, from low to normal, based on a cell's location within the tumor or on its periphery. In the hypoxic core of the tumor, cells are subjected to low oxygen concentrations, initiating upregulation of epidermal growth factor receptor (EGFR) and hypoxia-inducible factor 1 (HIF-1), which promote GBM proliferation and the ensuing aggressiveness [100, 102, 103, 124, 125]. Of the numerous genetic mutations thought to be involved in GBM, overexpression of EGFR is one of the most common due to its identification in approximately 50% of all primary GBM cases, and as a result, is thought to contribute to chemoresistance [11, 14, 25, 126-129]. Other oncogenes implicated in GBM progression and invasion include phosphoinositide 3-kinase (PI3K), which activates EGFR and protein kinase b (Akt); and MYC, which activates genes involved in glycolysis, mitochondrial function, and apoptosis, as well as interacts with HIF-1 to advance tumorigenicity [100, 103].

Contrary to oncogenes, tumor suppressor genes, such as p53 and phophatase and tensin homolog (PTEN), are known to be down-regulated in GBM [100, 103, 123]. P53 is the most well known tumor suppressor and is inactivated in a significant number of cancers, including GBM [100, 130]. Due to its inactivation, there is an induction of genetic instability and inhibition of DNA repair, which allows for the inhibition of programmed cell death, but enhancement of glycolysis [100, 123, 130-132]. P53 is also known to contribute to

mitochondrial maintenance both directly and indirectly, and as a result of its inactivation, assembly of complex IV in the OXPHOS/ETC (electron transport chain) pathway is inhibited, leading to impaired mitochondrial function [100, 103, 123]. In addition to inactivation of p53, loss of PTEN further enhances glycolysis via the upregulation of PI3K [103, 123].

Lastly, oxidative stress and the potential induction of apoptosis are also affected by the improper mitochondrial function exhibited in GBM. During OXPHOS in healthy cells, reactive oxygen species (ROS) are generated as a byproduct, which are eventually converted to less cytotoxic molecules that are quickly exported [103, 133]. However, in GBM, ROS is produced at significantly higher levels, leading to genomic and mitochondrial DNA damage that exacerbates mitochondrial dysfunction [134]. This includes interference with the OXPHOS pathway, as well as increases in ROS buffering enzymes, such as catalase, peroxiredoxins, superoxidase dismutase, and glutathione [99, 103, 110]. While increased levels of ROS should induce apoptosis in GBM, defects in the intrinsic apoptotic pathway allow unrestricted proliferation of these damaged cells, aiding tumor progression. The issues involved in impaired apoptosis include overexpression and activation of anti-apoptotic proteins, such as Bcl-2 and sBcl-XL, with simultaneous down-regulation of pro-apoptotic proteins Bcl-2-associated X and K (Bax and Bak) [99, 102, 103, 135, 136]. As a result, inhibition or activation of a number of the aforementioned proteins is known to enhance chemoresistance and GBM recurrence, necessitating development of more effective treatments to target these mutations.

Current Diagnosis and Treatment Strategies

As consistently stated, due to GBM's heterogeneous nature and aggressiveness, new therapeutic options are necessary. However, an initial examination of current diagnostic methods is needed in order to establish noted improvements in detection prior to focusing on

analyzing currently available, as well as in-development, treatments. Currently, GBM is diagnosed by a combination of medical history and physical exam, imaging tests, and biopsy. Initially, a patient presenting with any or all of the previously described signs and symptoms consults their physican and provides a complete medical history, including any potential familial history of cancer, and undergoes a physical exam to test brain and spinal cord performance. If obtained results appear abnormal, the patient is referred to a neurologist and/or neurosurgeon for further examination [2].

Once a preliminary exam has been performed, further testing involving imaging modalities, such as MRI (magnetic resonance imaging), CT (computed tomography), and PET (positron emisson tomography), are necessary to establish the presence of a tumor, as well as delinate the extent of tumor progression and invasion [2, 6, 7]. In MRI scans, which are believed to be the best means of detecting and diagnosing brain tumors, radio waves, powerful magnets, and a contrast dye called gadolinium are utilized. With high grade brain tumors, such as GBM, accumulation of a signficant amount of contrast agent is detected by the intense brightness seen on MRI scans [7]. However, only soft, brain tissue can be analyzed with MRIs, necessitating the use of other imaging methods to visualize and examine the surrounding bone for tumor-induced injury [2]. In addition to traditional MRI, perfusion MRI, magnetic resonance angiography, and magnetic resonance spectroscopy can be performed in conjunction to determine the blood flow and vasculature of the tumor, as well as its chemical and mineral makeup, respectively [2, 7]. With CT scans, as with MRIs, contrast dye is injected into the patient, but instead utilizes X-rays to perform visualization. While they do not provide as detailed images of the brain tissue and potential tumor, CT scans supply information regarding the position of the tumor within the bony skull to enable preparation for surgery [2, 6, 7]. In the final imaging option for brain tumor

diagnosis, PET, the radioactively labelled sugar fluorodeoxyglucose is injected and visualized. Since tumor cells undergo rapid proliferation, their utilization of significant amounts of glucose can be detected. While PET scanning is not as detailed as MRI or CT, it can be extremely valuable post-treatment as a means to confirm complete removal of the tumor [2].

Lastly, a tissue biopsy is performed to definitively establish the presence and type of cancer. As previously stated, imaging tests are performed in order to properly prepare the surgeon for a biopsy and either subsequent or simultaneous surgery, in order to establish operability, as well as prevent any poor post-surgical and/or treatment outcomes. Two types of biopsies exist when diagnosing GBM: a stereotactic (needle) biopsy or full surgical biopsy, referred to as a craniotomy [2, 6]. If the tumor is deemed to be too difficult for surgical removal, a needle biopsy is performed by making an incision, drilling a small hole through the skull, and inserting a thin needle into the brain to obtain a tissue sample that is then sent to a pathologist for tumor identification and grading, in order to enable determination of a proper treatment protocol [2, 6]. If imaging indicates that the tumor is operable, a craniotomy is done, allowing for simultaneous biopsy identification and grading and tumor debulking, if deemed feasible for successful and further treatment [2].

Once identified and graded, GBM treatment involves a combination of surgery, radiation therapy, and chemotherapy, as well as the use of newer, targeted therapy options, all of which will be summarized in the following paragraphs. As previously stated, surgery is the first line of defense against GBM; however, it is not considered curative due to the notorious invasiveness of GBM into fragile, healthy brain [2, 6, 7, 65]. As such, additional treatment modalities are necessary. Currently, the standard treatment protocol comprises a five day a week for six weeks dosing schedule of a total of 60 gray units radiation in conjunction with the chemotherapeutic

agent, temozolomide (TMZ), followed by administration of TMZ for five days a month every month to a pre-determined end point at which tumor regression is noted [6, 7, 14, 35, 65, 137]. With the current treatment regimen, median survival increased from 3 months to nearly 15 months post diagnosis [14, 65, 137].

Initial administration of radiotherapy (RT) post-surgery is shown to increase median survival by 9 months, and include conventional, external beam radiation; two- or three-dimensional (2D or 3D) conformal radiation (CRT); intensity modulated radiotherapy (IMRT); conformal proton radiation; stereotactic radiosurgery or radiotherapy; and brachytherapy [2, 6, 7]. Typically during GBM treatment, the first method for delivering radiotherapy is via high dose x-rays from outside the body called external beam radiation therapy (EBRT). However, with this method, healthy brain tissue surrounding the tumor is also targeted in order to reduce or eliminate the likelihood of recurrence from evading tumor cells [2, 6, 7]. Thus, in order to reduce this unwanted consequence, more focused external radiation is dispensed. In 3D-CRT and IMRT, several low dose radiation beams are targeted specifically at the tumor based on information obtained from MRI tests in order to preserve the vulnerable surrounding brain tissue, while with conformal photo radiotherapy, proton beams are used instead to x-rays to deliver higher doses of targeted radiation with significantly lower damage to the surrounding tissue [2, 6, 7]. However, conformal photon RT is shown to be most effective in tumors with delineated borders, which is not typical in GBM [2, 7]. For patients who have inoperable tumors or are not physically capable of undergoing cytoreductive surgery, stereotactic radiosurgery or radiotherapy are available options that deliver a sizeable dose of targeted radiation once or spread over several appointments, respectively. However, both methods are less frequently used compared to others for GBM patients due their undefined tumor edges and infiltration into the surrounding healthy

brain tissue [2, 6, 7]. Lastly, brachytherapy, when used in conjunction with low dose EBRT, can elicit notable tumor reduction due to the placement of radioactive material directly inside of or in close proximity to the tumor [2].

While radiotherapy is effective at reducing GBM tumor size, chemotherapy is typically used in combination to enhance tumor killing. For GBM, the most common and effective chemotherapeutic agent is TMZ, a cytotoxic drug that is capable of permeating the BBB and administered orally, unlike most chemotherapeutics that are given IV [2, 7, 14, 35, 137]. Recent studies have shown that patients that responded the best to TMZ treatment had a methylated or silenced DNA repair gene, O6-methylguanine–DNA methyltransferase (MGMT), further validating the need for analysis of the genome, proteome, and metabolome, and development of molecularly-targeted therapies [7, 11, 14, 35, 65, 138]. With that said, additional cytotoxic chemtherapeutics are available and in clinical use for GBM, including carmustine (BCNU), cisplatin, and lomustine (CCNU) [6, 7, 14, 35, 139, 140].

Carmustine, which is also known as bis-chloroethylnitrosourea (BCNU), is an alkylating agent that intercalates into DNA, preventing replication and transcription. Typically, BCNU is delivered via its impregnation on biodegradable wafers that are implanted directly into the tumor site during cytoreductive surgery, as a means to target cancer cells and reduce off-target side effects in the surrounding healthy brain tissue [2, 6, 14]. However, its usage as a GBM treatment has not increased since its development several decades ago due to lack of substanial improvements in survival rates compared to TMZ. Cisplatin is a platinum-based chemotherapeutic agent that also inserts itself into DNA to inhibit replication and transcription, ultimately leading to apoptosis. However, due to nephrotoxicity and increasing resistance, cisplatin use is minimized [141]. Lastly, lomustine, also known as N-(2-chloroethyl)-N'-

cyclohexyl-N-nitrosourea (CCNU), is another alkylating chemotherapeutic agent that is administered orally for the treatment of GBM. Like other nitrosourea compounds, it is able to easily permeate the BBB and can alter the structure and function of proteins, leading to their inactivation. As with many chemotherapeutics, CCNU can induce nephrotoxicity and impair immune function that can result in an increased likelihood of infection [142]. As a result, the above listed drugs are commonly used in combination, enabling reduction in the doses needed for treatment and potential lessening of side effects. Regardless, other medications are used simultaneously to treat the symptoms associated with GBM and its removal, including steroids to minimize brain swelling and anti-convulsants to prevent the occurrence of seizures in patients that have previously experienced them as a result of GBM [2, 6, 7].

If drug resistance develops or traditional chemotherapeutics demonstrate other mechanisms of ineffectiveness, targeted therapies are available, including anti-angiogenic compounds like bevacizumab [2, 7, 11, 14, 35, 65]. Bevacizumab is a monoclonal antibody targeted against VEGF that leads to an inhibition of the vasculature that aids tumor growth [2, 7, 11, 14, 35, 65]. Currently, bevacizumab is used in combination with TMZ, and has led to improvements in progression-free, but not overall, survival [35]. Additionally, bevacizumab is used as a salvage therapy, along with TMZ and other alkylating agents, to treat recurrent GBM, which befalls nearly 100% of patients [7, 11, 14, 35, 65]. With that said, other small molecules being considered as potential GBM therapies include those that target overexpressed growth factors and their receptors, such as EGF/EGFR (erlotinib), PDGF/PDGFR (imatinib), or transforming growth factor-β (AP12009); protein kinases and their receptors, such as the mammalian target of rapamycin (everolimus) or Akt (perifosine); and molecules involved in cell adhesion and migration, such as integrins (cilengitide) [2, 7, 11, 14, 65]. Lastly, tumor vaccines

and gene therapies are being developed as potential GBM treatments in order to induce the immune system to eliminate the tumor cells, enhance chemotherapeutic drug sensitivity, or enable proper function of tumor suppressing genes [2, 7, 11, 14]. Needless to say, additional new therapies must be developed, as well as methods to effectively deliver these and/or other compounds that have been previously discarded, due to their toxic side effects, across the BBB and into the tumor.

Methylene blue

Biological/Chemical Description

Methylene blue (MB), otherwise known as methylthioninium chloride, is a heterocyclic, cationic dye that was discovered in the late 1800s, and exists as a dark greenish blue (active) or colorless (inactive) compound due to its ability to undergo reversible photocatalysis (Fig. 3) [143, 144]. MB, whose molecular formula is ($C_{16}H_{18}ClN_3S$) and molecular weight is 319.85 g/mol, is a phenothiazine-derived drug with several medicinal applications that will be discussed in detail in a subsequent section [143-145]. During its photoreduction, active MB is reduced to inactive leucomethylene blue (LMB) by nicotinamide adenine dinucleotide phosphate (NADPH), which is reoxidized to MB by oxygen (O_2), as depicted in Figure 1 [143, 144, 146]. In its active form, MB has UV-Vis absorption peaks at ~665nm and 605nm, due to its presence as a monomer and dimer, respectively [147-149]. Additionally, it occurs in significantly smaller fractions following its metabolism as the demethylated forms, azure B and A, with mass spectrometry peaks at 284 (MB), 270 (azure B), and 256 (azure A) [144, 150, 151].

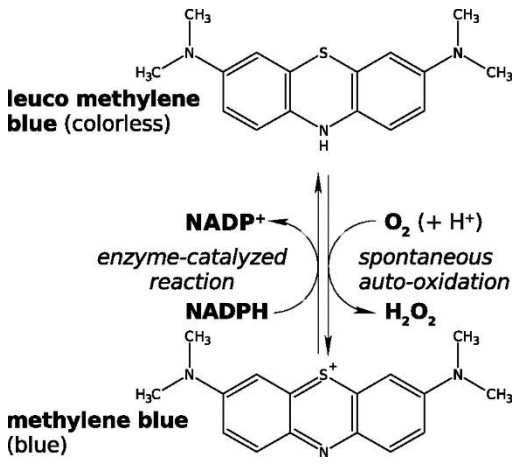

Figure 1 – Reversible photoreduction of methylene blue (MB) to leucomethylene blue (LMB) and vice versa [143,144]. MB is reduced by nicotinamide adenine dinucleotide phosphate (NADPH) to LMB, which is then oxidized back to MB by molecular oxygen (O_2).

MB affects several signaling pathways, including those involved in metabolism and energy production, as previously stated. MB is a known inhibitor of nitric oxide synthase (NOS), soluble guanylate cyclase, monoamine-oxidase A (MAO A), acetylcholine esterases (AchE), and disulfide reductases [143, 144, 146, 152-159]. In the case of NOS and guanylate cyclase, MB inhibits nitric oxide synthesis, which directly blocks guanylate cyclase by inducing oxidation of its active iron (heme) core. Once guanylate cyclase is inhibited, cyclic guanosine monophosphate (cGMP) accumulation is obstructed, preventing vasodilation and relaxation of the smooth muscle surrounding the blood vessels, both of which are necessary for tumor formation and progression [143, 144, 152-156]. MB also reversibly inhibits MAO A, leading to an increase in 5-hydroxytryptophan metabolism and its conversion to serotonin (ST); in most individuals this is of no concern, however, this becomes problematic and potentially fatal in patients taking selective serotonin uptake inhibitors due to an accumulation of ST that can cause neurotoxicity [144, 156, 157]. Lastly, MB reversibly inhibits AchE, leading to increased synaptic acetylcholine and enhanced cholinergic neurotransmission; as well as acts as a noncompetitive inhibitor and substrate of disulfide reductases, leading to its own enzymatic reduction by NADPH and subsequent re-oxidation by molecular oxygen to produce ROS such as

hydrogen peroxide [144, 146, 158, 159]. Through MB's direct and indirect effects on various signaling pathways, numerous diseases, including GBM, can be significantly impacted.

Common Historical and Current Medical Uses

As previously stated, MB was originally formulated as a textile dye in the late 1800s by the German chemist Heinrich Caro; within 15 years, it became what is considered the first synthetic drug when it was used by Guttmann and Ehrlich to treat malaria [143-145, 160-162]. While its use was eventually replaced by chloroquine and other drugs, there has been a resurgence of interest during the last decade in its use as an anti-malarial due to its disease- and cost-effectiveness [144, 161, 163-166]. Over the last 130 years, additional clinical applications have been established for MB including: staining and characterization of parasites, bacteria, and human cells; treatment of methemoglobinemia; treatment of cyanide and carbon monoxide poisoning; prevention and treatment of ifosfamide-induced neurotoxicity in cancer patients; prevention of urinary tract infections in the elderly; treatment of vasoplegia, cardiac arrest, and shock; use in photodynamic therapy (PDT) for cancer patients, including GBM; and treatment of depression, Alzheimer's disease (AD), and other neurological disorders, which will be discussed in detail in the following section [143, 144, 156, 167-194].

In the potentially deadly condition called methemoglobinemia, the red blood cell (RBC) protein hemoglobin is incapable of properly transporting and releasing its passenger molecule oxygen to tissues following circulation due to oxidation of the protein's heme (iron) molecule. In the utilization of MB to treat methemoglobinemia, MB is converted to its inactive, oxidized LMB form by RBC proteins, which is then able to reduce the troublesome methemoglobin to the functional hemoglobin following LMB's reversible transition back to MB [144, 146, 170, 186]. For the prevention and treatment of ifosfamide-induced neurotoxicity, MB acts to induce proper

functionality of the mitochondrial ETC following production of the toxic metabolite chloroacetaldehyde and buildup of nicotinamide adenine dinucleotide hydrogen (NADH). In this instance, MB serves as an electron acceptor that leads to a reversal of NADH accumulation, allowing for glucose production, as well as prevents the generation of chloroacetaldehyde through multiple mechanisms [144, 173, 186].

When treating vasoplegia, cardiac arrest, and septic shock, MB functions similarly to prevent issues related with nitric oxide synthesis and guanylate cyclase activation [143, 144, 174-182, 186, 195, 196]. As previously stated, dysregulation of NOS leads to improper activation of guanylate cyclase, which causes increased cGMP production and ultimately leads to dilation of blood vessels and a potentially deadly decrease in blood pressure. Following treatment with MB, patients experience improvements in blood pressure and cardiac function, and a reduction in brain injuries that typically coincide with cardiovascular complications [143, 179-181, 186].

In cancer patients, MB is used in a treatment referred to as PDT, which utilizes a specific wavelength light to excite photosensitizer molecules, in this case, MB, to induce tumor cell apoptosis, as well damage the tumor vasculature, by the production of ROS, [183-186, 197-201]. While PDT treatment is minimally invasive and less toxic than traditional cancer treatments, its shortcoming involves the depth and size of the tumor involved – being most effective in tumors that are close to the skin or organ surface (1cm), as well as being relatively small in size [202, 203]. Lastly, MB has demonstrated use as a neurotherapeutic, to treat conditions ranging for depression to AD; these topics will be discussed in detail in the following section.

Use as a Neurotherapeutic

Following its use as a medication compliance monitoring system for psychiatric patients, it was determined that MB could induce mood-enhancing effects in individuals suffering from depression, which has led to the development of other antidepressant compounds currently in use [156, 187, 188, 204, 205]. MB's effects in depressed patients is thought to result from its previously described role as an inhibitor of NOS and MAO, leading to increased levels of the mood-enhancing neurotransmitters serotonin and dopamine [204-207]. In addition, MB has been used to treat individuals diagnosed with traumatic brain injury [208, 209]. In these studies, MB was shown to reduce brain lesion size and associated behavioral deficits, post injury, through its known roles in improving mitochondrial function and ATP production and reducing ROS production, as well as by increasing autophagy, in order to protect neurons and prevent further damage, and impeding activation of the resident macrophages within the brain, microglia [208, 209].

Another area of interest for MB utilization as a neurotherapeutic has been in neurodegenerative disorders, such as Huntingtin's; Parkinson's; and Alzheimer's diseases, where MB is shown to enhance mitochondrial function, reduce neuronal loss and their associated behavioral deficits, and prevent and/or reduce accumulation of toxic metabolites known to induce and enhance disease progression [144, 186, 190, 192, 210-214]. In Huntingtin's disease, MB was shown to inhibit the aggregation of Huntingtin protein, leading to reduced neurotoxicity and behavioral loss, as well as improve mitochondrial function and ATP production [210, 212]; while in Parkinson's disease, disease progression was ameliorated following MB treatment due to a reduction in the degeneration of dopaminergic neurons, as well as improvements in the mitochondrial ETC, resulting in a reduction in ROS production and accumulation [211-214]. In

AD, MB targets not only mitochondrial function and cellular metabolism, but also inhibits the aggregation of two toxic proteins, tau and Aβ, as well as cholinesterase, in order to reverse/improve AD [144, 186, 190, 191, 193, 194, 205, 211-213, 215-223].

Lastly, as previously stated, MB has also demonstrated use as a potential therapy for GBM in the form of PDT [186, 201]. However, due to the typical size and depth of GBM, use of MB in its traditional compound state for PDT is unlikely [157, 158]. Currently, encapsulation of MB into a nanoparticulate platform is being considered in order to improve uptake by cancer cells and reduce off-target side effects in healthy brain and other cells [184, 224-232]. In the following section, nanotechnology, its medical applications, and potential use to treat GBM will be discussed.

Nanotechnology

Types of Nanotechnology in Medicine

Nanomedicine is a term for the medical applications of nanotechnology and their use in disease diagnostics and screening, imaging, drug delivery, or a combination (theranostics). Common types of nanomedical systems include dendrimers, liposomes, quantum dots, solid lipid nanoparticles, inorganic nanoparticles, polymeric nanoparticles, and hybrid nanoparticles [233-237]. Certain parameters are considered conducive for the use of any of the listed nanomedicines including, but not limited to: composition, size, surface charge and morphology, biocompatibility/biodegradability, cytotoxicity, and biodistribution. Regardless of type, nanomeds should be smaller than 200nm, to enable circulation and reduce elimination by the immune system; relatively uniform in size and shape; and induce little to no toxicity in healthy,

non-target cells due to composition or cargo [237-239]. Each nanomedicine type will be described and include their medical applications in the following sections.

Dendrimers are highly branched molecules with controllable size and shape based on the number and extent of branches; it is this extensive branching that makes them very stable and allows for increased loading capacity of drugs, imaging agents, and targeting ligands. While drug compounds can be attached at the ends of dendrimer branches, they can also be incorporated within the dendrimer during formulation, depending on the type of release kinetics needed. In addition, dendrimers are known to have uniform size distributions, however, they tend to be very small, which limits their cargo carrying capacity [234-237, 240, 241].

In contrast, liposomes are spherical vesicles with a lipid bilayer membrane composed of a single or combination of natural and/or synthetic phospholipids that can carry cargo such as drugs, peptides, antibodies, imaging agents, DNA/RNA, etc [234]. Due to their high biocompatibility, several liposomal formulations are currently in clinical use, primarily for infectious diseases and cancers, with the first and most well known being the liposomal doxorubicin Doxil [235-237, 242]. However, limitations exist for liposomes including a need for surface modifications to increase circulation time and enable immune system evasion, the potential for oxidation and hydrolysis of the phospholipid membrane, and a reliance of the degree of cargo encapsulation efficiency on the cargo's hydrophobicity [235-237, 242].

Another nanomedicine category called quantum dots (QDs) are inorganic fluorophores whose sizes are tunable to allow real-time imaging, resulting from their excitation across a wide range of wavelengths, but narrow emission spectra. Due to their capacity to undergo multiple rounds of excitation/emission, they are extremely photostable compared to other fluorophore molecules that are used in imaging and diagnostics. Additionally, similar to other nanomeds,

QDs can be modified with targeting moieties to allow for controlled cellular and sub-cellular uptake. However, disadvantages associated with QD use include their known ability to induce cytotoxicity in a variety of cell types due to degradation of their inorganic core, off-target effects on intracellular organelles, and the production of ROS during transport and degradation [239, 241, 243].

Similar in composition to liposomes, solid lipid nanoparticles (SLNs) are sub-micron sized lipid particles; however, they are composed of a solid phospholipid milieu instead of a bilayer with aqueous core that incorporates rather than encapsulates its cargo [234, 244]. While SLNs combine the advantages of other nanoparticle systems, such as enhanced bioavailability, without their inherent limitations, such as bioincompatibility and toxicity, they still must be coated with surfactants, such as polyethylene glycol (PEG); polyvinyl alcohol (PVA); or poloxamer/pluronic to reduce opsonization and elimination by the immune system [234, 236, 244, 245]. In addition, SLNs do exhibit a few other disadvantages that include reduced effectiveness in encapsulating hydrophilic drugs and short half-life due to their rapid removal by the reticuloendothelial system (RES), the spleen and liver's immune system [234, 244].

Another class of nanomeds is inorganic nanoparticles (NPs) that are sub-micron sized particles composed of either a metal oxide or metallic compound, such as gold, silica, or iron. Inorganic NPs are commonly used in MRI cancer imaging pre- and post-treatment due to their increased stability, as well as as drug delivery devices and in photothermal ablation therapy [237, 239, 241, 246-250]. However, even with their demonstrated clinical applications, their use must be diligently monitored due to an increased exposure to potentially toxic inorganic compounds and radiation associated with the NPs themselves, as well as the equipment required for their imaging; surface modifications with surfactants and targeting moieties to reduce/eliminate

opsonization and removal by the RES and off-target side effects; accumulation in eliminatory organs resulting in increased toxicity in the spleen, liver, and kidneys; and induction of hemolysis [237, 239, 241, 249, 250].

In contrast to inorganic NPs, polymeric NPs are a novel class of spherical carriers for drugs, peptides, DNA/RNA, etc. composed of either naturally-occurring (chitosan, dextran, albumin, alginate) or synthetic (polylactic acid [PLA], polyglycolic acid [PGA], polycyanoacrylate [PCA], polycaprolactone [PCL], poly(lactic-co-glycolic acid) [PLGA]) polymers and co-polymers [236, 237, 241, 251-253]. They can either encapsulate a drug, and reduce the need for its modification in order to maintain its efficacy and allow for its release according to the external environment, or have it covalently attached to the surface, reducing its non-specific release, but prolonging treatment unnecessarily; the type of drug incorporation will depend on the release needs and the preparation method chosen [237, 239, 241, 252]. Additional advantages of polymeric NPs include increased drug loading capacity; increased stability to enable a longer drug half-life and formulation storage period; biocompatibility/biodegradability; delivery by multiple administration routes; use in tissue engineering, in addition to their traditional applications; and ability to encapsulate other NPs to reduce/eliminate their noted drawbacks [236, 246, 251, 253, 254].

One of the most well known polymeric nanoparticulate drug delivery systems to date is the FDA-approved nanoformulation Abraxane, which is composed of the chemotherapeutic agent paclitaxel and the naturally-occurring polymer albumin [233, 255]. However, while naturally-occurring polymers have demonstrated applicability in drug development, their poor batch-to-batch reproducibility and increased degradation rate as such might make them less desirable, regardless of their intrinsic attributes [253]. Thus, the following paragraphs will

describe the differences between the types of synthetic polymeric NPs, as well as common surfactants used to coat them.

Regardless of the polymer type chosen, size and surface charge (otherwise referred to as zeta potential) are tunable, leading to an induction and enhancement of cellular and/or subcellular uptake, while preventing their elimination from the body [237, 246, 251-253, 256]. Typically, polymeric NPs smaller than 200nm are most desirable, as they allow proper passage through the circulation; can achieve enhanced permeation retention in tumors; and enhance target cell uptake, while reducing recognition and elimination by the RES [236, 246, 251, 253]. Additionally, these NPs can be surface modified, similarly to others, with surfactants (PEG, PVA, and poloxamers/pluronics) to reduce opsonization and enable passive targeting, and/or antibodies or peptides to increase uptake specificity in target cells [237, 246, 251-253, 256, 257].

Polylactic acid (PLA) is a biocompatible/biodegradable polymer that undergoes hydrolytic degradation into lactic acid monomers, which are then removed from the body during the Kreb's cycle [258, 259]. Similar to PLA, polyglycolic acid (PGA) is also biocompatible/biodegradable, however, it is broken down to glycolyic acid monomers [259]. PLA and PGA are non-toxic, non-immunogenic, and FDA-approved, making them desirable polymers in biomedical applications, where they are primarily used as implants for tissue and bone repair. However, due to their rapid degradation, their employment in drug delivery and as imaging nanocarriers is significantly reduced [259].

Another class of biodegradable polymer that has a sufficient degradation rate for development as a drug delivery system is polycyanoacrylate (PCA) [260]. However, due to its rapid degradation, PCA tends to exhibit decreased stability in an aqueous environment [261].

Additionally, PCA can be toxic due to the formation of formaldehyde by-products upon break down [262].

Polycaprolactone (PCL) is another biodegradable/biocompatible FDA-approved polymer with noted stability, allowing for its utility in sustained drug delivery and transport and as medical implants and surgical sutures to aid tissue engineering and wound healing [237, 263]. However, due to its known extended degradation rate (studies show the presence of PCL up to 4 years post application), its use in internal drug delivery as a sole formulation is limited compared to other listed polymers [264, 265].

Another commonly used polymer for biomedical applications is the biodegradable/biocompatible block copolymer, poly(lactic-co-glycolic acid) (PLGA). PLGA is broken down into lactic acid and glycolic acid monomers following hydrolysis of its polyester backbone, which undergo further degradation by the Kreb's cycle into carbon dioxide and water [251, 258, 266-268]. Due to its relatively complete degradation, PLGA is known to be minimally cytotoxic, and thus has been approved by the FDA as a drug delivery system [267, 268].

While it demonstrates an absolute break down, this can be tuned via alterations to PLGA's molecular weight and lactic acid to glycolic acid ratio, as well as drug content within PLGA-based nanoformulations [266-268]. Additionally, NPs prepared from PLGA can also exhibit changes in break down, as well as cellular uptake and sustained drug release, due to the aforementioned physico-chemical properties, as well as due to their size; size distribution (polydispersity index); surface morphology; surface charge (zeta potential); surface modifications with surfactants and/or targeting moieties; and manufacturing techniques [257, 266-273]. PLGA degradation rate is slower in higher molecular weight, longer polymers with

lower glycolic acid content, resulting in larger NPs; however, these NPs tend to have a lower initial drug encapsulation efficiency compared to smaller NPs made from smaller chain length PLGA with a higher glycolic acid composition [266-268].

As previously stated, NPs should be below 200nm in size in order to enhance cellular uptake and reduce elimination, thus, polymer composition is imperative [236, 246, 251, 253, 267, 268, 274]. With that said, smaller PLGA NPs, which exhibit a higher surface area to volume ratio, undergo a more rapid degradation rate than larger NPs, further establishing the importance of polymer composition [266, 268, 270]. In addition to size, a narrow size distribution, or polydispersity index (PDI), is also necessary to enhance NP uptake by target cells. On a scale of 0 to 1, the closer a batch of NPs' PDI is to 0, the more uniform its size is and reduced possibility of aggregation. Also, the rounder/smoother the PLGA NPs are, the higher their likelihood of uptake [275].

Lastly, the surface charge (zeta potential) of PLGA NPs influences their target cell uptake and overall biodistribution [256, 266, 267, 276, 277]. Positively charged NPs exhibit increased cellular internalization and the ability to escape lysosomal trafficking quickly, but reduced circulation half-life and availability for uptake [266, 267, 276, 277]. In contrast, with negatively charged NPs, there is increased circulation time, allowing for absorption of plasma proteins, primarily immunoglobulin G, during the process of opsonization; this leads to their increased uptake and elimination by phagocytes, thereby reducing their availability for uptake by their target cells [256, 276].

In order to obtain an optimum zeta potential and enhance target cell internalization, surface modifications are necessary and include coating with surfactants and/or attaching

targeting moieties. Some common surfactants used during PLGA NP formulation are PEG, PVA, and poloxamer (branded Pluronic), with descriptions of each to follow.

Polyethylene glycol (PEG) is a water and organic solvent-soluble FDA-approved polymer composed of multiple ethylene oxide molecules that is biocompatible, resulting in minimal toxicity and no immunogenicity [234, 246, 267, 277, 278]. To improve uptake of NPs by their target cells through passive targeting, a PEG coating is utilized, as it increases blood circulation half-life; reduces plasma protein absorption and opsonization, leading to reduced recognition and removal by the RES; and positively impacts biodistribution, further reducing elimination from the body prior to reaching the target cell/tissue [234, 246, 256, 267, 271, 277, 278]. Additionally, PEG can neutralize the surface charge of negative PLGA NPs, act as attachment points for targeting ligands, improve the circulation half-life of an encapsulated drug, and enhance accumulation of NPs within a tumor and its microenvironment to increase their therapeutic effect [246, 267, 277]. However, PEG has demonstrated limitations such as having poor biodegradation abilities, potential indication of immunogenicity upon repeated administration, and dichotomy of using low molecular versus high molecular weight PEG to allow proper break down; reduce the formation of ROS by-products; and reduce potential immunogenicity and toxicity [279].

Thus, another commonly used emulsifier available for biomedical applications is the water solube, non-ionic surfactant, polyvinyl alcohol (PVA). PVA is known to neutralize the surface charge of PLGA NPs and produce smaller, more uniformly distributed NPs with smooth surfaces [272, 280]. However, numerous disadvantages exist with the use of PVA, including: low coating efficiency; possible carcinogenicity; reduced biocompatibility; reduced drug loading capacity; induction of hypertension, CNS depression, and other side effects related to its residual

presence on the surface of NPs; aggregation in biological media; and decreased cancer cell uptake [272, 280, 281].

Due to PVA's overall poor utility in biomedical applications, another commonly employed class of surfactants is called poloxamers, which are also referred to as Pluronics. Poloxamers are non-ionic triblock copolymers composed of polypropylene and polyethylene oxides whose contents can be varied to improve their biomedical applications [269, 272, 273, 280, 282-285]. A frequently studied poloxamer for biomedical applications, particularly with PLGA NPs, is poloxamer 188, otherwise referred to as Pluronic F-68 (PF68). In the poloxamer designation, the first two digits relate to the molecular mass of polypropylene oxide and the last digit the percentage of polyethylene oxide content (18 x 100 = 1,800 g/mol polypropylene oxide in poloxamer 188 and 8 x 10% = 80% polyethylene oxide content in poloxamer 188); in the Pluronic description, the F involves its physical form at room temperature (flake = solid), while the first number concerns the molecular mass of polypropylene oxide and the last number the percentage of polyethylene oxide content (6 x 300 = 1,800 g/mol polyproylene content in PF68 and 8 x 10% = 80% polyethylene oxide content in PF68) [269].

PF68 has demonstrated advantages when used alone, as well as in combination as a NP surfactant. It has low immunogenicity and toxicity, with enhanced biocompatibility, as shown by its minimal side effects and proper elimination upon administration. Its noted effects upon physiology include inhibition of platelet and RBC aggregation; induction of mild lower back and leg pain; nausea; headaches; fatigue; prevention of bacterial infection during wound healing, without any direct antibacterial effects; induction of cell membrane recovery following damage; increased blood pressure, cardiac output, and blood flow to organs, without affecting heart rate; reduction in coronary blockage, leading to reduced risk and occurrence of heart attacks;

inhibition of uptake and release of the neurotransmitter norepinephrine; and the ability to easily permeate the BBB due to preferential adsorption of specific proteins involved in lipid transport (apolipoproteins) following IV administration [269, 271, 280, 285-288]. When used in conjunction with PLGA NPs, it can result in the formation of spherical, porous NPs with a monodisperse size distribution, as well as neutralization of the acidity that occurs during PLGA degradation and overall neutralization of NP surface charge [269, 272, 273, 284]. As a result, there is an enhancement in NP stability, in addition to drug stability and solubility, that subsequently increases NP target cell uptake and therapeutic effectiveness [269, 273, 282].

Thus, these advantages are critical for PF68's utilization as a chemotherapeutic delivery system. As stated, PF68 has demonstrated benefits that are amplified when used as a PLGA NP coating, especially for cancer applications. These include reduced interaction with plasma proteins and inhibition of opsonization, resulting in decreased elimination by the RES, but enhanced uptake by cancer cells for improved cytotoxicity; increased blood circulation half-life of PLGA NPs and drug cargo, resulting in increased therapeutic effectiveness; innate chemosensitization in multi-drug resistant (MDR) cancers; inhibition of ATP-binding cassette (ABC) proteins, drug efflux pumps (such as P-glycoprotein (P-gp)), and drug detoxification systems to overcome MDR; prevention of drug sequestration within cytoplasmic vesicles through alterations in organellar pH; depletion of ATP levels to further enhance MDR inhibition; and drastic reduction in tumor metastasis [257, 269, 272, 280, 283-285, 288-292]. With that said, the use of PF68 must be reserved as its repeated administration can lead to increased clearance, and ultimately, reduced therapeutic activity [257].

Regardless of the previously listed attributes, PLGA NPs, even in the presence of surfactants, have their limitations, including modest drug loading capacity that averages 1%, and

an initial burst release of drug compound that reduces the actual amount available for treatment [267, 268]. Thus, a final nanoparticle option, the hybrid NP (HNP), is available, with the most common being lipid-polymer hybrids. HNPs are composed of a hydrophobic polymer core; hydrophilic polymer shell; and lipid monolayer between the core-shell border, thus demonstrating advantages of polymeric NPs and liposomes without a number of each NP's inherent limitations [293-295]. The benefits of using HNPs include tunable size and surface charge, increased drug loading capacity and effective encapsulation of relatively water-insoluble drugs, enhanced stability during storage and experimentation due to lipid/polymer composition, biocompatibility/biodegradability, sustained drug release and increased therapeutic activity, superior blood circulation half-life, the ability to employ cell- or tissue-specific targeting ligands, and enhanced target cell uptake and cytotoxicity [293-295]. As a result, HNPs are gaining in development for drug delivery, as well as DNA/RNA delivery and diagnostic imaging [294, 295]. However, issues arise when considering their translation applications, such as improving the concentration of targeting ligands on the surface, completeness of lipid coverage around the NP surface, encapsulation of multiple therapeutics and/or imaging modalities, limited data on *in vivo* studies and their success, and development of scale-up procedures [294, 295]. With that said, no nanoformulation is completely ideal, making the type chosen dependent on available facilities, the disease(s) or biochemical pathway(s) being studied, and any potential translational applications.

Delivery of Polymeric Nanoparticles Across the BBB

The blood-brain barrier (BBB) is a biological barrier composed of endothelial cells, astrocytes, microglial (immune) cells, and pericytes that controls the transport of compounds into the brain from the circulation by physical (tight junctions) and metabolic (enzyme) means. Thus,

delivery of brain targeted therapeutics occurs through receptor, transporter, or adsorptive-mediated endocytosis by brain capillary endothelial cells (BCECs); transcytosis by BCECs; and/or following disruption of the BBB by other therapeutics or disease [241, 267, 296-306]. However, a majority of small molecule drugs are inhibited from obtaining passage across the BBB through most of the aforementioned methods due to the presence of drug efflux pumps, like ABC proteins and P-gp; thus, another transport system is required [241, 297-299, 302].

Polymeric nanoparticles (NPs), specifically PLGA NPs, which are becoming more frequently used as drug delivery mechanisms, have the ability to circumvent the BBB, the most immunologically and physically protected biological barrier [277, 297, 298, 300, 306-308]. In an *in vivo* mouse study, the brain was determined to be the fourth most common distribution site for PLGA NPs (~13% of total NPs) following IV administration, with those smaller than 200nm being more likely to accumulate there [270, 305]. This confirms that, on their own, PLGA NPs can permeate the BBB; however, by utilizing surface modifications to enable non-specific endocytosis (passive targeting through surfactant coating) or active targeting through ligand surface attachment, there can be an enhancement in NP uptake, reduced elimination by the RES, and improved therapeutic efficacy [267, 296-301, 303, 304, 306-312].

NPs typically cross the BBB by endocytosis or trancytosis by BCECs, however additional mechanisms have been hypothesized, including: enhanced accumulation by brain-blood capillaries and their adsorption to capillary walls; inhibition of efflux pumps by surfactant coatings; solubilization of cell membrane lipids of BCECs by surfactants; breaching tight junctions between BCECs solely due to the presence of NPs; or a combination of those listed [303, 306, 309, 312-315]. Studies have shown that moderate to highly negative/anionic NPs (-1 to -45 mV) have an increased likelihood of passage across the BBB following BCEC uptake and

are able to inhibit drug efflux by ABC pumps and other exporters, which can be enhanced upon surfactant coating [241, 304, 316].

As previously stated, some commonly used surfactants in NP formulation include PEG, PVA, poloxamers/Pluronics, and polysorbate/Tween 80, with recent studies demonstrating that poloxamer 188 (Pluronic F68/PF68) has the best capacity to enable NP permeation across the BBB upon comparison [296-299, 303, 306, 309, 311-314]. In addition to their potential role in lipid membrane solubilization, NP surfactants can adsorb plasma proteins, including apolipoproteins (Apo), on their surface to enhance transport across the BBB, leading to their mis-identification as self and delivery via receptor or adsorptive-mediated endocytosis [271, 298, 303, 317]. Coating with PF68 and Tween 80 also enable inhibition of efflux of NPs and their cargo by ABC transporters like P-gp, however, some BBB toxicity is noted with Tween 80, further establishing PF68 as a better alternative [303, 309]. Thus, naturally-derived coatings are also available, with demonstrated biocompatibility and reduced neurotoxicity to the BBB, and include glutathione and albumin [300, 301, 303]. Glutathione is a compound that guards against oxidative stress and also inhibits P-gp, demonstrating its effectiveness as a protective shell for NPs, as well as a cellular shield that prevents premature polymer degradation and drug release [300, 301, 303]. Lastly, albumin is a one of the most common blood serum proteins, which is typically found on the surface of NPs during their circulation [301, 303]. Studies have previously shown that albumin-coated NPs can easily permeate the BBB, yet do not induce toxicity even at very high concentrations, making albumin a potentially useful NP coating [301, 303].

In addition to surfactants, attachment of ligands on the surface of PLGA NPs, such as peptides and antibodies, is another effective means to enhance delivery and uptake across the

BBB and to target cells, while reducing recognition and elimination by the RES and efflux pumps [267, 299-301, 303, 304, 307, 309, 310]. Examples of brain ligand targeting moieties include thiamine; transferrin; lactoferrin; insulin; folate; and low density lipoproteins (LDLs), as their receptors are some of the most commonly expressed receptors at the BBB [267, 299-301, 303, 304, 307, 309, 310]. Thiamine is a compound (water soluble vitamin B) necessary throughout every stage of cellular function and maintenance that has receptors on the surface of endothelial cells along the BBB, making it a suitable targeting molecule for NPs. However, due to the presence of thiamine receptors throughout the body, its applicability in targeting the BBB is unlikely [300, 301, 303].

Next, transferrin, an endogenous peptide that was one of the first to be used in ligand-based NP, has a significant amount of receptors on the surface of BCECs, enabling its endocytosis and transport across the BBB [301, 303, 310]. However, its application has been limited due to the excessive presence of transferrin in circulation, which can outcompete transferrin-coated NPs for receptor binding sites and prevent their passage across the BBB. Instead, transferrin antibodies like Ox26 are being utilized as NP conjugates to enhance their BBB transport and uptake, as there is no concern for competion against the antibody's specific binding site [299, 303, 309, 310]. Another ligand option is lactoferrin, a transferrin member glycopeptide that also possesses a significant number of BBB cell surface receptors for binding [267]. Through its ligand-receptor interaction, transport across this strict biological barrier is possible, as well as the ability to influence numerous physiological processes that range from inhibiting inflammation to preventing carcinogenesis [267, 318]. While lactoferrin and transferrin are structurally similar, lactoferrin was shown to have a higher uptake across the BBB than the transferrin peptide or antibody, making it a more useful targeting moiety [319, 320].

Next, another available ligand used in targeting is insulin, the hormone necessary for proper sugar transport and utilization throughout the body. However, do to its rapid degradation and potential induction of hypoglycemia, the insulin ligand is not a feasible option [303, 309, 310]. Thus, insulin antibodies have been exploited for transport across the BBB, through receptor-mediated endocytosis and subsequent transcytosis, and have been shown to be more effective at binding transferrin receptors and enabling BBB permeation and cell uptake than Ox26, in addition to effectively binding its own receptors on BCECs [303, 309, 310, 321].

In addition to the above options is folic acid, water soluble vitamin B9 that is necessary for the production of DNA and RNA and vitamin B12-dependent methionine synthesis [322]. Folic acid is shown to have a significant amount of folate receptors present within, instead of on the surface of, BCECs of the BBB, particularly those with high affinity binding capabilities, reducing the likelihood of misguided drug delivery [322, 323]. In a study characterizing folate conjugated, PEG-coated polymeric NPs, there was a 10-fold higher affinity for the folate receptor compared to free folate, further establishing its utility as a BBB ligand [324]. A final option for brain targeting is through low-density lipoproteins (LDLs) such as Apo A, B, or E. As demonstrated, surfactant-coated NPs undergo enhanced BBB passage following adsorption of LDLs on the surface; thus, conjugation with any of a variety of available LDLs should enable a similar mechanism without the need for surfactants [271, 303, 309, 325]. This has been confirmed by several studies where Apo that were convalently attached to different NP formulations improved BBB uptake and delivery by receptor-mediated endocytosis and subsequent transcytosis, due to an increased presence of LDL receptors on the BBB surface [309, 315, 317, 325]. With that said, any of the above options are sufficient for enabling and enhancing passive or active targeting of NPs across the BBB and to the specific diseased brain

region; however, additional experimentation is necessary to establish their applicability in a clinical setting.

Applications of Polymeric Nanoparticles in Cancer

One clinical field experiencing signficant development of new polymeric nanotherapeutics is cancer, where treatments can "target" the tumor itself, the tumor vasculature, or the tumor microenvironment. Nearly every nanoformulation to date aimed at treating cancer involves some form of surface modification, either surfactant coating or attachment of a targeting ligand or a combination, in order to enhance uptake by the cancer cells and reduce potential side effects in healthy neighboring cells. Several studies that encapsulated model drugs such as coumarin in PVA, vitamin E, or PEG-coated PLGA NPs demonstrated their enhanced accumulation in breast and colon cancer cell lines compared to non-coated NPs following administration, confirming their utility as cancer drug delivery systems [278, 326]. To further establish those findings, other studies encapsulating chemotherapeutic agents in PF68 and PEG-coated polymeric NPs were developed to treat a myriad of cancer types *in vitro* and *in vivo*, as well as in human patients, and shown to induce cancer cell apoptosis, reduce antitumor activity and off-target effects, and increase survival rates [327-333]. In addition to traditional chemotherapy drugs, another compound with demonstrated anticancer activity is the plant extract curcumin. Recent studies from different labs have demonstrated its enhanced activity following administration *in vitro* and *in vivo* upon its encapsulation in different polymeric nanoformulations [334, 335]. While in other reports, the photosensitizer molecule methylene blue and its derivatives, which were encapsulated in surfactant-coated polymeric NPs, were able to enhance cytotoxicity in several different cancer cell lines upon administration and irradiation for PDT [230, 231, 336]. Thus, packaging drug compounds in surfactant-coated polymeric

nanoparticles can enhance their effectiveness, while reducing any toxic side effects that might transpire in healthy cells. However, to further eliminate the possibility of damage to healthy cells and tissue in close proximity to a tumor, use of targeting ligands is being explored.

As previously described, some common cell surface receptors include folate and transferrin, as well as biotin, which can be targeted for cancer drug nano-delivery. In recent papers, peptides that bind the aforementioned receptors have been conjugated to chemotherapeutic-loaded PLGA NPs and have demonstrated enhanced antiproliferative and cytotoxic activity, as well as improved cancer cell specific uptake, which led to reduced tumor growth upon comparison to free drug and non-targeted NPs [337-339]. However, use of these ligands is problematic due to their ubiquitous occurrence, requiring the utilization of more tumor cell and tissue-specific targeting moieties.

Various cancers have been targeted for their increased cell surface expression of integrins, growth factor receptors, and drug efflux pumps (P-gp) via conjugation of their peptide binding partners to surfactant-coated PLGA NPs that were loaded with several different chemotherapeutics. Upon administration of these nanoformulations, there was a noted induction of apoptosis and reduction in proliferation *in vitro*, with a subsequent inhibition of tumor growth and angiogenesis *in vivo* [328, 340-342]. While these ligands are improvements, further targeting enhancement is imperative. In the case of prostate cancer treatment, a common target is the transmembrane glycoprotein, prostate-specific membrane antigen (PSMA). Numerous drug and silencing RNA-loaded polymeric nanoformulations have utilized PSMA peptide aptamers and antibodies to enhance drug delivery and effectiveness, both *in vitro* and *in vivo*, with one (BIND-014) currently in clinical trials as a treatment for advanced and metastatic cancers [343-346]. Breast cancer is another malignancy with substantial nanotechnology-based

drug development underway. In one formulation, PVA-coated PLGA NPs loaded with bovine serum albumin as a model drug was covalently attached with a breast cancer specific mononclonal antibody and shown to bind its cell surface receptor and enable enhanced internalization in a co-culture with a colon cancer cell line compared to non-targeted NPs, while in another, Annexin A2 antibody-conjugated, PVA-coated PLGA NPs that were loaded with curcumin also had enhanced cell uptake and ultimately induced apoptosis in Annexin A2 overexpressing breast cancer cells [347, 348]. Lastly, melanoma cells treated with F3 (a peptide that binds the nucleoline receptor)-conjugated polyacrylic acid (PAA) NPs that were filled with methylene blue derivatives displayed significant cell death following PDT light treatments compared to PEGylated PAA NPs, substantiating the applications of nanotechnology in cancer therapy [228].

Applications of Polymeric Nanoparticles in Glioblastoma

As previously described, GBM is a highly aggressive, grade IV brain tumor that is cellularly and molecularly heterogenous, making development and utilization of treatment protocols difficult. In addition to surgery and radiation, some form of chemotherapy, typically temozolomide (TMZ), is used to reduce disease progression and extend survival; however, these treatments result in a median survival length of 15 months, demonstrating the need for better, more effective therapy options and the potential applicability of nanotechnology.

As stated in the former section on cancer nanoformulations, those developed to include surfactants and/or targeting moities might be most effective for GBM. Due to the presence of the BBB, surfactant-coated PLGA NPs could be useful, as they enhance passage across this restrictive biological barrier, as well as increase uptake in human GBM cell lines by the adsorption of plasma proteins [315]. In doxorubicin-loaded, PF68-coated PLGA and

polybutylcyanoacrylate NPs administered in a brain tumor rat model, the NPs were shown to easily permeate the BBB, as well as reduce and prevent further tumor growth that lead to increased survival times *in vivo* [313, 349, 350]. Additionally, GBM is known to express high levels of cell surface receptors for LDL such as Apo A and E, further establishing the use of surfactants on PLGA NPs as a means of protection and transport of drug compounds [304].

In Tween 80-coated polymeric NPs containing various chemotherapeutic agents, there was a noted increase in antiproliferative activity and reduction in tumor growth due to enhanced brain accumulation, particularly in the tumor, in xenograft rodent models; this effects resulted in extended survival rates in the animals, which could be applied to human GBM cases [351-353]. Similar anti-tumorigenic activities were observed in C6 and 9L rodent models administered PEGylated polymeric nanoformulations loaded with paclitaxel, as well as in C6 and RG2 cells treated with glutathione-coated PLGA NPs encapsulating taxane compounds [354-357]. Lastly, in methylene blue-loaded PAA NPs coated with PEG or Aerosol-OT, there was an increase in ROS levels that resulted in an increase in cytotoxicity in C6 rat cells following PDT irradiation, further demonstrating the effectiveness of surfactant-coated polymeric NPs in GBM [230, 231].

While surfactant coating can enhance NP uptake, it does not completely prevent internalization by healthy cells in close proximity to the tumor, thus utilization of targeting moieties can be an option. A commonly expressed receptor on the cell surface of the BBB, as well as many cancer types, including GBM, is transferrin. In a transferrin-conjugated PLGA NP formulation carrying doxorubicin and paclitaxel, an increase in tumor inhibition was observed following treatment both *in vitro* and *in vivo*; however, while this targeting ligand does occur at a higher rate in GBM, it is not tumor specific [358]. In other studies, RGD used singularly or in conjunction with an interleukin-13 peptide were conjugated to PEGylated polymeric NPs to

target GBM cells and their associated vasculature. The NPs, which were loaded with taxanes, were shown to enhance brain uptake, specifically at the tumor site, compared to non-targeted NPs, leading to increased antiproliferative, antiangiogenic activities and survival rates *in vitro* and *in vivo*, respectively [359-361]. Finally, polymeric NPs functionalized with an F3 peptide and PEG coating, or solely with PEG, were shown to boost methylene blue's cytotoxic abilities following irradiation *in vitro*, while reducing tumor burden in a 9L rat model, further demonstrating the applicability of polymeric-based nanotechnology as a means to effectively deliver chemotherapeutic agents to GBM [229, 362].

Objectives of Study

Hypothesis and Specific Aims

According to statistics from the American Cancer Society (ACS), of the estimated 1.7 million newly diagnosed cancer cases within the United States this year, nearly 1.4% (23,130) will be due to tumors of the brain and nervous system; additionally, of the 580,000 total cancer deaths, approximately 2.4% will be attributed to the aforementioned anatomical areas [363]. Although these figures are significantly lower than those of more recognized cancer types (breast, colorectal, lung, pancreatic, and prostate), brain-associated cancer prevalence is rising due to increased resistance to conventional treatment methods, leading to significantly lower survival rates [3, 7, 364]. Glioblastoma (GBM), a rapidly developing grade IV brain cancer that originates from supportive glial cells called astrocytes located primarily within the cerebrum, is considered the most common and aggressive primary human brain tumor due to poor prognosis (14 months maximum post-diagnosis with treatment) and substandard five-year survival rates (less than 10%) [3, 6-8]. With that said, GBM primarily remains localized to the brain, with

extracranial metastasis being very rare [9, 365]. While GBM can affect individuals of all ages, it occurs more frequently in adults, primarily middle-aged people between 45 and 65, with a gender disparity favoring men, as well as a slight racial discrepancy towards Caucasians [3, 7]. Currently, little is known about the actual cause of GBM, with research continuing in genetics, heredity, and environment, among others [7]. Due to GBM's recent reclassification into four molecular subtypes, additional treatments are necessary in order to more effectively treat this devastating disease and its heterogeneous nature [366-369].

With that said, methylene blue (MB), an established medicinal compound, has received increased attention during the last decade as a potential therapeutic for several brain disorders, in part due to its ability to permeate the blood-brain barrier. In a study performed by our collaborator, MB treatment was shown to increase oxygen consumption, reduce lactate production, and inhibit proliferation of U87 glioblastoma cells through reversal of the Warburg effect [370]. While MB has demonstrated utility, the challenge that arises is that delivery via either traditional oral or IV route provides reduced brain uptake compared to administered dosage [371], leading to overmedicating and potential toxicity. Using established techniques that improve drug delivery, MB could provide a better treatment option over current methods, allowing for healthier lifespans and increased survival rates.

A method with demonstrated improvements in drug delivery is via the encapsulation of compounds into polymeric nanoparticles (NPs) made from the biodegradable/biocompatible, FDA approved molecule, poly(lactide-co-glycide) (PLGA). Our lab has demonstrated the applicability of PLGA NP formulations as treatments for various cancers [334, 348, 372-374], with additional drug delivery advantages resulting from their sustained release abilities [334, 372] and preferential accumulation in the brain [375]. A study associated with the evaluation of

PLGA NPs in vivo, confirmed detectable accumulation of PLGA NPs (12.86%) in the brain of Balb/c mice [270]. Finally, other studies have shown the ability to encapsulate MB in different NP formulations for disease diagnosis and/or treatment, further demonstrating their feasibility [224-227, 231, 376-387].

As a result, the *objective* of this project was to develop and characterize a MB(OS)NP (methylene blue oleate salt-loaded polymeric nanoparticle) formulation and to investigate its permeability, uptake, and anti-proliferative effects in GBM models *in vitro*. We *hypothesized* that encapsulation of a sodium oleate conjugate of MB (MBOS) into PLGA NPs would inhibit GBM cell survival and proliferation through a reversal of the Warburg effect. Thus, to test the hypothesis, our aims were,

1) *To formulate and characterize MBOS-loaded PLGA NPs using particle size, surface charge, and morphological analysis.* Additionally, encapsulation efficiency, drug loading, and MBOS release will be determined to ensure that sufficient agent is available for effective treatment. This formulation will be compared to empty PLGA NPs, free MB, and free MBOS.

2) *To investigate the anti-proliferative effects of MBOS-loaded PLGA NPs in in vitro GBM models.* We will determine formulation efficacy based on altered mitochondrial and overall cell functions in the human GBM cell lines U87 and T98G following NP treatment. Cell metabolism (oxygen consumption; ATP production; glucose quantification), cell survival/death, and cell proliferation will be analyzed. Experiments will also be performed with empty PLGA NPs, free MB, and free MBOS.

- U87 – human GBM cell line with epithelial morphology; isolated from 44-year-old Caucasian male; WT p53, mutant PTEN, p16 del; temozolimide (TMZ)-sensitive

- T98G – human GBM cell line with fibroblast morphology; isolated from 61-year-old Caucasian male; mutant p53, mutant PTEN, p16 del; TMZ-insensitive

3) *To determine the bio-distribution of MBOS-loaded PLGA NPs in vivo.* We will establish the pharmacokinetics of drug-loaded NPs compared to free drug (MB and MBOS) to determine if an equivalent amount accumulates in plasma and tissues of CD-1 mice following administration and quantification at designated time points.

CHAPTER II

DEVELOPMENT AND CHARACTERIZATION OF METHYLENE BLUE OLEATE SALT-LOADED POLYMERIC NANOPARTICLES AND THEIR POTENTIAL APPLICATION AS A TREATMENT FOR GLIOBLASTOMA

Abstract

Glioblastoma (GBM) is an aggressive, grade IV brain tumor that develops from astrocytes located within the cerebrum, resulting in poor prognosis and survival rates following an accepted treatment regimen of surgery, radiation, and temozolomide. Thus, development of new therapeutics is necessary. During the last two decades, methylene blue (MB) has received increased attention as a potential neurotherapeutic due to its duality in brain cancers and neurodegenerative diseases. While MB is capable of easily permeating the blood-brain barrier, its therapeutic concentrations in GBM are known to induce off-target cytotoxicity and thus, another mode of drug delivery must be considered. To this end, encapsulation of formerly unusable compounds into nanoparticles (NPs) made from the biodegradable/biocompatible, FDA approved co-polymer poly(lactide-co-glycolide) (PLGA) has been more commonplace when developing novel therapeutics. In this study, we formulated and characterized Pluronic F68-coated PLGA NPs containing a sodium oleate conjugate of MB (MBOS) via solvent displacement. Conjugation of sodium oleate to MB was shown to reduce its release from PLGA NPs compared to unmodified MB, leading to potential improvements in drug accumulation and

therapeutic effectiveness. Our drug-loaded NP preparations, which were ~170 nm in size and had drug loading values of ~2%, were shown to reduce cell viability and cell compartment-specific, as well as overall cell, functions equivalently, if not more so, when compared to free drug in two GBM cell lines. Following bio-distribution analysis of free MBOS compared to its nano-encapsulated counterpart, drug-loaded NPs were shown to more effectively permeate the BBB, which could lead to improvements in therapeutic effectiveness upon further examination in a tumor-bearing mouse model. Based on these results, we believe that the further development and eventual utilization of this nanoformulation could lead to an effective GBM therapy that could extend patient survival rates. Keywords – methylene blue, nanomedicine, glioblastoma, brain tumor, neurotherapeutic

Introduction

According to statistics from the American Cancer Society (ACS), of the estimated 1.7 million newly diagnosed cancer cases within the United States this year, nearly 1.4% (23,130) will be due to tumors of the brain and nervous system; additionally, of the 580,000 total cancer deaths, approximately 2.4% will be attributed to the aforementioned anatomical areas [363]. Although these figures are significantly lower than those of more recognized cancer types (breast, colorectal, lung, pancreatic, and prostate), brain-associated cancer prevalence is rising due to increased resistance to conventional treatment methods - a combination of surgery, chemotherapy, and radiation - leading to significantly lower survival rates [3, 7, 364]. Glioblastoma (GBM), a rapidly developing grade IV brain cancer that originates from supportive glial cells called astrocytes, resulting in its classification as an astrocytoma, is located primarily within the cerebrum and considered the most common and aggressive primary human brain

tumor due to poor prognosis (15 months maximum post-diagnosis with treatment) and substandard five-year survival rates (less than 5%) [1-8]. While GBM can affect individuals of all ages, it occurs more frequently in adults, primarily middle-aged people between 45 and 65, with a gender disparity favoring men, as well as a slight racial discrepancy towards Caucasians [3, 7, 10, 14, 15].

GBM, like other cancers and cells undergoing rapid proliferation, depend on an inefficient energy producing process called aerobic glycolysis to generate adenosine 5'-triphosphate (ATP) and other metabolic precursors for successive colony expansion through a phenomenon referred to as the Warburg effect [99, 107, 388, 389]. In the Warburg effect, highly proliferative cells, including cancers such as GBM, exhibit irregular mitochondrial behavior that results from disjointed energy metabolism, leading to a dependence on cytosolic glycolysis for energy [102, 390-392]. While decades of research have established the Warburg phenomenon and associated mitochondrial dysfunction as a consequence of compounding genetic mutations, the concept continues to be an intriguing aspect in the development and progression of cancer, specifically GBM, and thus, provides an avenue for the development of novel therapies.

Methylene blue (MB), also referred to as methylthioninium chloride, is a water soluble compound that was discovered in the late 1870s and originally used as a histological dye. MB, which has a proven safety record and demonstrated versatility in clinical applications, has been used to treat maladies ranging from chemotherapy-induced encephalopathy and can act as a photodynamic therapy (PDT) in cancer patients to more historical conditions such as cyanide poisoning and malaria [171, 172, 186, 211, 371, 393-395]. In the case of various diseases, including GBM, MB has been shown to target dysfunctional mitochondria by acting as an electron carrier via its reversible photoreduction to inactive leucomethylene blue (LMB) to aid

cytochrome c reduction, bypass complex II, increase oxygen consumption, and increase the production of reactive oxygen species (ROS) [216, 396-402]. While MB shows promise as a neurotherapeutic due to these benefits, as well as its ability to easily permeate the blood-brain barrier (BBB), the challenge arises when administering MB to patients. In order to achieve the necessary accumulation of drug concentration for treatment, a higher-than-required dose must be given, leading to potential overmedicating and off-target toxicity [371]. As a result, additional drug delivery methods must be considered.

Traditional modes of drug delivery across the BBB involve disruption of the BBB, which if still intact during the disease state, can lead to infection; lipidation of small molecules; and delivery of anti-sense or non-viral DNA [403]. Due to recent advances in nanotechnology, its applications have been considered as possible mechanisms for more effective drug delivery across the BBB, ranging from encapsulation in liposomes and polymeric nanoparticles to direct conjugation to antibodies [253, 296, 298, 404-407]. Over the past few decades, nanoparticle drug development has grown because of its wide versatility of applications and formulations. In accordance with the previous statement, nanoparticle delivery of drugs for GBM has grown due to the need for more effective treatments that can maneuver the BBB. While numerous options are currently available for developing nanodrug delivery systems, including liposomes; solid lipid nanoparticles; polymeric nanoparticles; hybrid nanoparticles; dendrimers; and nanotubes, this study focuses on the application of polymeric nanoparticles, derived from the synthetic co-polymer poly(lactide-co-glycide) (PLGA). PLGA was the first FDA-approved co-polymer for medical use, is biocompatible/biodegradable via its non-enzymatic hydrolysis at its ester linkages to lactic and glycolic acids, and has confirmed brain accumulation in *in vivo* studies [270, 408-410]. Some of the advantages afforded by PLGA NPs as drug delivery systems include: their

ability to encapsulate numerous compounds; provide targeted drug delivery using surface functionalization with antibodies/peptides; allow tunable sizing; can be prepared from various matrices; improve therapeutic efficacy of drugs due to reduced clearance; can be used for various administration routes, reduce toxic side effects; and traverse biological barriers, including the blood-brain barrier (BBB), skin, and tight junctions of various epithelial layers [253]. PLGA NPs are thought to obtain passage through the BBB via receptor-mediated endocytosis in brain capillary endothelial cells, which results from either covalent attachment of targeting ligands or coating with certain chemicals that enable adsorption of specific plasma proteins for improved circulation and distribution [406]. Methods that are being considered in order to improve PLGA NP passage through the BBB, as well as improve tumor uptake, include active targeting via surface conjugation with antibodies or BBB receptor ligands and use of surfactants [411].

While MB-loaded NP formulations have been developed in the last several years to treat various conditions, the concern with utilizing MB in a PLGA NP is due to its high water solubility. PLGA NPs tend to encapsulate hydrophobic and lipophilic drugs more effectively than hydrophilic drugs; therefore, modifications to MB are necessary that enable prolonged entrapment within the NP until delivery to the target site without affecting its normal chemical functions. To this end, we formulated a methylene blue oleate salt (MBOS) conjugate and encapsulated it within PLGA NPs. In this study, we tested the hypothesis that encapsulation of MBOS in PLGA NPs would elicit minimally equivalent *in vitro* effects in multiple GBM cell lines when compared to free MB, as well as free MBOS, based on the reversal of mitochondrial dysfunction and supposed reduction in off-target side effects. Additionally, we sought to determine the biodistribution of MBOSNPs compared to free MB and MBOS, as a means to

confirm any potential clinical applications toward improving disease progression and reducing drug-associated toxicity.

Experimental Procedures

1. Cell Culture and Other Reagents

U87 MG (U87) were gifts from Dr. ShaoHua Yang (University of North Texas Health Science Center), while T98G cells were obtained from American Type Culture Collection (ATCC). Both were cultured as previously described 55. MB was purchased from Calbiochem. Sodium oleate, Pluronic F68, glucose oxidase/peroxidase solution, O-dianisidine dihydrochloride, and D-(+)-glucose were obtained from Sigma-Aldrich. PLGA 50:50 DLG 8E was purchased from Lakeshore Biomaterials. Pierce protein reagent was obtained from ThermoScientific, D-luciferin sodium salt from Regis Technologies, and QuantiLum recombinant luciferase from Promega.

2. Preparation of Methylene blue oleate salt

In pre-weighed 250 mL glass beaker containing a stir bar, 100 mg sodium oleate (SO) was dissolved in 100 mL distilled, deionized (DDI) H2O. 50 mg MB was added to 5 mL dehydrated ethanol and mixed, then combined with SO solution and allowed to stir overnight at room temperature in a fume hood to prepare the MBOS solution. The following day, 100 mL chloroform was added to the MBOS solution, stirred for 5 minutes, then placed at room temperature in a fume hood for at least 24 hours to obtain complete partitioning of the organic and aqueous layers. After achieving layer separation, the H2O layer containing free MB was removed, and the beaker containing the MBOS chloroform solution returned to stirrer under vacuum in fume hood for 72 hours until chloroform has completely evaporated and layer of

MBOS coating remained. To determine the final amount of mg of MBOS obtained, the beaker was removed from stirring and re-weighed.

3. Preparation and Characterization of MBOSNPs

3.1 Preparation of MBOSNPs - To generate MBOSNPs (Figure 1), 3 mg MBOS was combined in 1 mL acetone, placed on a mini vortexer until completely dissolved, then 10 mg PLGA added and returned to vortexer until PLGA was in solution. While MB and PLGA solution was vortexing, 1% PF68 in DDI H2O was prepared and 3 mL filtered through a 0.45 micron syringe filter. Once MB and PLGA solution was obtained, it was added to PF68 solution and placed under compressed nitrogen gas until acetone has evaporated and organic solvent odor no longer remained (~1 hour). Next, the NP sample was transferred to a 50 mL 10K cut-off Amicon tube, where ~10 mL DDI H2O was added, then centrifuged at 3500 rpm for 20 minutes at 4°C. Once the flow through was discarded, centrifuge/wash step was repeated 2x more for 20 minutes, then 30 minutes. Once washes were concluded, 5% sucrose in DDI H2O was added to NP sample to obtain 1 mL total volume. The liquid MBOSNPs were transferred to a pre-weighed cryovial, placed at -80°C overnight, then moved to a cooled, pressurized lyophilizer (ATR, Inc.) for 72 hours. Upon removal from lyophilizer, sample was stored at -20°C until needed. Empty, blank NPs were also generated, analyzed, and tested in subsequent in vitro assays for comparison at the highest "treatment" concentration for drug-loaded NPs.

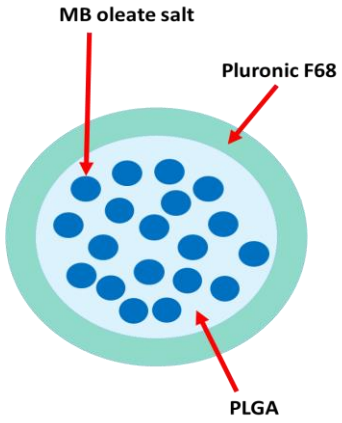

Figure 1 – Schematic representation of MBOSNPs. MBOS, produced by chloroform extraction to reduce water solubility and release, was encapsulated within the co-polymer PLGA via solvent displacement, and subsequently coated with the surfactant Pluronic F68 and lyophilized. Abbreviations: MBOSNPs, methylene blue oleate salt-loaded nanoparticles; MBOS, methylene blue oleate salt; PLGA, poly(D,L-lactide-co-glycolide).

3.2 Physico-chemical Characterization of MB(OS)NPs - Prior to freezing and lyophilizing, as well as post, particle size and zeta potential were analyzed via a Malvern Zetasizer Nano ZS. Briefly, a small amount of lyophilized NPs was resuspended in 1 mL DDI H_2O, vortexed for 30 seconds, then transferred to a disposable cuvette (Sarstedt) for analysis of particle size (in nm) by dynamic light scattering. The sample was then transferred to a disposable capillary cell (Malvern) for analysis of zeta potential. For each NP batch, the mean diameter ± S.D. for three measurements was determined. The polydispersity index (PDI) was also quantified to establish particle size distribution.

3.3 Drug Loading and Encapsulation Efficiency Determination by UV/Vis Spectrophotometry - Drug loading and encapsulation efficiencies were determined post-production by mixing 5 mg lyophilized MBOSNPs in 1mL acetone, placing in a 37°C incubator shaker for 4 hours, then

centrifuging at 14,000 rpm at room temperature for 5 minutes to precipitate residual PLGA. The acetone component containing MBOS was then analyzed via the UV/Vis spectrophotometry component of a Nanodrop (ThermoScientific) at 645nm, with values compared to an MBOS standard curve.

3.4 Transmission Electron Microscopy (TEM) - Following acquisition of the lyophilized final product, MBOSNPs were also analyzed for shape and surface morphology via TEM. Briefly, a small amount of NP was resuspended in 1 mL DDI H_2O, then diluted 1:10. A drop (~5 µL) of diluted, resuspended MBOSNP sample was deposited on a discharged carbon grid, allowed to dry for 1 minute, carefully blotted, and a drop of 2% uranyl acetate added with a 1-minute dry time and subsequent blotting. Once negatively stained, the NP sample was on examined under a Tecani Spirit Biotwin at the University of Texas Southwestern Medical Center's Electron Microscopy Core Facility.

3.5 MBOS Release Kinetics – To determine the rate of MBOS release from the NPs, MBOSNPs containing at least 0.5 mg MBOS (~30mg) was weighed out and added to 2 mL 1X PBS in 8 MWCO dialysis tubing. The dialysis tubing containing sample was then placed in a 250 mL glass beaker containing 100 mL 1X PBS as a "sink" under constant stirring at room temperature. At designated time points, 1 mL of 1X PBS from the "sink" was collected, replaced with fresh PBS, and analyzed at 645nm via the UV/Vis spectrophotometry component of a Nanodrop (ThermoScientific), with values compared to an MBOS standard curve.

4. <u>In Vitro Analyses</u>

4.1 Cellular Bioenergetics Analysis – Assay was performed according to manufacturer's directions and as previously described [370], where U87 and T98G cells were plated at 30,000 cells/well in an XF24 plate and allowed to attach overnight. Media was replaced an hour before

onset of the assay with XF24 media, and then, rotenone/antimycin A mix, FCCP, and oligomycin were diluted in XF24 media and loaded into the provided cartridge to obtain final concentrations of 100 nM, 300 nM, and 1 µg/mL, respectively. MB, MBOS, or MBOSNP treatments, at pre-determined concentration, were also inserted into the cartridge. Addition of the compounds into the medium took place at designated time points, and oxygen consumption was examined using a Seahorse Bioscience XF24 Extracellular Flux Analyzer.

4.2 Liquid Colony Formation Assay – Cells were seeded into 6-well culture plates (Falcon) at a concentration of 50 cells/well in 1 mL DMEM high glucose with pyruvate (Gibco), 10% FBS, and 1% Pen/Strep. Treatments were added to each well to obtain a pre-determined final concentration in 2 mL/well total volume. Plates were incubated for 4 weeks undisturbed, and only carefully received a media change at week 3 with or without drug treatments if colonies were not visible. Following completion of the 4-week incubation period, colonies were stained as previously described [370]. Culture plates were placed on ice and gently washed twice with ice-cold PBS; next, colonies were fixed with ice-cold methanol for 10 minutes, which was removed to allow for staining; plates were then relocated to the bench-top, where the colonies were stained with 0.5% crystal violet in 25% methanol for 10 minutes, which was removed; finally, plates were washed by immersion in cold, running tap water until the water ran clear and placed upside down on absorbent paper to allow overnight drying. Stained colonies were counted, with the number and size documented.

4.3 ATP Quantification – U87 and T98G cells were seeded into 6-well plates at 200,000 cells/well in 1 mL DMEM high glucose with pyruvate (10% FBS and 1% Pen/Strep) and allowed to grow overnight. The next day, media was replaced with MB, MBOS, or MBOSNPs at desired concentrations and analyzed at specified 24 hour increments. Following a modified

protocol outlined in an ATP kit obtained from Life Technologies, cells were washed twice with PBS, then lysed with 150 uL of ATP assay buffer (500 mM Tricine buffer, pH 7.8, 100 mM $MgSO_4$, 2 mM EDTA, and 2 mM sodium azide) containing 1% Triton X-100, dislodged by scraping with a pipette tip, and transferred to 1.5 mL Eppendorf tubes on ice for 5 minutes. 10 uL of cell lysate was then added in triplicate to a white 96-well plate, also containing ATP standards. Before reading the plate, 100 uL of ATP assay buffer containing 90 µg/mL D-luciferin, 20 µM DTT, and 25 µg/mL Luciferase) was added to each well. Luminescence was calculated using a Tecan Infinite F200 plate reader. Protein concentration was also determined using the Pierce 660 nm Protein Assay (660 nm absorbance), with ATP production standardized to protein values.

4.4 Glucose Quantification – Glucose was measured per instructions from a kit manufactured by Sigma-Aldrich. Briefly, 200,000 U87 and T98G cells were seeded into a 6-well plate and incubated overnight. On the subsequent day, media was removed and exchanged with 2 mL fresh DMEM high glucose (4.5 g/L glucose) contained pre-determined MB, MBOS, or MBOSNP concentrations. After designated times, medium was removed, diluted 1:100 in glucose assay buffer (glucose oxidase, horseradish peroxidase, and O-dianisidine), then added to a 96-well plate at a 1:3 dilution in glucose assay buffer. The plate was then incubated at 37°C and 5% CO_2 for 30 minutes, and the reactions halted by the addition of 66 uL of 12N sulfuric acid. Absorbance values were evaluated at 540 nm on a Biotek Synergy 2 plate reader.

4.5 Cell Viability – U87 and T98G cells were seeded at 750 cells/well in 100 µL DMEM high glucose with pyruvate (10% FBS and 1% Pen/Strep) in a black, 96-well flat-bottomed plate, and allowed to attached overnight. The following day, 50 µL media containing varying concentrations of MB, MBOS, or MBOSNP was added designated wells and incubated at 37°C

overnight. The next morning, the plates were washed with 200 µL/well 1X PBS, which was removed and replaced with 95 µL calcein AM reagent at 1:1000 dilution in 1X PBS. Plates were incubated at 37°C for 5-10 minutes, protected from light, and read via a Tecan Infinite F200 plate reader at 485/530 excitation/emission fluorescence.

5. In Vivo Bio-distribution

All animal studies were performed at the University of Texas Southwestern Medical Center's Preclinical Pharmacology Core, with practices following Institutional Animal Care and Use Committee and National Institute of Health guidelines. Female mice (CD-1 background, 5-6 weeks old) were used for all bio-distribution studies. Mice were administered a single intravenous (IV) dose of either MB (in 95% PBS/5% DI H_2O), MBOS (in 10% DMSO/10% Cremophor EL/80% PBS), or MBOSNP (in 100% PBS) via lateral tail vein at 8 mg/kg treatment concentration, and then euthanized by CO_2 inhalation at selected time points and blood sample obtained by cardiac puncture. Plasma was processed from whole blood by centrifugation of EDTA-treated blood for 10 minutes at 9,600 x g, then stored at -80°C until analyzed. In addition, kidneys, spleen, lung, liver, and brain were removed, weighed, flash frozen, then homogenized in a 3-fold volume of PBS for further analysis and stored at -80°C. For standard curve construction, 100 µL of blank plasma (Bioreclamation, LLC) or tissue homogenate was infused with 2 µL of varying concentrations of MB or MBOS, then processed as described below. Next, 100 µL of each sample (plasma or tissue homogenate) was crashed with 200µL methanol + 0.1% formic acid + 50 ng/mL (final concentration) n-benzyl benzamide internal standard, vortexed for 15 seconds, incubated at room temperature for 10 minutes, then centrifuged at 16,000 x g for 5 minutes at 4°C. 250 µL of supernatant was then transferred to an Eppendorf tube, centrifuged as previously described, then 195 µL of supernatant transferred to

an HPLC vial with insert for analysis by HPLC-MS/MS (AB Sciex 3200 QTrap). An Agilent C18 XDB column (50 x 4.6 mm, 5 micron packing) was used for chromatography with the following conditions: 0-1.5 minutes in 90% Buffer A (water + 0.1% formic acid), 1.5-2 minutes in 100% Buffer B (acetonitrile + 0.1% formic acid), 2-3.5 minutes in 100% Buffer B, and 3.6-4.5 minutes in 90% Buffer A. MB was detected with the mass spectrometer in MRM (multiple reaction monitoring) mode by following the precursor to fragment ion transitions: 284.1/268.0 (intact MB) and 270.0/254.0 (demethylated MB), while the internal n-benzyl benzamide was detected using a 212.1/91.1 transition. The limit of detection (LOD) was set at the standard concentration providing an analyte signal three-fold above blank matrix. The limit of quantification (LOQ) was set at the lowest standard concentration which upon back-calculation gave a measured concentration within 20% of nominal and which was above the LOD. Per UTSW's lab SOPs, samples falling below LOQ and above LOD are assigned a value of ½ LOQ. Samples falling below LOQ and LOD are assigned a value of 0. Tissue concentrations of MB were corrected by subtracting residual compound remaining in the vasculature. Reference values for tissue vasculature provided in Kwon, 2001 were used for this calculation [412]. Pharmacokinetic parameters for MB were calculated using the noncompartmental analysis tool in Phoenix WinNonlin.

6. Statistical Analysis

All data are given as the means ± S.E. The difference in significance among groups with one independent variable was determined by one-way ANOVA with Dunnett's multiple comparisons test for intended comparisons between groups when significance was identified. The difference in significance among groups where two independent variables occurred was established by two-way ANOVA with Dunnett's multiple comparisons test for arranged

comparisons between groups when significance was identified. For all tests, $p < 0.05$ was deemed significant.

Results and Discussion

Characterization of MBOSNPs

Following analysis of numerous batches of MBOSNPs, an average particle size of 166.95 ± 63.1 nm was determined. Based on data reported by other publications, the value of our nanoformulations was determined to be within an acceptable range compared to other MB- or MBOS-loaded nanoparticle formulations (Table 1) [381, 386, 413]. Additionally, the size distributions (PDI) associated with the formulations ranged from 0.287 to 0.387, allowing for consistent particle size within and among the batches. Due to the small size and relatively uniform distribution of the NP formulations, enhanced cellular uptake and rapid passage through the bloodstream to the target tissue is expected. Finally, the zeta potential of the drug-loaded nanoparticles exhibited values of approximately -32mV (Table 1). Nanoparticles exhibiting surface charge values between -1 and -45 mV have been shown to increase the likelihood of BBB permeation, as well as enhance their stability [304]. These values were also determined for empty, blank nanoparticles and deemed comparable to the drug-loaded formulation (at -38.33 ± 11.66 mV) (Table 1). Simultaneously, the average drug loading and encapsulation efficiencies for MBOSNPs were also determined to be ~2% and 29% (Table 1), respectively. These values were also found to be comparable to previously published nanoformulations containing MB or MBOS [381, 386, 413].

Table 1 – Physico-chemical characteristics of methylene blue oleate salt-loaded polymeric nanoparticles (MBOSNPs) compared to blank, non-drug-loaded polymeric nanoparticles (BNPs)

Nanoparticle Type	Average Particle Size	Average Polydispersity Index (PDI)	Average Zeta Potential	Average Drug Loading	Average Encapsulation Efficiency
MBOSNPs	166.95 ± 63.1nm	0.287 ± 0.1	-32.12 ± 4.98mV	2.21 ± 0.74%	29.16 ± 7.47%
BNPs	132.25 ± 17.99nm	0.186 ± 0.06	-38.33 ± 11.66mV	N/A	N/A

Six batches of MBOSNPs and BNPS were analyzed for the aforementioned characteristics, then their values averaged. Figures denote mean ± SD. Particle size, PDI, and zeta potential were ascertained from NP samples evaluated in triplicate using a ZetaSizer Nano ZS (Malvern). Drug loading and encapsulation efficiency values for MBOSNPs were determined utilizing MBOS dissolved in acetone for standard curve comparison via UV/Vis spectrophotometry component of Nanodrop (ThermoScientific) at 645nm.

In addition to the aforementioned physico-chemical characterizations of MBOSNPs and BNPs, the size and surface morphology were evaluated by TEM, as illustrated in Figure 2, with a subsequent release kinetic profile obtained, as shown in Figure 3. From TEM analysis, we were able to obtain a graphical representation of the overall, and expected, spherical morphology of the blank and drug-loaded NPs, as well as confirm the size and size distribution data acquired from the previously performed physico-chemical analysis. Following formulation and preliminary characterization of MBOSNPs, release kinetic studies were also performed in order to determine the peak release, as well as overall release profile. Several batches of drug-loaded NPs with similar physico-chemical characteristics were analyzed to obtain uniform data. After analysis concluded at 14 days, the peak drug release was found to occur at 24 hours, with a gradual reduction in release over time (Figure 3).

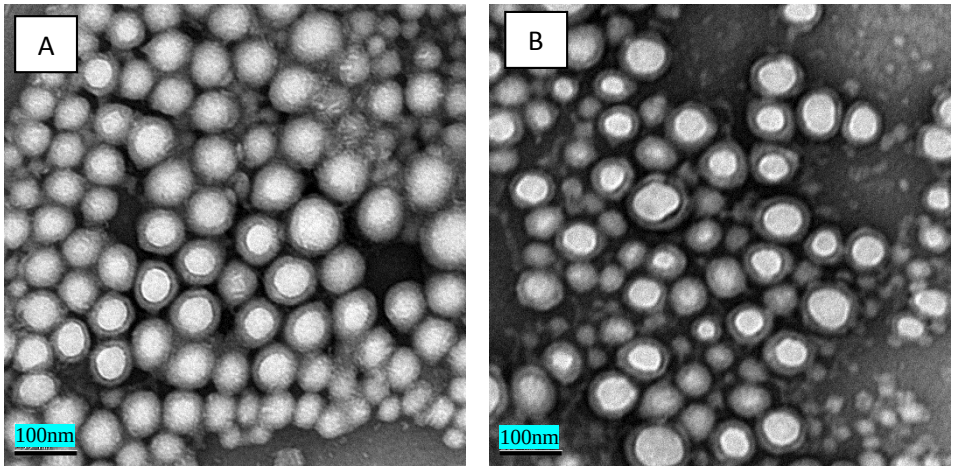

Figure 2 – TEM images of Blank NPs (A) and MBOSNPs (B). Lyophilized NPs were resuspended in DDI H_2O, then further diluted 1:10 in DDI H_2O and processed by negative staining for analysis. Both sets of NPs display a spherical shape with a dark, outer ring depicting the Pluronic F68 layer and lighter, inner core of PLGA. Scale bar set to 100 nm.

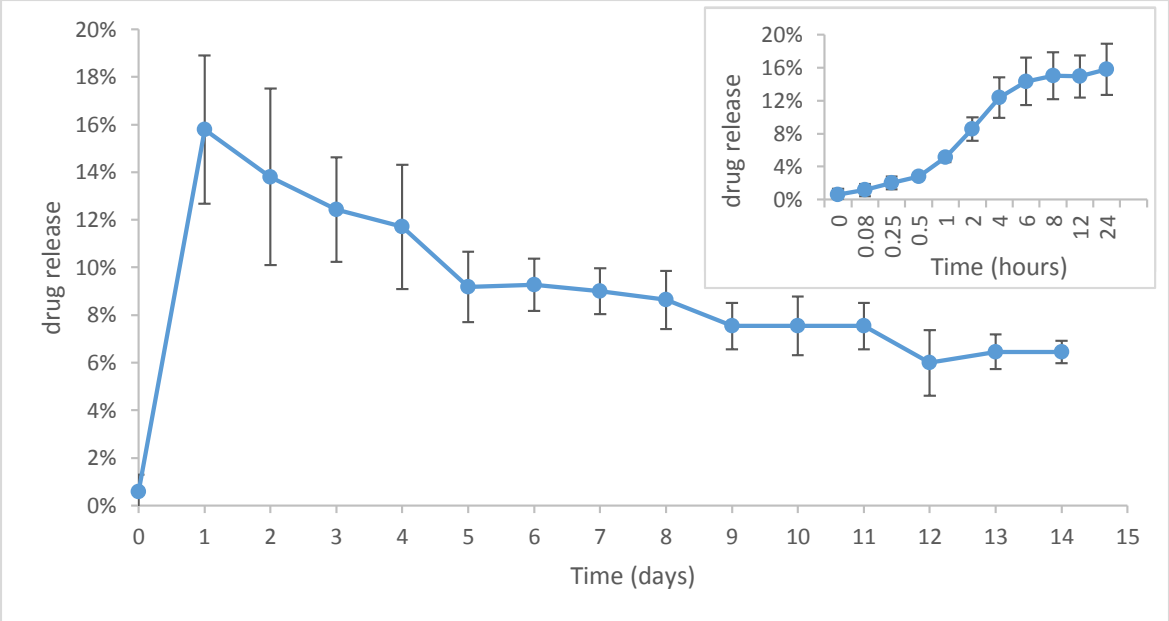

Figure 3 – Cumulative Release Kinetic Profile of MBOS from MBOSNPs. Following addition of drug-loaded NPs to PBS in 8MWCO dialysis tubing, PBS from "sink" was collected at the designated time points at 28°C under constant stirring. Peak release occurred at 24hrs (~16%) and gradually decreased until final sample collection at 14 days. Decrease in MBOS release possibly

due to conversion of MBOS to MB, then LMB due to exposure to light, resulting in variability in quantified concentration by UV/Vis spectrophotometry. Inset graph illustrates % MBOS release values between 0 and 24 hours. N = 3.

MB(OS)NPs Impair Cellular Metabolism in U87 and T98G Cells

We assessed the effects of MB, MBOS, and MBOSNPs on metabolic processes and their by-products at concentrations between 100 nM and 10 µM in U87 and T98G cells. In U87 cells treated with 10 µM MB or MBOSNP, there was a significant increase in oxygen consumption rates (OCR) (Figure 4, B and C), which was not seen with the lower treatment concentration (Figure 4, A and C). However, with T98G cells, the increase in OCR following 10 µM MB and MBOSNP treatments was more pronounced at 1.6-fold (Figure 4, E and F), with an additional noted increase with both 1 µM treatments (Figure 4, D and F).

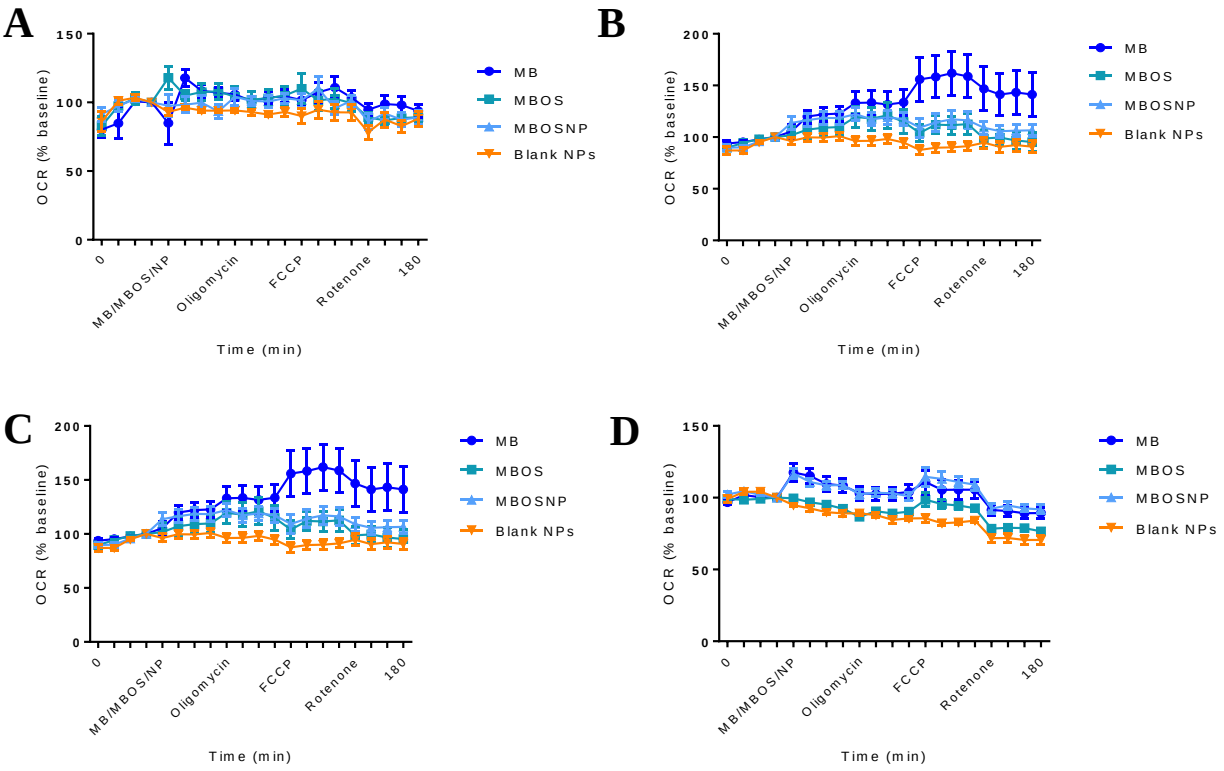

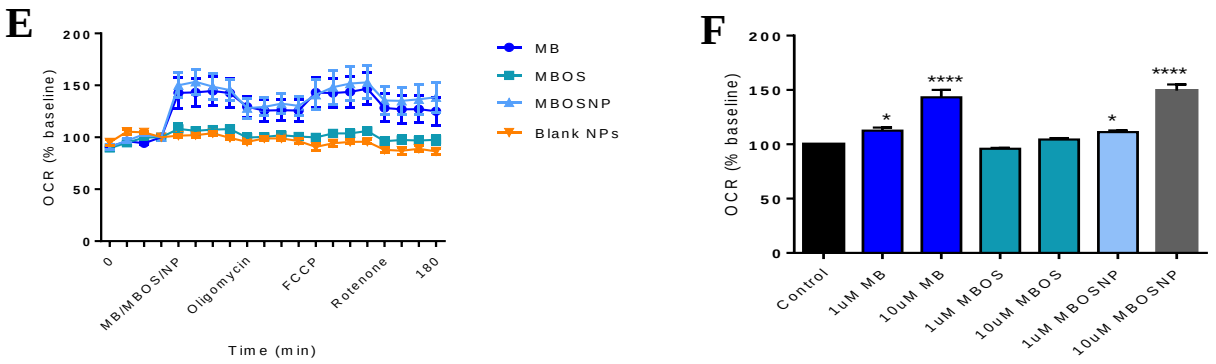

Figure 4 – MBOSNPs increase OCR in U87 and T98G cells. A and B, OCR of U87 cells following 1 and 10 µM treatments, including BNPs, respectively. C, MB and MB(OS)NPs significantly increased U87 cell OCR at 10 µM. D and E, OCR of T98G cells following 1 and 10 µM treatments, including BNPs, respectively. F, MB and MBOSNPs significantly increased T98G cell OCR at 1 and 10 µM. N = 3. * indicates $p < 0.05$ and **** indicates $p \leq 0.0001$ by 1-way ANOVA and Dunnett's multiple comparisons test.

To determine the long-term effects of MBOSNPs on cellular bioenergetics, we treated U87 and T98G cells with 10 µM MB, MBOS, and MBOSNPs for 24, 48, or 72 hours and then measured ATP production (24 or 48 hours) and glucose utilization (24, 48, or 72 hours). ATP levels were increased in 24 hours in both cell lines with 10 µM MBOSNP, and 10 µM MB in U87 cells compared to control (Figure 5, A and B). However, an increase in ATP production was not observed by 48 hours, possibly due to a reduction in cell viability and/or number. When quantifying sample glucose based on the original media glucose concentration (4.5 g/L), all 10 µM treatments resulted in significant increases at 48 hours compared to untreated cells in U87 cells (Figure 5, C through E), but only in 10 µM MB at 48 and 72 hours in T98G cells (Figure 5, F through H). Cell fitness and number may also be implicated in the lack of significant glucose utilization after 48 hours in all 10 µM treatments, regardless of cell line.

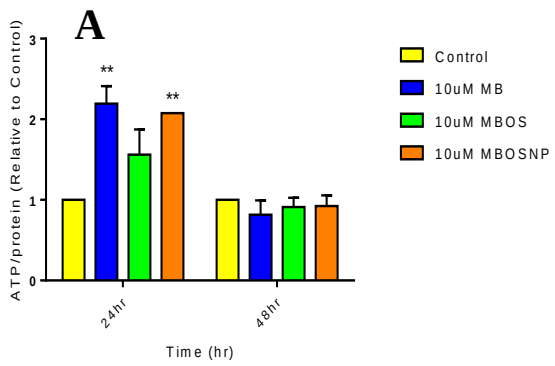
A
ATP/protein (Relative to Control)
Control
10uM MB
10uM MBOS
10uM MBOSNP
24hr
48hr
Time (hr)

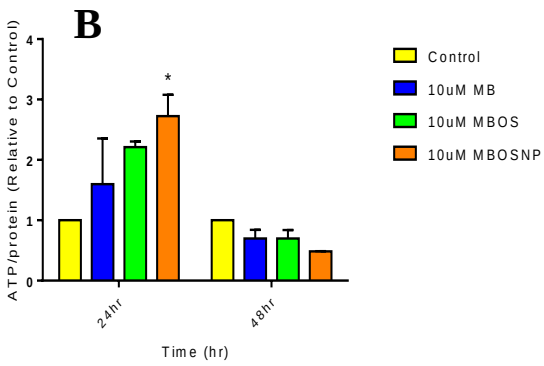
B
ATP/protein (Relative to Control)
Control
10uM MB
10uM MBOS
10uM MBOSNP
24hr
48hr
Time (hr)

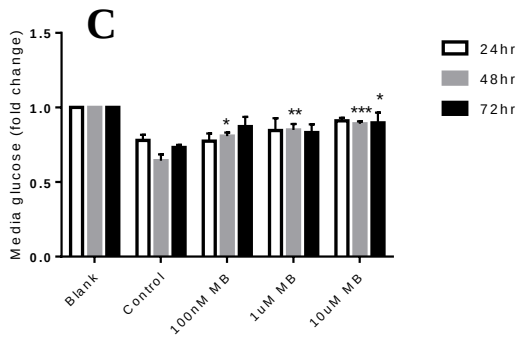
C
Media glucose (fold change)
24hr
48hr
72hr
Blank
Control
100nM MB
1uM MB
10uM MB

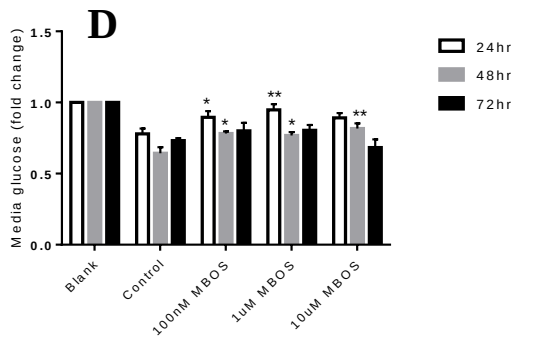
D
Media glucose (fold change)
24hr
48hr
72hr
Blank
Control
100nM MBOS
1uM MBOS
10uM MBOS

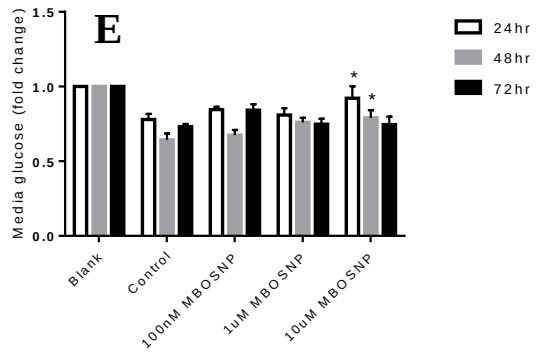
E
Media glucose (fold change)
24hr
48hr
72hr
Blank
Control
100nM MBOSNP
1uM MBOSNP
10uM MBOSNP

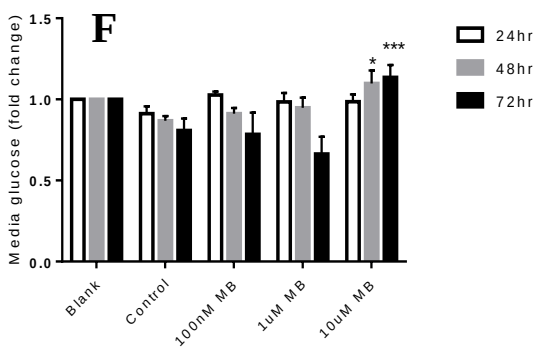
F
Media glucose (fold change)
24hr
48hr
72hr
Blank
Control
100nM MB
1uM MB
10uM MB

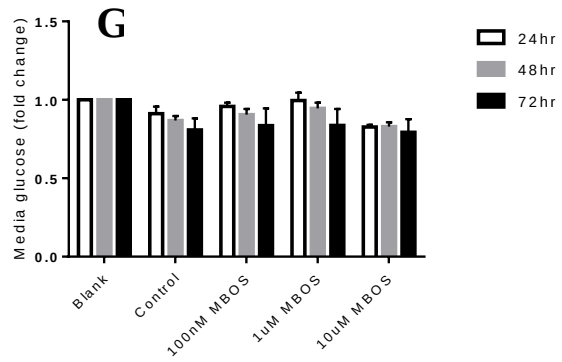
G
Media glucose (fold change)
24hr
48hr
72hr
Blank
Control
100nM MBOS
1uM MBOS
10uM MBOS

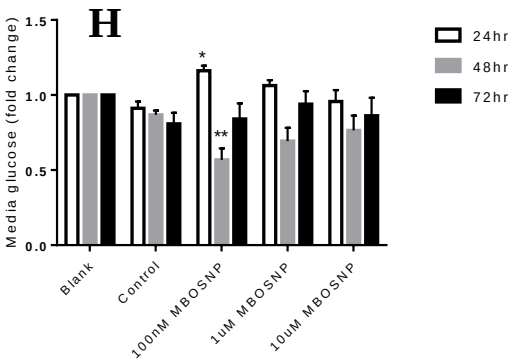
H
Media glucose (fold change)
24hr
48hr
72hr
Blank
Control
100nM MBOSNP
1uM MBOSNP
10uM MBOSNP

Figure 5 – MBOSNPs alter cellular bioenergetics. A, MB and MBOSNPs increased ATP production at 24 hrs in U87 cells. B, MBOSNPs increased ATP production at 24 hrs in T98G cells. C-E, Effects of varying concentrations of MB, MBOS, and MBOSNPs on glucose quantification in U87 cells at 24, 48, and 72 hrs. F-H, Effects of varying concentrations of MB, MBOS, and MBOSNPs on glucose quantification in T98G cells at 24, 48, and 72 hrs. N = 4. * indicates $p < 0.05$, ** indicates $p \leq 0.01$, *** indicates $p \leq 0.001$ by 2-way ANOVA and Dunnett's multiple comparisons test.

MBOSNPs Inhibit In vitro Tumor Growth

To elucidate how changes in GBM metabolism and bioenergetics following MBOSNP treatment influenced tumor growth, we assessed cell viability and anchorage-dependent colony formation in U87 and T98G cells. Based on preliminary studies (unpublished), neither cell line exhibited a significant reduction in cell viability until 96 hours when analyzing a concentration range from 100 nM to 100 µM of MB, MBOS, and MBOSNPs (Figure 6, A and B). Once the IC_{50} dose range was narrowed down to between 10 and 100 µM, an extended time course was performed. In T98G cells treated with 10 µM MB or MBOSNPs for 24 and 72 hours, there was an initial reduction in cell viability by 25% that stayed consistent through 144 hours with MB(OS)NP treatment, but increased by an additional ~50% following MB treatment (Figure 6, F and H). However, with the same treatment concentration for MBOS, there was no significant reduction in T98G cell viability until 144 hours (Figure 6G). With U87 cells, 10 µM MB did not induce cell death until 72 and 144 hours, with an increase in cell viability following a 24-hour treatment (Figure 6C). According to previously published data, low concentrations of MB have been shown to enhance cell viability by augmenting mitochondrial function[211], which could explain this observation. A similar trend in cell viability following MB treatment was also noted

with MBOS treatments, with a reduction in cell survival not seen until 144 hours (Figure 6D). However, in U87 cells treated with even the lowest concentration of MBOSNPs (10 µM), a significant reduction in cell viability was detected at all three time points (Figure 6E). In both cell lines, the IC_{50} for MBOSNP treatment was determined to be 10 µM, which was observed to induce similar, if not better, reduction in cell viability when compared to free MB, but especially free MBOS.

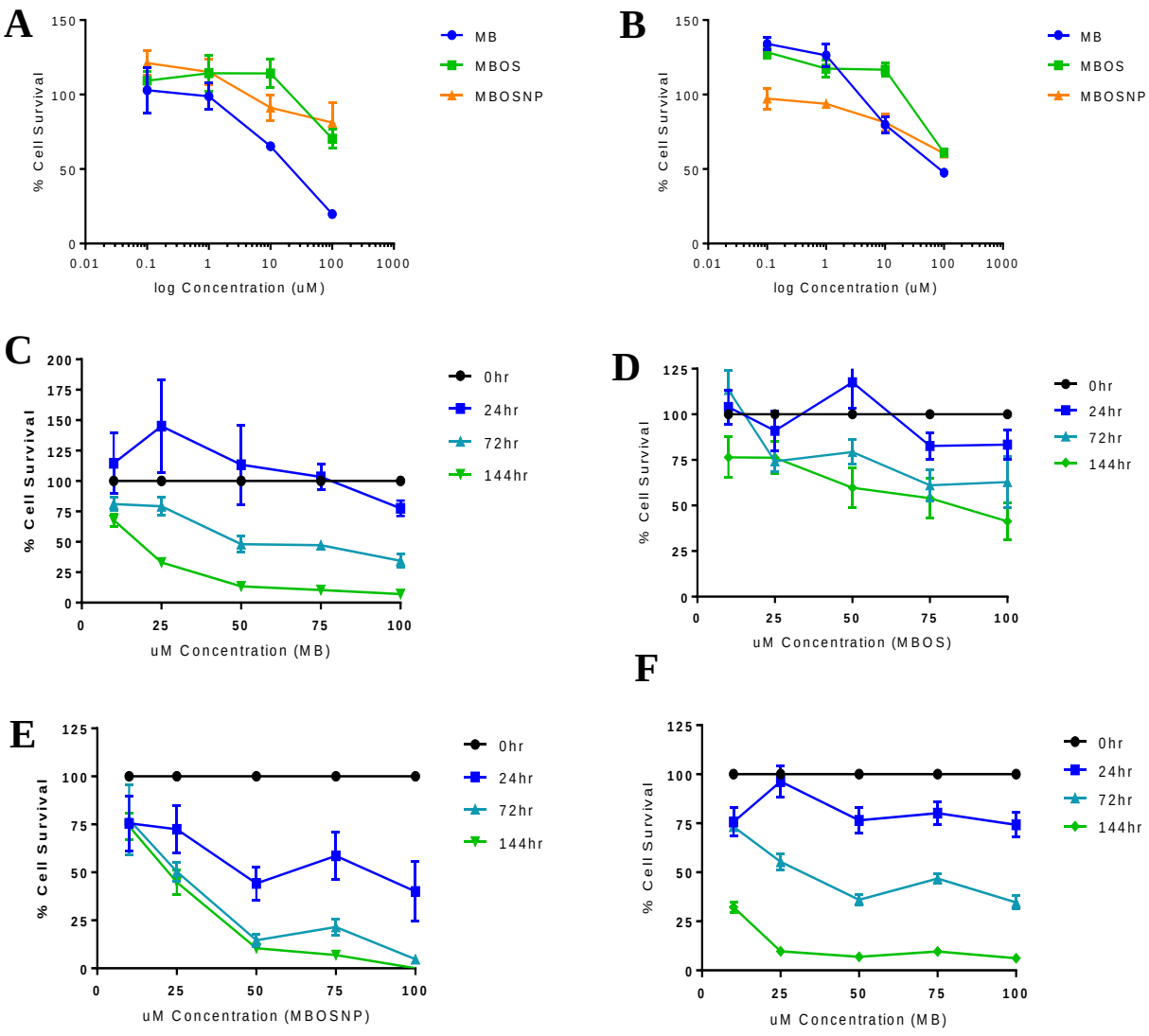

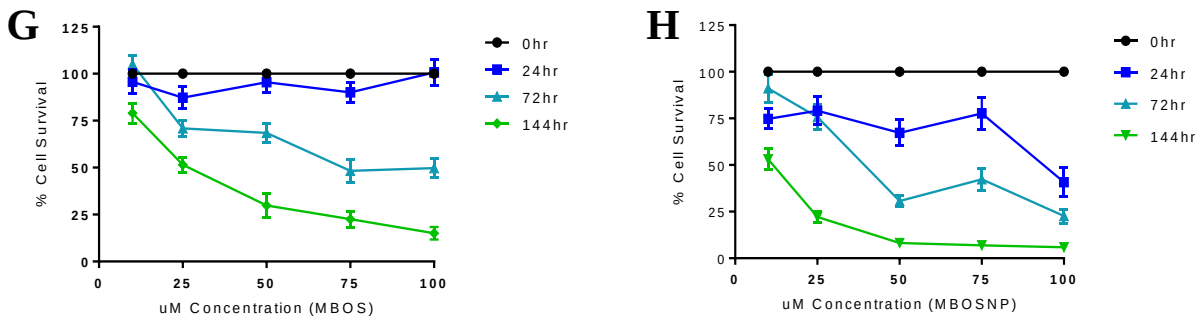

Figure 6 – MBOSNPs inhibit U87 and T98G cell survival. A and B, Cell survival analysis at 96 hrs post treatment in U87 and T98G cells, respectively. C-E, U87 cell survival following varying MB/MBOS/MBOSNP treatment concentrations at 24, 72, and 144 hrs. C, Reduction in viability not noted at lowest concentration (10 µM) until 72 hrs. D, U87 cell viability reduced at lowest concentration at 144 hrs. E, U87 cell viability reduced at lowest concentration beginning at 24 hrs. F-H, T98G cell survival following varying MB/MBOS/MBOSNP treatment concentrations at 24, 72, and 144 hrs. F, T98G viability reduced at lowest concentration beginning at 24 hrs, with drastic reduction at 144 hrs. G, T98G viability not noted until 144 hrs. H, T98G cell viability reduced following lowest treatment concentration starting at 24 hrs, with drastic reduction at 144 hrs. Based on these data, the IC_{50} for MBOSNP was 10 µM. Additionally, MBOSNP treatment seemed to demonstrate a comparable, if not more effective, reduction in cell viability to free MB. N = 3. Abbreviations: MBOSNPs, methylene blue oleate salt-loaded polymeric nanoparticles; MB, methylene blue; MBOS, methylene blue oleate salt.

In addition to cell viability analysis, U87 and T98G cells were treated as previously described to determine the effects of MBOSNPs on cell proliferation. Following a 4-week liquid colony formation assay and subsequent examination of the average size and number of colonies, MBOSNP treatment was shown to be as effective as free MB, and more effective than free MBOS, at inhibiting cell proliferation in U87 and T98G cells at identical treatment

concentrations (Figures 7 and 8, respectively). In both cell lines, the colonies obtained following 10 µM MB and MBOSNP treatments were on average fewer and smaller than their untreated, control cell counterparts (Figures 7 and 8). For U87 cells, both colony size and number were significantly reduced following 10 µM MBOSNP treatment (Figure 7, E and F), while only size was reduced to a comparable level by the same MB concentration (Figure 7A). In U87 cells treated with MBOS, little to no difference in colony size and number of colonies was produced regardless of treatment concentration compared to untreated U87 cells (Figure 7, C and D). In T98G cells, all treatments produced similar outcomes as occurred with U87 cells, such that 10 µM MB significantly reduced the average size and number of T98G colonies (Figure 8, A and B), while the same concentration of MBOSNP only significantly impacting average size, but not colony number (Figure 8, E and F). However, 10 µM MBOS did induce a change in average T98G colony size, but in the inverse direction (Figure 8C), which was also seen but with the lowest concentration in U87 cells. Supplemental Figures 1 and 2 further illustrate the difference in average colony size and number of colonies for each treatment and concentration. Based on these statistical and graphical data, MBOSNP treatment demonstrated an ability to not only inhibit GBM cell viability, but also proliferation.

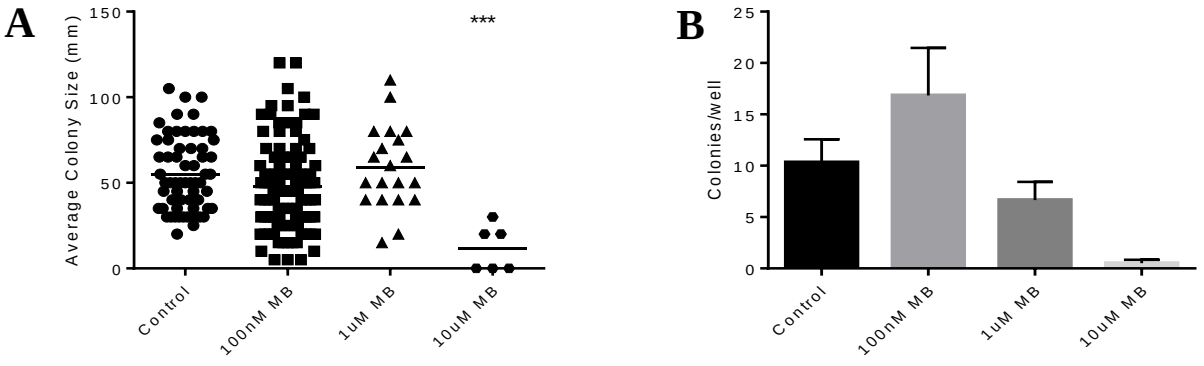

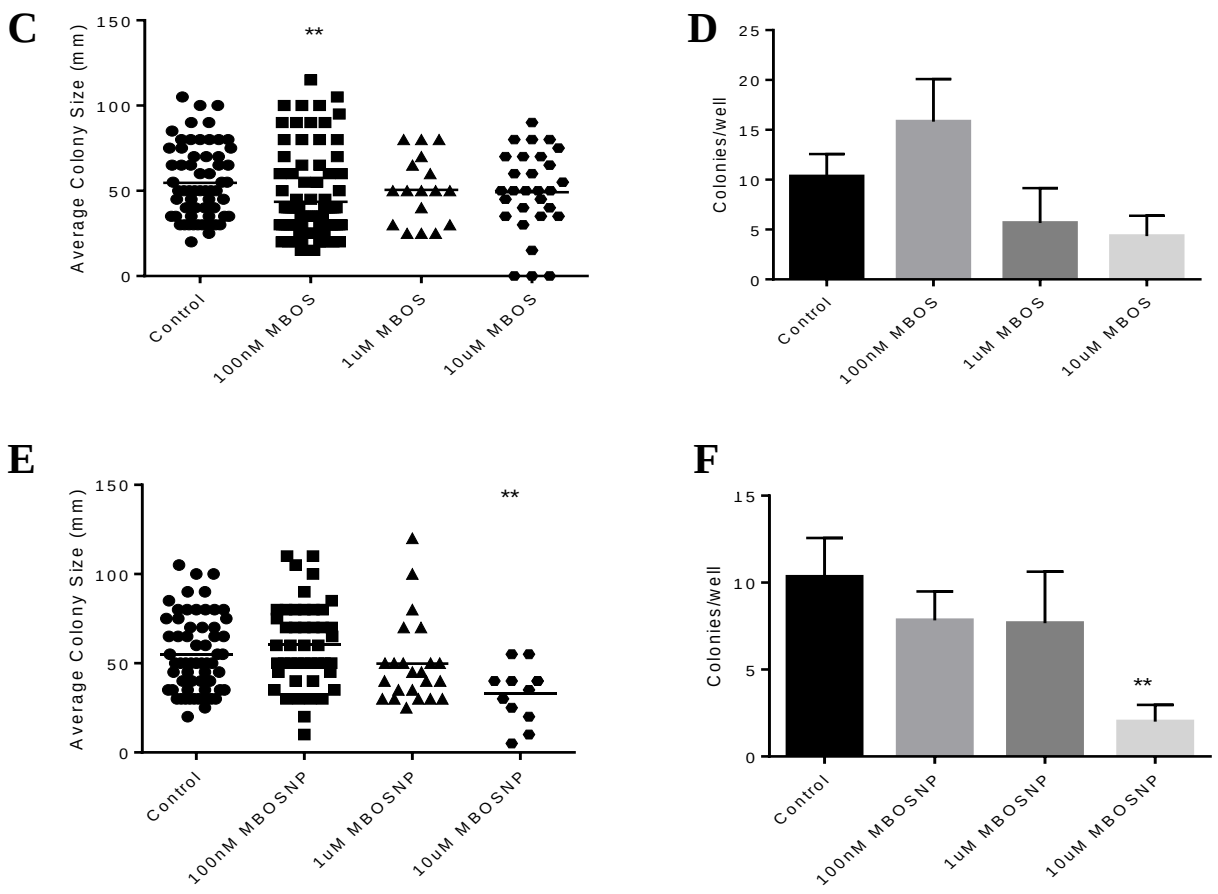

Figure 7 – MBOSNP treatment inhibits U87 cell proliferation. A, 10 μM MB treatment significantly reduced average colony size compared to control. B, 10 μM MB treatment reduced average number of U87 colonies. C, 100 nM, but not 1 or 10 μM MBOS, treatment significantly reduced average colony size compared to control. D, MB treatment all concentrations had no effect on average number of U87 colonies. E, 10 μM MBOSNP treatment significantly reduced average colony size compared to control. F, 10 μM MBOSNP treatment reduced average number of U87 colonies. N = 3. ** indicates $p \leq 0.01$, *** indicates $p \leq 0.001$ by 1-way ANOVA and Dunnett's multiple comparisons test.

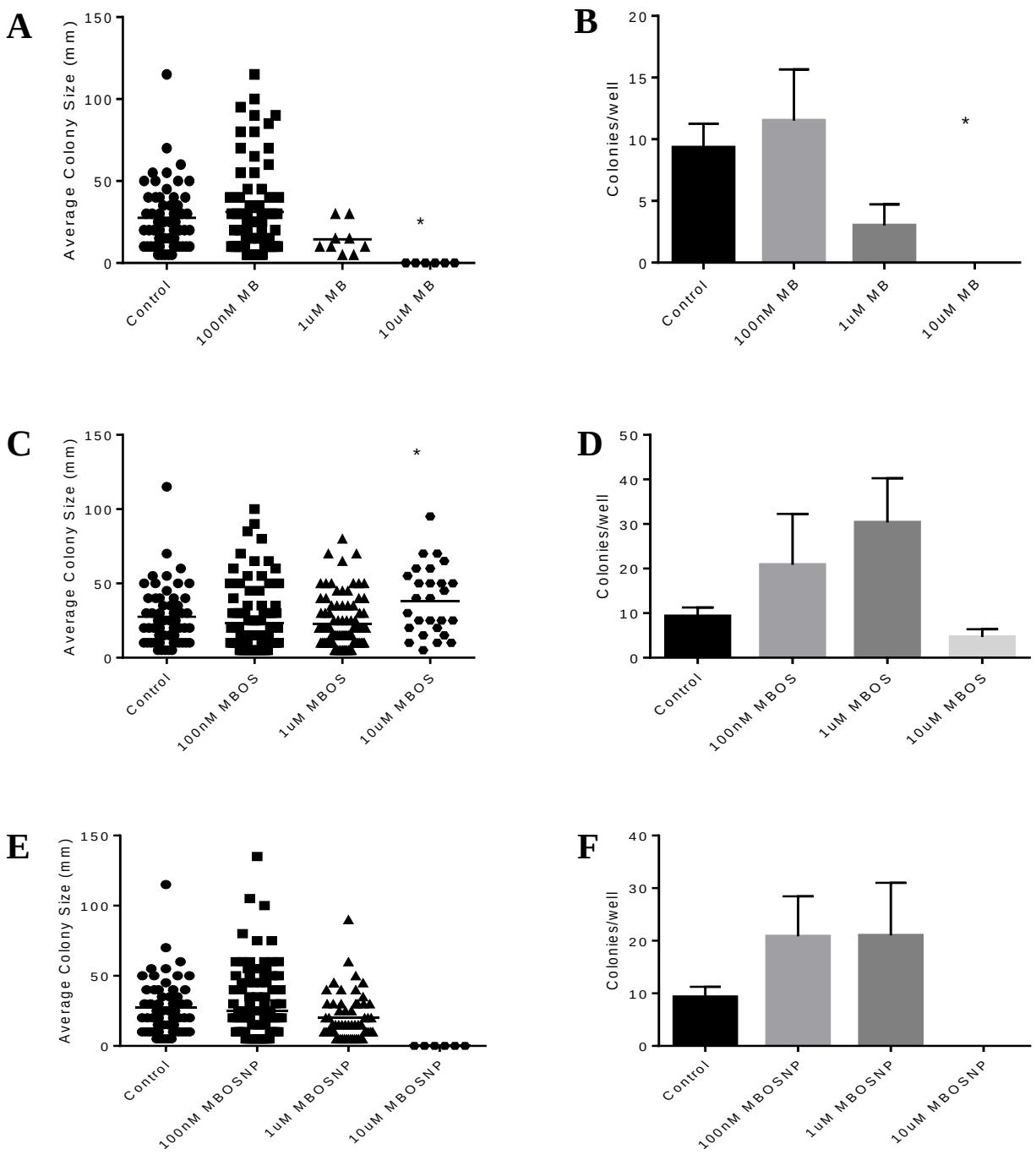

Figure 8 – MBOSNP treatment inhibits T98G cell proliferation. A, 10 µM MB treatment significantly reduced average colony size compared to control. B, 10 µM MB treatment significantly reduced average number of T98G colonies. C, 10 µM MBOS treatment significantly increased average colony size compared to control. D, MB treatment all concentrations had no

effect on average number of T98G colonies. E, 10 μM MBOSNP treatment significantly reduced average colony size compared to control. F, 10 μM MBOSNP treatment reduced average number of T98G colonies. N = 3. * indicates $p < 0.05$, ** indicates $p \leq 0.01$ by 1-way ANOVA and Dunnett's multiple comparisons test.

Bio-distribution of MBOSNPs

We further determined the biodistribution of our nanoformulations. Following an initial analysis of MB and MBOS by LC-MS/MS, we found that both compounds produced chemical peaks at 284 and 270, but with inverted component ratios (i.e. MB had a 20:1 ratio of 284:270 mw species, while MBOS had a 15:1 ratio of 270:284 mw species). Through further evaluation, it was determined that the 284 mw species was intact MB, while the 270 mw species was demethylated at some position on MB. While the difference in species ratios in MB and MBOS did not appear to result in functional inactivity *in vitro*, a similar assumption was reached in regards to *in vivo* effects.

Following treatment administration and tissue collection, free MB exhibited the highest drug concentrations across the designated time points, regardless of tissue type (Figure 9 and Table 2). However, due to the aforementioned issue involving the differences in mw species ratios for MB and MBOS, it was determined that the best comparison would be between concentrations of free MBOS and MBOSNPs recovered from the plasma and tissues. Upon doing so, it was determined that overall, MBOS exhibited better tissue accumulation following administration compared to MBOSNPs containing the same MBOS concentration (Figure 9 and Table 2). However, using the drug concentration values obtained (area under the curve – AUC), it was established that MBOSNPs were more effective at crossing the BBB than free MBOS by 1.6-fold (Table 2), due to the presence of the PF68 coating. As a result, this provides for a

potential application for the drug-loaded NPs as a GBM therapy upon further formulation optimization and scale up.

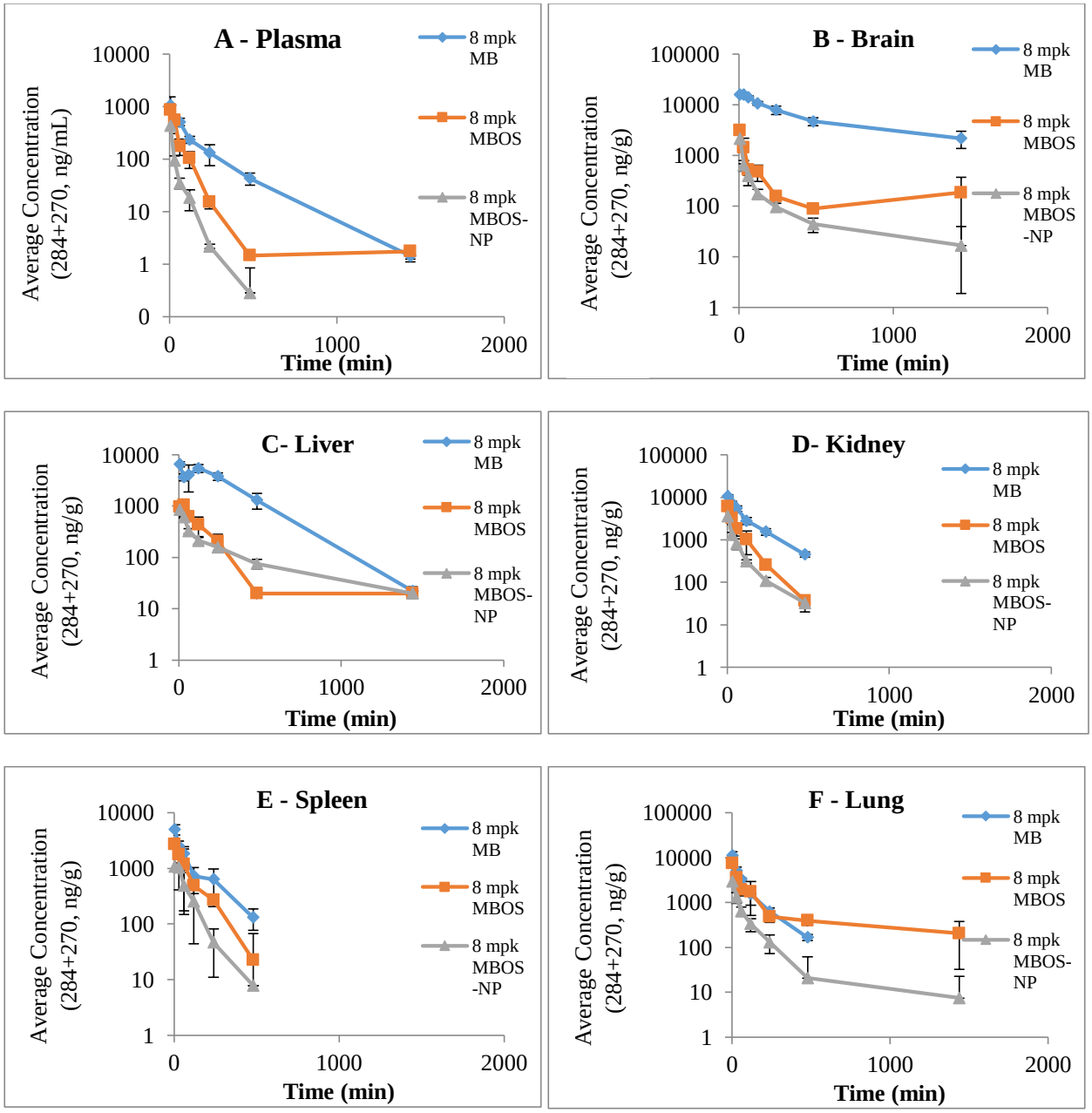

Figure 9 – Bio-distribution of MB, MBOS, and MBOSNPs at 8 mg/kg (8mpk) drug concentration. Following administration of each treatment, blood and tissues were collected from CD-1 mice and analyzed by LC-MS/MS for 284 and 270 mw species (intact versus demethylated MB) at designated time points. The ng/mL or g drug concentrations per plasma volume or tissue

weight, respectively, was obtained and plotted according to WinNonlin Noncompartmental PK parameters. In all samples, free MB had the highest concentration, followed by free MBOS, then MBOSNPs.

Table 2 – PK study values for area under the curve (AUC) in min*ng/mL for plasma or min*ng/g for tissues.

Tissue	MB	MBOS	MB(OS)NP
Plasma	127,828 ± 7,507	52,659 ± 3,247	14,358 ± 1,109
Brain	7,626,056 ± 340,435	333,423 ± 46,799	142,258 ± 8,764
Liver	2,391,840 ± 162,972	172,265 ± 12,683	149,236 ± 5,744
Kidney	1,230,440 ± 40,621	423,681 ± 36,095	189,473 ± 6,653
Spleen	500,163 ± 41,386	244,660 ± 25,905	101,203 ± 15,207
Lung	765,373 ± 39,324	939,911 ± 76,188	187,453 ± 16,075

In all samples, free MB had the highest drug concentration present, followed by free MBOS, then MB(OS)NPs. Due to mw ratio differences, even without MB consideration included, MBOS was still higher than MB(OS)NPs in all tissues. However, when examining the most effective therapy for passage across the BBB (Brain AUC/Plasma AUC), MB(OS)NPs were superior to free MBOS due to its PF68 surfactant coating.

Conclusions

Due to the aggressive nature of GBM that results in sub-standard survival rates beyond two years, development of new therapies is required in order to more effectively treat the disease. While a cure for GBM is unlikely in the near future, advancements toward better identifying genes responsible for its growth and progression are possible. As a result, the

utilization of formerly rejected compounds could be beneficial in treating GBM, if proper delivery systems are employed.

In this study, we were able to repurpose the photosensitizer methylene blue as a potential GBM chemotherapeutic, by encapsulating it within nanoparticles composed of the synthetic co-polymer, PLGA. These NPs, which were formulated through solvent displacement, were coated with PF68 to enhance BBB passage, and then analyzed by DLS for particle size, size distribution (PDI), and zeta potential (surface charge). Additionally, particle size and surface morphology were analyzed by TEM, with drug loading and encapsulation efficiency performed by UV-Vis at 645nm. The resultant drug-loaded PLGA NPs obtained were below size restrictions for passage across the BBB (<200nm), which was confirmed by their enhanced ability to permeate the BBB compared to free MBOS and accumulate in the brain tissue, even at lower concentrations than free MBOS. Furthermore, MBOSNPs induced comparable, if not better, levels of cell death and inhibition of cell proliferation to free MB and MBOS, while inducing similar or greater degrees of cellular and metabolic changes in U87 and T98G cells *in vitro*, demonstrating their potential application as a treatment for GBM.

However, due to the variability in mw species ratios between MB and MBOS/MBOSNPs, a definitive comparison of their accumulations was not possible. Thus, this precluded an accurate determination of the effectiveness of MBOSNPs compared to free drug *in vivo*. With that said, we were able to determine that MBOSNPs were more efficient at permeating the BBB than free MBOS, establishing their potential application as a neurotherapeutic for GBM. However, toxicological studies on free MBOS (and MBOSNPs) are imperative, as there is currently no data available on how the compound might affect animals, and ultimately humans, upon administration. Nevertheless, a forthcoming xenograft mouse

model study is necessary to fully elucidate if the outcomes demonstrated in cultured cells could be translated into a tumor-bearing animal.

Supplemental Data

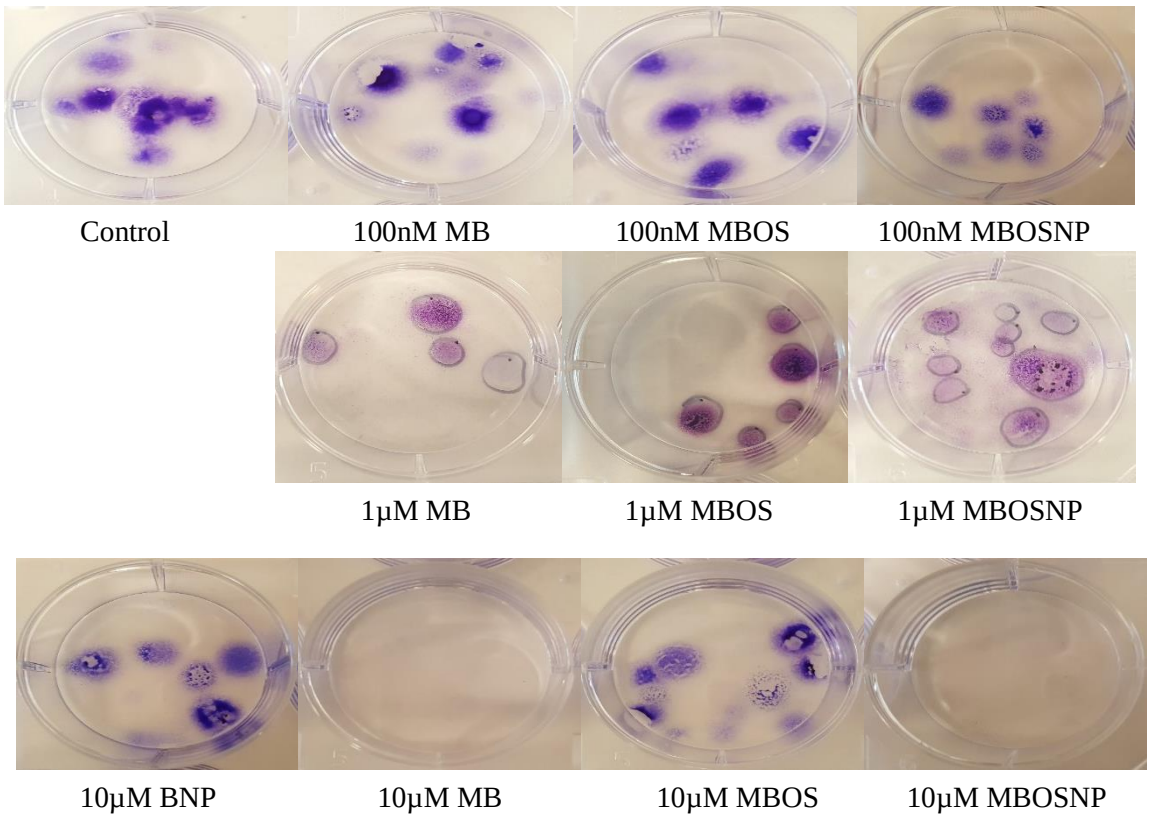

Supplemental Figure 1 – Effects of MBOSNPs on U87 cell proliferation. As treatment concentrations increased, average colony size and number of colonies decreased. At 10 µM MB and MBOSNP, little to no cells were detectable by visual examination, and those that were present were significantly smaller than untreated U87 cells. All MBOS treatment concentrations had similar sized colonies, as well as number of colonies. MBOSNP treatments compared to BNP-treated U87 cells to establish effect of PLGA, with no visible effect identified.

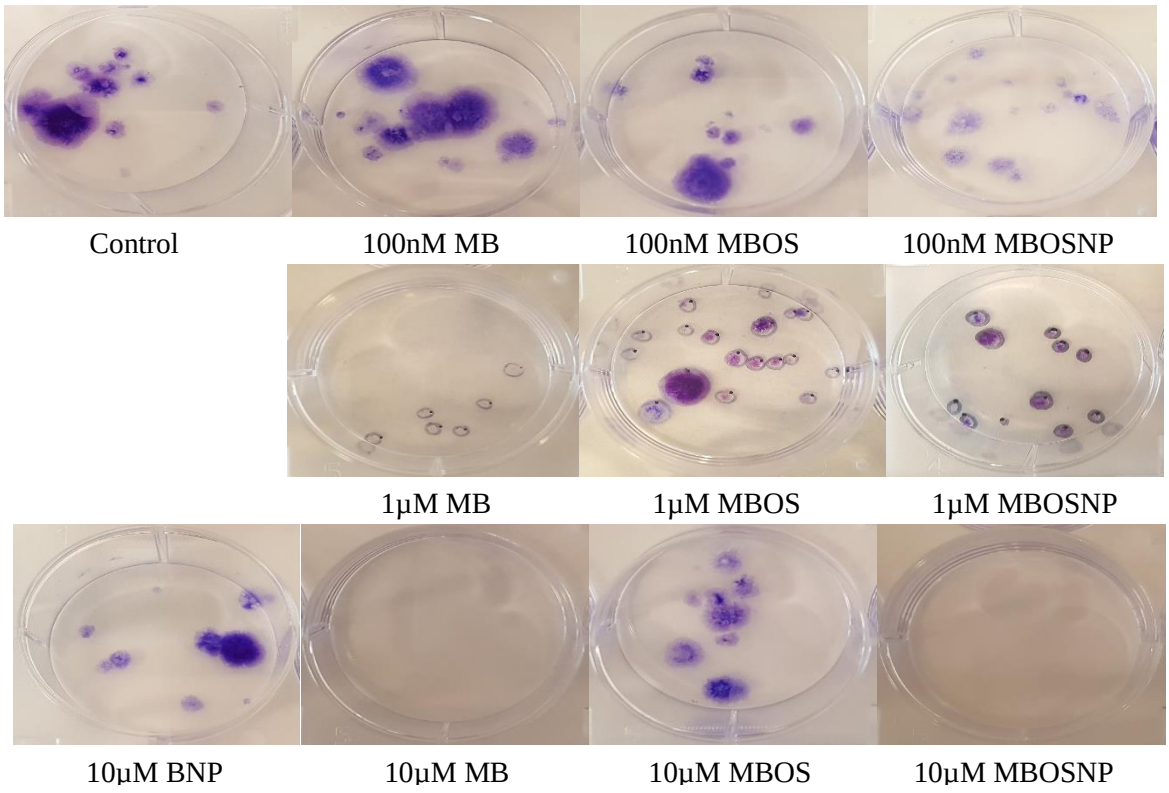

Supplemental Figure 2 – Effects of MBOSNPs on T98G cell proliferation. As treatment concentrations increased, average colony size and number of colonies decreased. At 10 µM MB and MBOSNP, little to no cells were detectable by visual examination, and those that were present were significantly smaller than untreated T98G cells. All MBOS treatment concentrations had similar sized colonies, as well as number of colonies. MBOSNP treatments compared to BNP-treated T98G cells to establish effect of PLGA, with no visible effect identified.

CHAPTER III

SUMMARY

As previously stated, glioblastoma (GBM) is a highly aggressive, molecularly heterogeneous grade IV human brain tumor with inferior survival periods that average 15 months post-diagnosis and treatment, and 5-year survival rates in the single digits. Current treatment regimens for GBM include a combination of cytoreductive surgery to remove the bulk of the tumor without severely damaging the neighboring healthy brain tissue, radiation to further eliminate any undetected tumor cell niches, and chemotherapy to inhibit additional growth and prevent recurrence as much as possible. However, this treatment protocol has only minimally improved GBM patient survival numbers and lengths over the last several decades due to increased toxicity in healthy tissues and organs upon repeated exposure, as is needed in order to eliminate GBM and prevent relapse, and a rise in drug resistance, rendering the development of new therapies and drug delivery systems imperative.

Current research in the field of GBM therapy development has focused on targeted therapies against cell surface and sub-cellular compartment ligands and receptors, as well as the application of nanotechnology-based drug delivery systems. In the most promising studies, ligand-conjugated nanoparticles containing various traditional chemotherapeutic agents, as well as other drug compounds with lesser known uses in oncology, have been used to treat GBM in vitro and in vivo, with a few undergoing different phases of clinical trials. However, to date, only a handful of nanoformulations, primarily liposomal, have made it into the clinic as

oncotherapies, potentially due to issues related to the composition of the preparations that are not discovered until administration to patients in significant numbers. Thus, extensive investigation during the development of these nanoformulations is imperative.

Methylene blue (MB), a photosensitizer molecule that undergoes a reversible catalysis that can lead to the production of reactive oxygen species (ROS), is being considered as a potential chemotherapeutic in conjunction with PDT. MB, which has a long history of medical uses that range from methemoglobinemia to an anti-malarial, has demonstrated applications in cancer, including GBM, due to the aforementioned excessive production of ROS and subsequent induction of cell death, as well as an ability to improve the functionality in mitochondria that is lost during pathogenesis. In GBM, mitochondria are known to undergo dysfunction that leads to improper performance of the electron transport chain (ETC); rapid, but inefficient ATP synthesis; and increased consumption of glucose to maintain and enhance tumor mass. Thus, MB could be a potential compound in the treatment of GBM.

While MB can easily permeate the BBB, which is key to treating any neurological disease, the concentrations needed to induce therapeutic actions tend to be excessive, and can lead to nephrotoxicity, in addition to other undesirable side effects. As a result, nanotechnology-based drug delivery systems could be a viable option. Current MB-loaded nanoparticles (NPs) with applications for GBM have revolved around invasive intracranial delivery and laser irradiation in PDT to produce ROS and inhibit tumor cell growth and disease progression. However, due to MB's noted cytotoxic and metabolic effects, encapsulation in and administration of polymeric NPs without the involvement of PDT is a potential avenue that has not been explored for cancer therapy, specifically for GBM.

In this study, a MB conjugate prepared by chloroform extraction of MB and sodium oleate was loaded into poly(D,L-lactic-co-glycolic acid) (PLGA) NPs that were coated with the surfactant poloxamer-188/pluronic F68 (PF68) to enhance BBB passage via the adsorption of plasma proteins on the surface. Thus, methylene blue oleate salt (MBOS)-loaded PLGA NPs were developed and characterized for their potential application as a GBM treatment. Following formulation and optimization, NPs obtained were within an acceptable size range (<200nm) that would enable enhancement of BBB passage and increased uptake by GBM cells, while reducing recognition and elimination by the various components of the immune system (reticuloendothelial system (RES), macrophages, and the spleen), as well as that by hepatic clearance.

MBOS-loaded PLGA NPs (MBOSNPs) were shown to induce cell death in cultured U87 and T98G GBM cell lines at levels comparable to, if not better, than free MB or MBOS. Additionally, they were able to equivalently inhibit cell proliferation due to a decrease in tumor cell colony number and size as demonstrated *in vitro*. Furthermore, MBOSNPs were able to impair cellular bioenergetic pathways in GBM, as noted by reductions in ATP production and glucose utilization. As a result of the positive outcomes seen *in vitro*, the potential brain accumulation, and ultimately inhibition of tumor growth, of the nanoformulation was investigated.

Prior to initiation of a pharmacokinetic (PK) study, MB and MBOS samples were analyzed by LC-MS/MS for confirmation of compound similiarities. Upon completion of the preliminary assessment, it was determined that while both compounds had similar chemical components, the ratios of the two major molecular weight (mw) species identified in each were drastically different. While both had peaks at 284 and 270 via mass spectrometry, the ratios of

each component was reversed in MB and MBOS; with MB composed primarily of the 284 mw species that corresponded to a fully methylated MB molecule, while MBOS' principal constituent was the 270 mw species that corresponded to a singularly demethylated MB molecule. While this chemical difference did not appear to result in a loss of activity *in vitro*, nothing was known about what might happen upon its administration *in vivo*. Due to this significant discrepancy between the two test compounds, further comparison would be focused on MBOS and MBOSNPs.

Following IV dosing with free MB, free MBOS, and MBOSNPs in CD-1 mice and collection of their plasma and tissues at designated time points, it was determined that between the three treatments, free MB exhibited the highest accumulation across all samples, followed by MBOS and MBOSNPs. As previously stated, even with the elimination of MB from the comparison, free MBOS showed better tissue accumulation following administration compared to MBOSNPs. However, it was noted that between the two treatments, MBOSNPs exhibited a better ability to vacate the circulation and permeate the blood-brain barrier (BBB), as demonstrated by a 1.6-fold higher value associated with the difference between the area under the curve (AUC) for brain than plasma compared to free MBOS. While drug accumulation did not appear as high in brain tissue following MBOS treatment compared to MBOSNPs, the NPs did exhibit a better capacity for BBB transport than free drug, providing for the potential continued development and optimization of MBOSNPs for GBM treatment. Additionally, a gender comparison following treatment administration would be necessary to analyze these effects, as GBM is known to be more common in men than women. However, to accurately determine their utility, MBOSNPs, in addition to free MB and MBOS, would need to be examined in a glioblastoma tumor-bearing mouse model, which was beyond the scope and time

limitations of this study. Regardless, these MBOSNPs may still show promise as a treatment for GBM in the future.

References

1. *Brain Tumor Statistics*. 2015 [cited 2016 June 21]; Available from: http://www.abta.org/about-us/news/brain-tumor-statistics/.
2. *Brain and spinal cord tumors in adults*. 2016, American Cancer Society: Atlanta, Georgia.
3. Barnholtz-Sloan, J.S., A.E. Sloan, and A.G. Schwartz, *Chapter 25 - Cancer of the brain and other central nervous system*. 2004, National Cancer Institute: Bethesda, MA.
4. *CBTRUS, Statistical report: primary brain tumors in the United States, 2000-2004*. 2008: Chicago, IL.
5. Dunn, G.P., M.L. Rinne, J. Wykosky, G. Genovese, S.N. Quayle, I.F. Dunn, et al., *Emerging insights into the molecular and cellular basis of glioblastoma.* Genes Dev, 2012. **26**(8): p. 756-84.
6. *Understanding glioblastoma*. 2012, National Brain Tumor Society: Watertown, MA.
7. *Glioblastoma and malignant astrocytoma*. 2012, American Brain Tumor Association: Chicago, IL.
8. *What you need to know about brain tumors*, U.S.D.o.H.a.H. Services, Editor. 2009, National Institutes of Health - National Cancer Institute: Rockville, MD.
9. Mourad, P.D., L. Farrell, L.D. Stamps, M.R. Chicoine, and D.L. Silbergeld, *Why are systemic glioblastoma metastases rare? Systemic and cerebral growth of mouse glioblastoma.* Surg Neurol, 2005. **63**(6): p. 511-9; discussion 519.
10. Jellinger, K., *Glioblastoma multiforme: Morphology and biology.* Acta Neurochirurgica, 1978. **42**: p. 5-32.

11. Kanu, O.O., A. Mehta, C. Di, N. Lin, K. Bortoff, D.D. Bigner, et al., *Glioblastoma multiforme: a review of therapeutic agents.* Expert Opinion on Therapeutic Targets, 2009. **13**(6): p. 701-18.

12. Engelhard, H.H., J.L. Villano, K.R. Porter, A.K. Stewart, M. Barua, F.G. Barker, et al., *Clinical presentation, histology, and treatment in 430 patients with primary tumors of the spinal cord, spinal meninges, or cauda equina.* J Neurosurg Spine, 2010. **13**(1): p. 67-77.

13. Adams, H., K.L. Chaichana, J. Avendaño, B. Liu, S.M. Raza, and A. Quiñones-Hinojosa, *Adult cerebellar glioblastoma: understanding survival and prognostic factors using a population-based database from 1973 to 2009.* World Neurosurg, 2013. **80**(6): p. e237-43.

14. Adamson, C., O.O. Kanu, A. Mehta, C. Di, N. Lin, A.K. Mattox, et al., *Glioblastoma multiforme: a review of where we have been and where we are going.* Expert Opin Investig Drugs, 2009. **18**(8): p. 1061-83.

15. Ohgaki, H., *Genetic pathways to glioblastomas.* Neuropathology, 2005. **25**(1): p. 1-7.

16. Thakkar, J.P., T.A. Dolecek, C. Horbinksi, Q.T. Ostrom, D.D. Lightner, J.S. Barnholtz-Sloan, et al., *Epidemiologic and molecular prognostic review of glioblastoma.* Cancer Epidemiology, Biomarkers, and Prevention, 2014. **23**(10): p. 1985-96.

17. Huse, J.T., E. Holland, and L.M. DeAngelis, *Glioblastoma: molecular analysis and clinical implications.* Annu Rev Med, 2013. **64**: p. 59-70.

18. Ohgaki, H., K. Watanabe, A. Peraud, W. Biernat, A. von Deimling, M.G. Yasargil, et al., *A case history of glioma progression.* Acta Neuropathol, 1999. **97**: p. 525-32.

19. Scherer, H.J., *Cerebral astrocytomas and their derivatives.* Am J Cancer, 1940. **40**: p. 159-98.

20. Ohgaki, H. and P. Kleihues, *The definition of primary and secondary glioblastoma.* Clin Cancer Res, 2013. **19**(4): p. 764-72.

21. Ostrom, Q.T., H. Gittleman, P. Farah, A. Ondracek, Y. Chen, Y. Wolinsky, et al., *CBTRUS statistical report: Primary brain and central nervous system tumors diagnosed in the United States in 2006-2010.* Neuro Oncol, 2013. **15**(Suppl 2): p. ii1-56.

22. Chakrabarti, I., M. Cockburn, W. Cozen, Y.P. Wang, and S. Preston-Martin, *A population-based description of glioblastoma multiforme in Los Angeles County, 1974-1999.* Cancer, 2005. **104**: p. 2798-806.

23. Ohgaki, H., P. Dessen, B. Jourde, S. Horstmann, T. Nishikawa, P.L. Di Patre, et al., *Genetic pathways to glioblastoma: a population-based study*. Cancer, 2004. **64**(19): p. 6892-9.

24. Xie, D., Y.X. Zeng, H.J. Wang, J.M. Wen, Y. Tao, J.S. Sham, et al., *Expression of cytoplasmic and nuclear Survivin in primary and secondary human glioblastoma.* Br J Cancer, 2006. **94**(1): p. 108-14.

25. Watanabe, K., O. Tachibana, K. Sata, Y. Yonekawa, P. Kleihues, and H. Ohgaki, *Overexpression of the EGF receptor and p53 mutations are mutually exclusive in the evolution of primary and secondary glioblastomas.* Brain Pathol, 1996. **6**(3): p. 217-23.

26. Karcher, S., H.H. Steiner, R. Ahmadi, S. Zoubaa, G. Vasvari, H. Bauer, et al., *Different angiogenic phenotypes in primary and secondary glioblastomas.* Int J Cancer, 2006. **118**(9): p. 2182-9.

27. Schwartzbaum, J.A., J.L. Fisher, K.D. Aldape, and M. Wrensch, *Epidemiology and molecular pathology of glioma.* Nat Clin Pract Neurol, 2006. **2**(9): p. 494-503; quiz 1 p following 516.

28. Godard, S., G. Getz, M. Delorenzi, P. Farmer, H. Kobayashi, I. Desbaillets, et al., *Classification of human astrocytic gliomas on the basis of gene expression: a correlated group of genes with angiogenic activity emerges as a strong predictor of subtypes.* Cancer Res, 2003. **63**(20): p. 6613-25.

29. Schrock, E., S. du Manoir, T. Veldman, B. Schoell, J. Wienberg, M.A. Ferguson-Smith, et al., *Multicolor spectral karyotyping of human chromosomes.* Science, 1996. **273**(5274): p. 494-7.

30. Louis, D.N., A. von Deimling, R.Y. Chung, M.P. Rubio, J.M. Whaley, R.H. Eibl, et al., *Comparative study of p53 gene and protein alterations in human astrocytic tumors.* J Neuropathol Exp Neurol, 1993. **52**(1): p. 31-8.

31. Kleihues, P. and H. Ohgaki, *Phenotype vs genotype in the evolution of astrocytic brain tumors.* Toxicol Pathol, 2000. **28**(1): p. 164-70.

32. Ohgaki, H. and P. Kleihues, *Genetic alterations and signaling pathways in the evolution of gliomas.* Cancer Sci, 2009. **100**(12): p. 2235-41.

33. Ohgaki, H. and P. Kleihues, *Genetic pathways to primary and secondary glioblastoma.* Am J Pathol, 2007. **170**(5): p. 1445-53.

34. Wrensch, M., Y. Minn, T. Chew, M. Bondy, and M.S. Berger, *Epidemiology of primary brain tumors: current concepts and review of the literature.* 4, 2002. **4**(278-99).

35. Omuro, A. and L.M. DeAngelis, *Glioblastoma and other malignant gliomas: a clinical review*. JAMA, 2013. **310**(17): p. 1842-50.

36. Hodges, L.C., J.L. Smith, A. Garrett, and S. Tate, *Prevalence of glioblastoma multiforme in subjects with prior therapeutic radiation.* J Neurosci Nurs, 1992. **24**(2): p. 79-83.

37. Bondy, M.L., M.E. Scheurer, B. Malmer, J.S. Barnholtz-Sloan, F.G. Davis, D. Il'yasova, et al., *Brain tumor epidemiology: consensus from the Brain Tumor Epidemiology Consortium.* Cancer, 2008. **113**(7 Suppl): p. 1953-68.

38. Pearce, M.S., J.A. Salotti, M.P. Little, K. McHugh, C. Lee, K.P. Kim, et al., *Radiation exposure from CT scans in childhood and subsequent risk of leukaemia and brain tumours: a retrospective cohort study.* Lancet, 2012. **380**(9840): p. 499-505.

39. Nichols, K.E., D. Malkin, J.E. Garber, J.F. Fraumeni, Jr., and F.P. Li, *Germ-line p53 mutations predispose to a wide spectrum of early-onset cancers.* Cancer Epidemiol Biomarkers Prev, 2001. **10**(2): p. 83-7.

40. Navas-Acien, A., M. Pollan, P. Gustavsson, and N. Plato, *Occupation, exposure to chemicals and risk of gliomas and meningiomas in Sweden.* Am J Ind Med, 2002. **42**(3): p. 214-27.

41. Krishnan, G., M. Felini, S.E. Carozza, R. Miike, T. Chew, and M. Wrensch, *Occupation and adult gliomas in the San Francisco Bay Area.* J Occup Environ Med, 2003. **45**(6): p. 639-47.

42. Zheng, T., K.P. Cantor, Y. Zhang, S. Keim, and C.F. Lynch, *Occupational risk factors for brain cancer: a population-based case-control study in Iowa.* J Occup Environ Med, 2001. **43**(4): p. 317-24.

43. Hochberg, F., P. Toniolo, P. Cole, and M. Salcman, *Nonoccupational risk indicators of glioblastoma in adults.* J Neurooncol, 1990. **8**(1): p. 55-60.

44. Demers, P.A., T.L. Vaughan, and R.R. Schommer, *Occupation, socioeconomic status, and brain tumor mortality: a death certificate-based case-control study.* J Occup Med, 1991. **33**(9): p. 1001-6.

45. Wrensch, M., M. Lee, R. Miike, B. Newman, G. Barger, R. Davis, et al., *Familial and personal medical history of cancer and nervous system conditions among adults with glioma and controls.* Am J Epidemiol, 1997. **145**(7): p. 581+-93.

46. El-Zein, R., A.Y. Minn, M. Wrensch, and M. Bondy, *Epidemiology of brain tumors*. 2nd ed. Cancer in the Nervous System, ed. L. V.A. 2002, New York, New York: Oxford University Press.

47. Ichimura, K., H. Ohgaki, P. Kleihues, and V.P. Collins, *Molecular pathogenesis of astrocytic tumours.* J Neurooncol, 2004. **70**(2): p. 137-60.

48. Brenner, A.V., M.S. Linet, H.A. Fine, W.R. Shapiro, R.G. Selker, P.M. Black, et al., *History of allergies and autoimmune diseases and risk of brain tumors in adults.* Int J Cancer, 2002. **99**(2): p. 252-9.

49. Schlehofer, B., M. Blettner, N. Becker, C. Martinsohn, and J. Wahrendorf, *Medical risk factors and the development of brain tumors.* Cancer, 1992. **69**(10): p. 2541-7.

50. Schlehofer, B., M. Blettner, S. Preston-Martin, D. Niehoff, J. Wahrendorf, A. Arslan, et al., *Role of medical history in brain tumour development: results from the international adult brain tumour study.* Int J Cancer, 1999. **82**(2): p. 155-60.

51. Schwartzbaum, J., A. Ahlbom, B. Malmer, S. Lönn, A.J. Brookes, H. Doss, et al., *Polymorphisms associated with asthma are inversely related to glioblastoma multiforme.* Cancer Res, 2005. **65**(14): p. 6459-65.

52. Schwartzbaum, J., F. Jonsson, A. Ahlbom, S. Preston-Martin, S. Lönn, K.C. Söderberg, et al., *Cohort studies of association between self-reported allergic conditions, immune-related diagnoses and glioma and meningioma risk.* Int J Cancer, 2003. **106**(3): p. 423-8.

53. Wiemels, J.L., J.K. Wiencke, J. Patoka, M. Moghadassi, T. Chew, A. McMillan, et al., *Reduced immunoglobulin E and allergy among adults with glioma compared with controls.* Cancer Res, 2004. **64**(2): p. 8468-73.

54. Wiemels, J.L., J.K. Wiencke, J.D. Sison, R. Miike, A. McMillan, and M. Wrensch, *History of allergies among adults with glioma and controls.* Int J Cancer, 2002. **98**(4): p. 609-15.

55. Wrensch, M., A. Weinberg, J. Wiencke, R. Miike, J. Sison, J. Wiemels, et al., *History of chickenpox and shingles and prevalence of antibodies to varicella-zoster virus and three other herpesviruses among adults with glioma and controls.* Am J Epidemiol, 2005. **161**(10): p. 929-38.

56. Tang, J., W. Shao, M.T. Dorak, Y. Li, R. Miike, E. Lobashevsky, et al., *Positive and negative associations of human leukocyte antigen variants with the onset and prognosis of adult glioblastoma multiforme.* Cancer Epidemiol Biomarkers Prev, 2005. **14**(8): p. 2040-4.

57. Schwartzbaum, J.A., Y. Xiao, Y. Liu, S. Tsavachidis, M.S. Berger, M.L. Bondy, et al., *Inherited variation in immune genes and pathways and glioblastoma risk.* Carcinogenesis, 2010. **31**(10): p. 1770-7.

58. Lachance, D.H., P. Yang, D.R. Johnson, P.A. Decker, T.M. Kollmeyer, L.S. McCoy, et al., *Associations of high-grade glioma with glioma risk alleles and histories of allergy and smoking.* Am J Epidemiol, 2011. **174**(5): p. 574-81.

59. Linos, E., T. Raine, A. Alonso, and D. Michaud, *Atopy and risk of brain tumors: a meta-analysis.* J Natl Cancer, 2007. **99**(20): p. 1544-50.

60. Forsyth, P.A. and J.B. Posner, *Headaches in patients with brain tumors: a study of 111 patients.* Neurology, 1993. **43**(9): p. 1678-83.

61. Glantz, M.J., B.F. Cole, P.A. Forsyth, L.D. Recht, P.Y. Wen, M.C. Chamberlain, et al., *Practice parameter: anticonvulsant prophylaxis in patients with newly diagnosed brain tumors. Report of the Quality Standards Subcommittee of the American Academy of Neurology*. Neurology, 2000. **54**(10): p. 1886-93.

62. Virchow, R., *Die Krankhaften Geschwulste*. 1863, Berlin: Hirschwald. 492.

63. Globus, J.H. and I. Strauss, *Spongioblastoma multiforme: a primary malignant form of brain neoplasm; its clinical and anatomical features.* Arch Neurol Psychiat, 1925. **14**(2): p. 139-91.

64. Bailey, P. and H. Cushing, *A classification of tumors of the glioma group on histogenetic basis with correlated study of prognosis*. 1926, Philadelphia, PA: J.B. Lipponcott. 175.

65. Agnihotri, S., K.E. Burrell, A. Wolf, S. Jalali, C. Hawkins, J.T. Rutka, et al., *Glioblastoma, a brief review of history, molecular genetics, animal models and novel therapeutic strategies.* Arch Immunol Ther Exp (Warsz), 2013. **61**(1): p. 25-41.

66. Kersting, G., *Tissue culture of human gliomas*. Progress in Neurological surgery, ed. H. Krayenbuhl, P.E. Maspes, and W.H. Sweet. Vol. 2. 1968, Chicago, IL: Year Book Med Publ.

67. Zulch, K.J., *Biology and morphology of glioblastoma multiforme.* Acta Radiol Ther, 1969. **8**(1-2): p. 65-77.

68. Luse, S.A., *Electron microscopic studies of brain tumors.* Neurology, 1960. **10**: p. 881-905.

69. Raimondi, A.J., *Ultrastructure and the biology of human brain tumors*, in *Progress of Neurological Surgery*, H. Krayenbuhl, P.E. Maspes, and W.H. Sweet, Editors. 1966, Year Book Medical Publisher: Chicago. p. 1-36.

70. *World Health Organization classification of tumors: pathology and genetics of tumors of the nervous system*. 3rd ed. Vol. 1. 2000, Lyon: IARC Press.

71. Reardon, D.A., J.N. Rich, H.S. Friedman, and D.D. Bigner, *Recent advances in the treatment of malignant astrocytoma.* J Clin Oncol, 2006. **24**(8): p. 1253-65.

72. Burger, P.C., F.S. Vogel, S.B. Green, and T.A. Strike, *Glioblastoma multiforme and anaplastic astrocytoma. Pathologic criteria and prognostic implications.* Cancer, 1985. **56**(5): p. 1106-11.

73. Miller, C.R. and A. Perry, *Glioblastoma.* Arch Pathol Lab Med, 2007. **131**(3): p. 397-406.

74. Engelhard, H.H. and D.G. Groothuis, *The blood-brain barrier: structure, function, and response to neoplasia*, in *Gliomas*, M.D. Berger and C.B. Wilson, Editors. 1999, Saunders: Philadelphia. p. 115-21.

75. Schneider, S.W., T. Ludwig, L. Tatenhorst, S. Braune, H. Oberleithner, V. Senner, et al., *Glioblastoma cells release factors that disrupt blood-brain barrier features.* Acta Neuropathol, 2004. **107**(3): p. 272-6.

76. Wolburg, H., S. Noell, P. Fallier-Becker, A.F. Mack, and K. Wolburg-Buchholz, *The disturbed blood-brain barrier in human glioblastoma.* Mol Aspects Med, 2012. **33**(5-6): p. 579-89.

77. Pronin, I.N., A.I. Holodny, and A.V. Petraikin, *MRI of high-grade glial tumors: correlation between degree of contrast enhancement and the volume of surrounding edema.* Neuroradiology, 1997. **39**(5): p. 348-50.

78. Liebner, S., A. Fischmann, G. Rascher, F. Duffner, E.H. Grote, H. Kalbacher, et al., *Claudin-1 and claudin-5 expression and tight junction morphology are altered in blood vessels of human glioblastoma multiforme.* Acta Neuropathol, 2000. **100**(3): p. 323-31.

79. Wolburg, H., K. Wolburg-Buchholz, J. Kraus, G. Rascher-Eggstein, S. Liebner, S. Hamm, et al., *Localization of claudin-3 in tight junctions of the blood-brain barrier is selectively lost during experimental autoimmune encephalomyelitis and human glioblastoma multiforme.* Acta Neuropathol, 2003. **105**(6): p. 586-92.

80. Papadopoulos, M.C., S. Saadoun, C.J. Woodrow, D.C. Davies, P. Costa-Martins, R.F. Moss, et al., *Occludin expression in microvessels of neoplastic and non-neoplastic human brain.* Neuropathol Appl Neurobiol, 2001. **27**(5): p. 384-95.

81. Rascher, G., A. Fischmann, S. Kroger, F. Duffner, E.H. Grote, and H. Wolburg, *Extracellular matrix and the blood-brain barrier in glioblastoma multiforme: spatial segregation of tenascin and agrin.* Acta Neuropathol, 2002. **104**(1): p. 85-91.

82. Binder, D.K. and M.S. Berger, *Proteases and the biology of glioma invasion.* J Neurooncol, 2000. **56**(2): p. 149-58.

83. Nuttall, R.K., C.J. Pennington, J. Taplin, A. Wheal, V.W. Yong, P.A. Forsyth, et al., *Elevated membrane-type matrix metalloproteinases in gliomas revealed by profiling proteases and inhibitors in human cancer cells.* Mol Cancer Res, 2003. **1**(5): p. 333-45.

84. Pietsch, T., M.M. Valter, H.K. Wolf, A. von Deimling, H.J. Huang, W.K. Cavenee, et al., *Expression and distribution of vascular endothelial growth factor protein in human brain tumors.* Acta Neuropathol, 1997. **93**(2): p. 109-17.

85. Machein, M.R., J. Kullmer, B.L. Fiebich, K.H. Plate, and P.C. Warnke, *Vascular endothelial growth factor expression, vascular volume, and capillary permeability in human brain tumors.* Neurosurgery, 1999. **44**(4): p. 740-1.

86. Machein, M.R. and K.H. Plate, *VEGF in brain tumors.* J Neurooncol, 2000. **50**(1-2): p. 109-20.

87. Lamszus, K., J. Laterra, M. Westphal, and E.M. Rosen, *Scatter factor/hepatocyte growth factor (SF/HGF) content and function in human gliomas.* Int J Dev Neurosci, 1999. **17**(5-6): p. 517-30.

88. Kurpad, S.N., X.G. Zhao, C.J. Wikstrand, S.K. Batra, R.E. McLendon, and D.D. Bigner, *Tumor antigens in astrocytic gliomas.* Glia, 1995. **15**(3): p. 244-56.

89. Chi, D.D., R.E. Merchant, R. Rand, A.J. Conrad, D. Garrison, R. Turner, et al., *Molecular detection of tumor-associated antigens shared by human cutaneous melanomas and gliomas.* Am J Pathol, 1997. **150**(6): p. 2143-52.

90. Brooks, W.H., H.D. Caldwell, and R.H. Mortara, *Immune responses in patients with gliomas.* Surg Neurol, 1974. **2**(6): p. 419-23.

91. Brooks, W.H., M.G. Netsky, D.E. Normansell, and D.A. Horwitz, *Depressed cell-mediated immunity in patients with primary intracranial tumors. Characterization of a humoral immunosuppressive factor.* J Exp Med, 1972. **136**(6): p. 1631-47.

92. Brooks, W.H., T.L. Roszman, M.S. Mahaley, and R.E. Woosley, *Immunobiology of primary intracranial tumours. II. Analysis of lymphocyte subpopulations in patients with primary brain tumours.* Clin Exp Immunol, 1977. **29**(1): p. 61-6.

93. Roszman, T.L. and W.H. Brooks, *Immunobiology of primary intracranial tumours. III. Demonstration of a qualitative lymphocyte abnormality in patients with primary brain tumours.* Clin Exp Immunol, 1980. **39**(2): p. 395-402.

94. Roszman, T.L., W.H. Brooks, and L.H. Elliott, *Immunobiology of primary intracranial tumors. VI. Suppressor cell function and lectin-binding lymphocyte subpopulations in patients with cerebral tumors.* Cancer, 1982. **50**(7): p. 1273-9.

95. Roszman, T.L., L.H. Elliott, and W.H. Brooks, *Proliferative potential of T-cell lymphocytes from gliomas.* J Neurosurg, 1992. **77**(5): p. 820-1.

96. Menzies, C.B., M. Gunar, D.G. Thomas, and P.O. Behan, *Impaired thymus-derived lymphocyte function in patients with malignant brain tumour.* Clin Neurol Neurosurg, 1980. **82**(3): p. 157-68.

97. Zou, J.P., L.A. Morford, C. Chougnet, A.R. Dix, A.G. Brooks, N. Torres, et al., *Human glioma-induced immunosuppression involves soluble factor(s) that alters monocyte cytokine profile and surface markers.* J Immunol, 1999. **162**(8): p. 4882-92.

98. Galarraga, J., D.J. Loreck, J.F. Graham, R.L. DeLaPaz, B.H. Smith, D. Hallgren, et al., *Glucose metabolism in human gliomas: correspondence of in situ and in vitro metabolic rates and altered energy metabolism.* Metab Brain Dis, 1986. **1**(4): p. 279-91.

99. Ordys, B.B., S. Launay, R.F. Deighton, J. McCulloch, and I.R. Whittle, *The role of mitochondria in glioma pathophysiology.* Mol Neurobiol, 2010. **42**(1): p. 64-75.

100. Marie, S.K.N. and S.M.O. Shinjo, *Metabolism and brain cancer.* Clinics, 2011. **66**(S1): p. 33-43.

101. Zhou, Y., Y. Zhou, T. Shingu, L. Feng, Z. Chen, M. Ogasawara, et al., *Metabolic alterations in highly tumorigenic glioblastoma cells: Preference for hypoxia and high dependency on glycolysis.* J Biol Chem, 2011. **286**(37): p. 32843-53.

102. Nagy, A., K. Eder, M.A. Selak, and B. Kalman, *Mitochondrial energy metabolism and apoptosis regulation in glioblastoma.* Brain Res, 2015. **1595**: p. 127-42.

103. Fogg, V.C., N.J. Lanning, and J.P. MacKeigan, *Mitochondria in cancer: at the crossroads of life and death.* Chin J Cancer, 2011. **30**(6): p. 526-39.

104. Furnari, F.B., T. Fenton, R.M. Bachoo, A. Mukasa, J.M. Stommel, A. Stegh, et al., *Malignant astrocytic glioma: genetics, biology, and paths to treatment.* Genes Dev, 2007. **21**(21): p. 2683-710.

105. Ziegler, D.S., A.L. Kung, and M.W. Kieran, *Anti-apoptosis mechanisms in malignant gliomas.* J Clin Oncol, 2008. **26**(3): p. 493-500.

106. Seyfried, T.N. and P. Mukherjee, *Targeting energy metabolism in brain cancer: review and hypothesis.* Nutr Metab (Lond), 2005. **2**: p. 30-8.

107. Vander Heiden, M.G., L.C. Cantley, and C.B. Thompson, *Understanding the Warburg effect: the metabolic requirements of cell proliferation.* Science, 2009. **324**(5930): p. 1029-33.

108. Dickinson, A., K.Y. Yeung, J.F. Donoghue, M.J. Baker, R.D. Kelly, M. McKenzie, et al., *The regulation of mitochondrial DNA copy number in glioblastoma cells.* Cell Death Differ, 2013. **20**(12): p. 1644-53.

109. Yeung, K.Y., A. Dickinson, J.F. Donoghue, G. Polekhina, S.J. White, D.K. Grammatopoulos, et al., *The identification of mitochondrial DNA variants in glioblastoma multiforme.* Acta Neuropathol Commun, 2014. **2**: p. 1-20.

110. Deighton, R.F., T. Le Bihan, S.F. Martin, A.M. Gerth, M. McCulloch, J.M. Edgar, et al., *Interactions among mitochondrial proteins altered in glioblastoma.* J Neurooncol, 2014. **118**(2): p. 247-56.

111. Lloyd, R.E., K. Keatley, T.J. Littlewood, B. Meunier, W.V. Holt, Q. An, et al., *Identification and functional prediction of mitochondrial complex III and IV mutations associated with glioblastoma.* Neuro Oncol, 2015. **17**(7): p. 942-52.

112. Larsen, C., *Genetic and molecular abnormalities of glioblastoma (GBM).* Bull Cancer, 2010. **97**(11): p. 1389-407.

113. Gogvadze, V., S. Orrenius, and B. Zhivotovsky, *Mitochondria in cancer cells: what is so special about them?* Trends Cell Biol, 2008. **18**(4): p. 165-73.

114. Tennant, D.A., R.V. Duran, H. Boulahbel, and E. Gottieb, *Metabolic transformation in cancer.* Carcinogenesis, 2009. **30**(8): p. 1269-80.

115. Andersson, A.K., L. Ronnback, and E. Hansson, *Lactate induces tumour necrosis factor-alpha, interleukin-6 and interleukin-1beta release in microglial- and astroglial-enriched primary cultures.* J Neurochem, 2005. **93**(5): p. 1327-33.

116. Imamura, K., T. Noguchi, and T. Tanaka, *Regulation of isozyme patterns of pyruvate kinase in normal and neoplastic tissues,* in *Markers of Human Neuroectodermal Tumors,* G.E.J. Staal and C.W.M. van Veelen, Editors. 1986, CRC Press: Boca Raton, Florida. p. 191-222.

117. Guminska, M., J. Ignacak, T. Kedryna, and B. Stachurska, *Tumor-specific pyruvate kinase isoenzyme M2 involved in biochemical strategy of energy generation in neoplastic cells.* Acta Biochim Pol, 1997. **44**(4): p. 711-24.

118. Mazurek, S., C.B. Boschel, F. Hugo, and E. Eigenbrodt, *Pyruvate kinase type M2 and its role in tumor growth and spreading.* Semin Cancer Biol, 2005. **15**(4): p. 300-8.

119. Christofk, H.R., M.G. Vander Heiden, M.H. Harris, A. Ramanathan, R.E. Gerszten, R. Wei, et al., *The M2 splice isoform of pyruvate kinase is important for cancer metabolism and tumour growth.* Nature, 2008. **452**(7184): p. 230-3.

120. Mukherjee, J., J.J. Phillips, S. Zheng, J. Wiencke, S.M. Ronen, and R.O. Pieper, *Pyruvate kinase M2 expression, but not pyruvate kinase activity is up-regulated in a grade-specific manner in human glioma.* PLoS One, 2013. **8**(2): p. e57610.

121. Lee, H.C., C.M. Chang, and C.W. Chi, *Somatic mutations of mitochondrial DNA in aging and cancer progression.* Ageing Res Rev, 2010. **9**(Suppl 1): p. S47-58.

122. Chae, Y.C., A. Angelin, S. Lisanti, A.V. Kossenkov, K.D. Speicher, H. Wang, et al., *Landscape of the mitochondrial Hsp90 metabolome in tumours.* Nat Commun, 2013. **4**: p. 2139.

123. Levine, A.J. and A.M. Puzio-Kuter, *The control of the metabolic switch in cancers by oncogenes and tumor suppressor genes.* Science, 2010. **330**(3009): p. 1340-4.

124. Velpula, K.K., A. Bhasin, S. Asuthkar, and A.J. Tsung, *Combined targeting of PDK1 and EGFR triggers regression of glioblastoma by reversing the Warburg effect.* Cancer Res, 2013. **73**(24): p. 7277-89.

125. Semenza, G.L., *Hif-1: upstream and downstream of cancer metabolism.* Curr Opin Genet Dev, 2010. **20**(1): p. 51-6.

126. (TCGA), T.C.G.A.R.N., *Comprehensive genomic characterization defines human glioblastoma genes and core pathways.* Nature, 2008. **455**(7216): p. 1061-8.

127. Wuchty, S., A. Vazquez, S. Bozdag, and P.O. Bauer, *Genome-wide associations of signaling pathways in glioblastoma multiforme.* BMC Med Genomics, 2013. **6**: p. 11.

128. Shinojima, N., K. Tada, S. Shiraishi, T. Kamiryo, M. Kochi, H. Nakamura, et al., *Prognostic value of epidermal growth factor receptor in patients with glioblastoma multiforme.* Cancer Res, 2003. **63**(20): p. 6962-70.

129. Wong, A.J., S.H. Bigner, D.D. Bigner, K.W. Kinzler, S.R. Hamilton, and B. Vogelstein, *Increased expression of the epidermal growth factor receptor gene in malignant gliomas is invariably associated with gene amplification.* Proc Natl Acad Sci U S A, 1987. **84**(19): p. 6899-903.

130. Prives, C. and P.A. Hall, *The p53 pathway.* J Pathol, 1999. **187**(1): p. 112-26.

131. Vogelstein, B. and K.W. Kinzler, *p53 function and dysfunction.* Cell, 1992. **70**(4): p. 523-6.

132. Newcomb, E.W., W.J. Madonia, S. Pisharody, F.F. Lang, M. Koslow, and D.C. Miller, *A correlative study of p53 protein alteration and p53 gene mutation in glioblastoma multiforme.* Brain Pathol, 1993. **3**(3): p. 229-35.

133. Ott, M., V. Gogvadze, S. Orrenius, and B. Zhivotovsky, *Mitochondria, oxidative stress and cell death.* Apoptosis, 2007. **12**(5): p. 913-22.

134. Weinberg, F. and N.S. Chandel, *Reactive oxygen species-dependent signaling regulates cancer.* Cell Mol Life Sci, 2009. **66**(23): p. 3663-73.

135. Nakasu, S., Y. Nakasu, H. Noioka, M. Nakajima, and J. Handa, *bcl-2 protein expression in tumors of the central nervous system.* Acta Neuropathol, 1994. **88**(6): p. 520-6.

136. Krakstad, C. and M. Chekenya, *Survival signalling and apoptosis resistance in glioblastomas: opportunities for targeted therapies.* Mol Cancer, 2010. **9**: p. 135.

137. Stupp, R., W.P. Mason, M.J. van den Bent, M. Weller, B. Fisher, M.J. Taphoorn, et al., *Radiotherapy plus concomitant and adjuvant temozolomide for glioblastoma.* N Engl J Med, 2005. **352**(10): p. 987-96.

138. Hegi, M.E., A.C. Diserens, T. Gorlia, M.F. Hamou, N. de Tribolet, M. Weller, et al., *MGMT gene silencing and benefit from temozolomide in glioblastoma.* N Engl J Med, 2005. **352**(10): p. 997-1003.

139. Westphal, M., D.C. Hilt, E. Bortey, P. Delavault, R. Olivares, P.C. Warnke, et al., *A phase 3 trial of local chemotherapy with biodegradable carmustine (BCNU) wafers (Gliadel wafers) in patients with primary malignant glioma.* Neuro Oncol, 2003. **5**(2): p. 79-88.

140. Brem, H., S. Piantadosi, P.C. Burger, M. Walker, R.G. Selker, N.A. Vick, et al., *Placebo-controlled trial of safety and efficacy of intraoperative controlled delivery by biodegradable polymers of chemotherapy for recurrent gliomas. The Polymer-brain Tumor Treatment Group.* Lancet, 1995. **345**(8956): p. 1008-12.

141. Dasari, S. and P.B. Tchounwou, *Cisplatin in cancer therapy: Molecular mechanisms of action.* Eur J Pharmacol, 2015. **740**: p. 364-78.

142. *Lomustine*. 2016; Available from: https://pubchem.ncbi.nlm.nih.gov/compound/lomustine#section=Information-Sources.

143. Miclescu, A. and L. Wiklund, *Methylene blue, an old drug with new indications?* J Rom Anest Terap Int, 2010. **17**(1): p. 35-41.

144. Schirmer, R.H., H. Adler, M. Pickhardt, and E. Mandelkow, *"Lest we forget you--methylene blue..."*. Neurobiol Aging, 2011. **32**(12): p. 2325 e7-16.

145. Wainwright, M. and L. Amaral, *The phenothiazinium chromophore and the evolution of antimalarial drugs.* Trop Med Int Health, 2005. **10**(6): p. 501-11.

146. Buchholz, K., R.H. Schirmer, J.K. Eubel, M.B. Akoachere, T. Dandekar, K. Becker, et al., *Interactions of methylene blue with human disulfide reductases and their orthologues from Plasmodium falciparum.* Antimicrob Agents Chemother, 2008. **52**(1): p. 183-91.

147. Bergmann, K. and C.T. O'Konski, *A spectroscopic study of methylene blue monomer, dimer, and complexes with montmorillonite.* J Phys Chem, 1963. **67**(10): p. 2169-77.

148. Ghasemi, J.B. and M. Miladi, *Association equilibrium of methylene blue by spectral titration and chemometrics analysis: a thermodynamic study.* J Chin Chem Soc, 2009. **56**(3): p. 459-68.

149. Morgounova, E., Q. Shao, B.J. Hackel, D.D. Thomas, and S. Ashkenazi, *Photoacoustic lifetime contrast between methylene blue monomers and self-quenched dimers as a model for dual-labeled activatable probes.* J Biomed Opt, 2013. **18**(5): p. 056004.

150. Yang, F., X. Shifei, Z. Liu, J. Chen, Y. Lin, B. Qiu, et al., *Analysis of methylene blue and its metabolites in blood by capillary electrophoresis/electrospray ionization mass spectrometry.* Electrophoresis, 2011. **32**(6-7): p. 659-64.

151. Kubuki, S., K. Shibano, K. Akiyama, Z. Homonnay, E. Kuzmann, M. Ristic, et al., *Decomposition mechanism of methylene blue caused by metallic iron-maghemite mixture.* Hyperfine Interact, 2013. **218**(1): p. 47-52.

152. Mayer, B., F. Brunner, and K. Schmidt, *Inhibition of nitric oxide synthesis by methylene blue.* Biochem Pharmacol, 1993. **45**(2): p. 367-74.

153. Mayer, B., F. Brunner, and K. Schmidt, *Novel actions of methylene blue.* Eur Heart J, 1993. **14**(Suppl 1): p. 22-6.

154. Tsai, S.C., R. Adamik, V.C. Manganiello, and M. Vaughan, *Regulation of activity of purified guanylate cyclase from liver that is unresponsive to nitric oxide.* Biochem J, 1983. **215**(3): p. 447-55.

155. Juffermans, N.P., M.G. Vervloet, C.R.G. Daemen-Gubbels, J.M. Binnekade, M. de Jong, and A.B.J. Groeneveld, *A dose-finding study of methylene blue to inhibit nitric oxide actions in the hemodynamics of human septic shock.* Nitric Oxide, 2010. **22**(4): p. 275-80.

156. Harvey, B.H., I. Duvenhage, F. Viljoen, N. Scheepers, S.F. Malan, G. Wegener, et al., *Role of monoamine oxidase, nitric oxide synthase and regional brain monoamines in the antidepressant-like effects of methylene blue and selected structural analogues.* Biochem Pharmacol, 2010. **80**(10): p. 1580-91.

157. Ramsay, R.R., C. Dunford, and P.K. Gillman, *Methylene blue and serotonin toxicity: inhibtion of monoamine oxidase A (MAO A) confirms a theoretical prediction.* Br J Pharmacol, 2007. **152**(6): p. 946-51.

158. Augustinsson, K., *Methylene blue as an inhibitor of acetylcholine-esterase.* Acta Chem Scand, 1950. **4**: p. 536-42.

159. Pfaffendorf, M., T.A. Bruning, H.D. Batink, and P.A. van Zwieten, *The interaction between methylene blue and the cholinergic system.* Br J Pharmacol, 1997. **122**(1): p. 95-8.

160. Faber, P., A. Ronald, and B.W. Millar, *Methylthioninium chloride: pharmacology and clinical applications with special emphasis on nitric oxide mediated vasodilatory shock during cardiopulmonary bypass.* Anaesthesia, 2005. **60**(6): p. 575-87.

161. Schirmer, R.H., B. Coulibaly, A. Stich, M. Scheiwein, H. Merkle, J. Eubel, et al., *Methylene blue as an antimalarial agent.* Redox Rep, 2003. **8**(5): p. 272-5.

162. Wainwright, M. and K.B. Crossley, *Methylene blue - a therapeutic dye for all seasons.* J Chemother, 2002. **14**(5): p. 431-43.

163. Coulibaly, B., A. Zoungrana, F.P. Mockenhaupt, R.H. Schirmer, C. Klose, U. Mansmann, et al., *Strong gametocytocidal effect of methylene blue-based combination therapy against falciparum malaria: a randomized controlled trial.* PLoS One, 2009. **4**: p. e5318.

164. Ohrt, C., Q. Li, N. Obaldia, R. Im-Erbsin, L. Xie, and J. Berman, *Efficacy of intravenous methylene blue, intravenous artesunate, and their combination in preclinical models of malaria.* Malar J, 2014. **13**: p. 415-23.

165. Mwangi, V.I., R.M. Mumo, D.M. Kiboi, S.A. Omar, Z.W. Ng'ang'a, and H.S. Ozwara, *Methylene blue inhibits lumefantrine-resistant Plasmodium berghei.* J Infect Dev Ctries, 2016. **10**(6): p. 635-42.

166. Wirjanata, G., B.F. Sebayang, F. Chalfein, Prayoga, I. Handayuni, L. Trianty, et al., *Potent ex vivo activity of naphthoquine and methylene blue against drug-resistant clinical isolates of Plasmodium falciparum and Plasmodium vivax.* Antimicrob Agents Chemother, 2015. **59**(10): p. 6117-24.

167. Barcia, J.J., *The Giemsa stain: its history and applications.* Int J Surg Pathol, 2007. **15**(3): p. 292-6.

168. Cajal, S., *El azul de metileno en los centros nerviosos.* Rev Trimest Microgr, 1896. **1**: p. 151-203.

169. Ehrlich, P., *Uber die Methylenblaureaktion der lebenden Nerven-substanz.* Dstch Med Wochenschr, 1886. **12**: p. 49-52.

170. Boylston, M. and D. Beer, *Methemoglobinemia: a case study*. Critical Care Nurse, 2002. **22**(4): p. 50-5.

171. Brooks, M.M., *Methylene blue as antidote for cyanide and carbon monoxide poisoning.* JAMA, 1933. **100**(1): p. 59.

172. Kupfer, A., C. Aeschlimann, B. Wermuth, and T. Cerny, *Prophylaxis and reversal of ifosfamide encephalopathy with methylene-blue.* Lancet, 1994. **343**(8900): p. 763-4.

173. Pelgrims, J., F. De Vos, J. Van den Brande, D. Schrijvers, A. Prove, and J.B. Vermorken, *Methylene blue in the treatment and prevention of ifosfamide-induced encepalopathy: report of 12 cases and a review of the literature.* Br J Cancer, 2000. **82**(2): p. 291-4.

174. Kofidis, T., M. Struber, M. Wilhemi, M. Anssar, A. Simon, W. Harringer, et al., *Reversal of severe vasoplegia with single-dose methylene blue after heart transplantation.* J Thorac Cardiovasc Surg, 2001. **122**(4): p. 823-4.

175. Leyh, R.G., T. Kofidis, M. Struber, S. Fischer, K. Knobloch, B. Wachsmann, et al., *Methylene blue: the drug of choice for catecholamine-refractory vasoplegia after cardiopulmonary bypass?* J Thorac Cardiovasc Surg, 2003. **125**(6): p. 1426-31.

176. Levin, R.L., M.A. Degrange, G.F. Bruno, C.D. Del Mazo, D.J. Taborda, J.J. Griotti, et al., *Methylene blue reduces mortality and morbidity in vasoplegic patients after cardiac surgery.* Ann Thorac Surg, 2004. **77**(2): p. 496-9.

177. Ozal, E., E. Kuralay, V. Yildirim, S. Kilic, C. Bolcal, N. Kücükarslan, et al., *Preoperative methylene blue administration in patients at high risk for vasoplegic syndrome during cardiac surgery.* Ann Thorac Surg, 2005. **79**(5): p. 1615-9.

178. Evora, P.R., P.J. Riberio, and J.C. de Andrade, *Methylene blue administration in SIRS after cardiac operations.* Ann Thorac Surg, 1997. **63**(4): p. 1212-3.

179. Miclescu, A., S. Basu, and L. Wiklund, *Methylene blue added to a hypertonic-hyperoncotic solution increases short-time survival in experimental cardiac arrest.* Crit Care Med, 2006. **34**(11): p. 2806-13.

180. Wiklund, L., H.S. Sharma, and S. Basu, *Circulatory arrest as a model for studies of global ischemic injury and neuroprotection.* Ann N Y Acad Sci, 2005. **1053**: p. 205-19.

181. Preiser, J.C., P. Lejeune, A. Roman, E. Carlier, D. De Backer, M. Leeman, et al., *Methylene blue administration in septic shock: a clinical trial.* Crit Care Med, 1995. **23**(2): p. 259-64.

182. Gachot, B., J.P. Bedos, B. Verber, M. Wolff, and B. Regnier, *Short-term effects of methylene blue on hemodynamics and gas exchange in humans with septic shock.* Intensive Care Med, 1995. **21**(12): p. 1027-31.

183. Tardivo, J.P., A. Del Giglio, C.S. de Oliveira, D.S. Gabrielli, H.C. Junqueira, D.B. Tada, et al., *Methylene blue in photodynamic therapy: From basic mechanisms to clinical applications.* Photodiagnosis Photodyn Ther, 2005. **2**(3): p. 175-91.

184. Simmer, K.A., *Improved efficacy of localized brain tumor therapy using photosensitive nanoparticles*, in *Biophysics*. 2014, University of Michigan: Ann Arbor, Michigan. p. 128.

185. Simmer, K.A., H.J. Hah, Y.K. Lee, O. Sagher, D.A. Orringer, M.A. Philbert, et al., *Towards glioma intra-operative photodynamic therapy: targeted photo-active nanoparticles in a brain tumor window model.* Int J Nanomed Nanosurg, 2015. **1**(2): p. 1-8.

186. Ginimuge, P.R. and S.D. Jyothi, *Methylene blue: Revisited.* J Anaesth Clin Pharmacol, 2010. **26**(4): p. 517-20.

187. Bodoni, P., *Dell'azione sedativa del bleu di metilene in varie forme di psicosi.* Clin Med Ital, 1899. **38**: p. 217-22.

188. Ehrlich, P. and A. Leppmann, *Uber Schmerzstillende Wirkung des Methylblau.* Dtsch Med Wochenschr, 1890. **16**: p. 493-4.

189. Kristiansen, J.E., *Dyes, antipsychotic drugs, and antimicrobial activity. Fragments of a development, with a special reference to the influence of Paul Ehrlich.* Dan Med Bull, 1989. **36**(2): p. 178-85.

190. Oz, M., D.E. Lorke, and G.A. Petroianu, *Methylene blue and Alzheimer's disease.* Biochem Pharmacol, 2009. **78**(8): p. 927-32.

191. Atamna, H. and R. Kumar, *Protective role of methylene blue in Alzheimer's disease via mitochondria and cytochrome c oxidase.* J Alzheimers Dis, 2010. **20 Suppl 2**: p. S439-52.

192. Medina, D.X., A. Caccamo, and S. Oddo, *Methylene blue reduces abeta levels and rescues early cognitive deficit by increasing proteasome activity.* Brain Pathol, 2011. **21**(2): p. 140-9.

193. Congdon, E.E., J.W. Wu, N. Myeku, Y.H. Figueroa, M. Herman, P.S. Marinec, et al., *Methylthioninium chloride (methylene blue) induces autophagy and attenuates tauopathy in vitro and in vivo.* Autophagy, 2012. **8**(4): p. 609-22.

194. Lin, A.L., E. Poteet, F. Du, R.C. Gourav, R. Liu, Y. Wen, et al., *Methylene blue as a cerebral metabolic and hemodynamic enhancer.* PLoS One, 2012. **7**(10): p. e46585.

195. Grayling, M. and C.D. Deakin, *Methylene blue during cardiopulmonary bypass to treat refractory hypotension in septic endocarditis.* J Thorac Cardiovasc Surg, 2003. **125**(2): p. 426-7.

196. Kwok, E.S.H. and D. Howes, *Use of methylene blue in sepsis: a systematic review.* J Intensive Care Med, 2006. **21**(6): p. 359-63.

197. Chen, Y., W. Zheng, Y. Li, J. Zhong, J. Ji, and P. Shen, *Apoptosis induced by methylene-blue-mediated photodynamic therapy in melanomas and the involvement of mitochondrial dysfunction revealed by proteomics.* Cancer Sci, 2008. **99**(10): p. 2019-27.

198. Lim, E.J., C.H. Oak, J. Heo, and Y.H. Kim, *Methylene blue-mediated photodynamic therapy enhances apoptosis in lung cancer cells.* Oncol Rep, 2013. **30**(2): p. 856-62.

199. Lu, Y., R. Jiao, X. Chen, J. Zhong, J. Ji, and P. Shen, *Methylene blue-mediated photodynamic therapy induces mitochondria-dependent apoptosis in HeLa cell.* J Cell Biochem, 2008. **105**(6): p. 1451-60.

200. Samy, N.A., M.M. Salah, M.F. Ali, and A.M. Sadek, *Effect of methylene blue-mediated photodynamic therapy for treatment of basal cell carcinoma.* Lasers Med Sci, 2015. **30**(1): p. 109-15.

201. Lee, Y.S. and R.D. Wurster, *Methylene blue induces cytotoxicity in human brain tumor cells.* Cancer Lett, 1995. **88**: p. 141-5.

202. Vrouenraets, M.B., G.W. Visser, G.B. Snow, and G.A. Van Dongen, *Basic principles, applications, in oncology, and improved selectivity of photodynamic therapy.* Anticancer Res, 2003. **23**(1B): p. 505-22.

203. Capella, M.A. and L.S. Capella, *A light in multidrug resistance: photodynamic treatment of multi-drug resistant tumors.* J Biomed Sci, 2003. **10**(4): p. 361-6.

204. Naylor, G.J., A.H. Smith, and P. Connelly, *A controlled trial of methylene blue in severe depressive illness.* Biol Psychiatry, 1987. **22**(5): p. 657-9.

205. Oz, M., D.E. Lorke, M. Hasan, and G.A. Petroianu, *Cellular and molecular actions of methylene blue in the nervous system.* Med Res Rev, 2011. **31**(1): p. 93-117.

206. Wegener, G., V. Volke, and R. Rosenberg, *Endogenous nitric oxide decreased hippocampal levels of serotonin and dopamine in vivo.* Br J Pharmacol, 2000. **130**(3): p. 575-80.

207. Dhir, A. and S.K. Kulkarni, *Involvement of nitric oxide (NO) signaling pathway in the antidepressant action of bupropion, a dopamine reuptake inhibitor.* Eur J Pharmacol, 2007. **568**(1-3): p. 177-85.

208. Talley Watts, L., J.A. Long, J. Chemello, S. Van Koughnet, A. Fernandez, S. Huang, et al., *Methylene blue is neuroprotective against mild traumatic brain injury.* J Neurotrauma, 2014. **31**(11): p. 1063-71.

209. Zhao, M., F. Liang, H. Xu, W. Yan, and J. Zhang, *Methylene blue exerts a neuroprotective effect against traumatic brain injury by promoting autophagy and inhibiting microglial activation.* Mol Med Rep, 2016. **13**(1): p. 13-20.

210. Sontag, E.M., G.P. Lotz, N. Agrawal, A. Tran, R. Aron, G. Yang, et al., *Methylene blue modulates huntingtin aggregation intermediates and is protective in Huntington's disease models.* J Neurosci, 2012. **32**(32): p. 11109-19.

211. Rojas, J.C., A.K. Bruchey, and F. Gonzalez-Lima, *Neurometabolic mechanisms for memory enhancement and neuroprotection of methylene blue.* Prog Neurobiol, 2012. **96**(1): p. 32-45.

212. Yang, S.H., W. Li, N. Sumien, M. Forster, J.W. Simpkins, and R. Liu, *Alternative mitochondrial electron transfer for the treatment of neurodegenerative diseases and cancers: Methylene blue connects the dots.* Prog Neurobiol, 2015.

213. Poteet, E., A. Winters, L.J. Yan, K. Shufelt, K.N. Green, J.W. Simpkins, et al., *Neuroprotective actions of methylene blue and its derivatives.* PLoS One, 2012. **7**(10): p. e48279.

214. Mocko, J.B., A. Kern, B. Moosmann, C. Behl, and P. Hajieva, *Phenothiazines interfere with dopaminergic neurodegeneration in Caenorhabditis elegans models of Parkinson's disease.* Neurobiol Dis, 2010. **40**(1): p. 120-9.

215. Gharib, A. and H. Atamna, *Methylene blue induces mitochondrial complex IV and improves cognitive function in old mice*, in *Neurodegeneration: Theory, Disorders and Treatments*, A.S. McNeill, Editor. 2011, Nova Science Publishers, Inc. p. 63-86.

216. Gonzalez-Lima, F., B.R. Barksdale, and J.C. Rojas, *Mitochondrial respiration as a target for neuroprotection and cognitive enhancement.* Biochem Pharmacol, 2014. **88**(4): p. 584-93.

217. Appleby, B.S., D. Nacopoulos, N. Milano, K. Zhong, and J.L. Cummings, *A review: treatment of Alzheimer's disease discovered in repurposed agents.* Dement Geriatr Cogn Disord, 2013. **35**(1-2): p. 1-22.

218. Hochgrafe, K., A. Sydow, D. Matenia, D. Cadinu, S. Konen, O. Petrova, et al., *Preventive methylene blue treatment preserves cognition in mice expressing full-length pro-aggregant human Tau.* Acta Neuropathol Commun, 2015. **3**: p. 25.

219. Deiana, S., C.R. Harrington, C.M. Wischik, and G. Riedel, *Methylthioninium chloride reverses cognitive deficits induced by scopolamine: comparison with rivastigmine.* Psychopharmacology (Berl), 2009. **202**(1-3): p. 53-65.

220. Wischik, C.M., P.C. Edwards, R.Y.K. Lai, M. Roth, and C.R. Harrington, *Selective inhibition of Alzheimer disease-like tau aggregation by phenothiazines.* Proc Natl Acad Sci U S A, 1996. **93**(20): p. 11213-8.

221. Crowe, A., M.J. James, V.M. Lee, A.B. Smith, 3rd, J.Q. Trojanowski, C. Ballatore, et al., *Aminothienopyridazines and methylene blue affect Tau fibrillization via cysteine oxidation.* J Biol Chem, 2013. **288**(16): p. 11024-37.

222. Necula, M., L. Breydo, S. Milton, R. Kayed, W.E. van der Veer, P. Tone, et al., *Methylene blue inhibits amyloid Abeta oligomerization by promoting fibrillization.* Biochemistry, 2007. **46**(30): p. 8850-60.

223. Paban, V., C. Manrique, M. Filali, S. Maunoir-Regimbal, F. Fauvelle, and B. Alescio-Lautier, *Therapeutic and preventive effects of methylene blue on Alzheimer's disease pathology in a transgenic mouse model.* Neuropharmacology, 2014. **76 Pt A**: p. 68-79.

224. Andhariya, N., B. Chudasama, R.V. Mehta, and R.V. Upadhyay, *Nanoengineering of methylene blue loaded silica encapsulated magnetite nanospheres and nanocapsules for photodynamic therapy.* Journal of Nanoparticle Research, 2011. **13**(9): p. 3619-3631.

225. El-Fattah, A., M. Al-Saadi, L. El-Khordagui, and S. Kandil, *Amphiphilic methoxy poly (ethylene glycol)/poly(ε-caprolactone) diblock copolymers as biomaterials for methylene blue nanoencapsulation.* International Journal of Chemical and Applied Biological Sciences, 2014. **1**(5): p. 32.

226. Hah, H.J., G. Kim, Y.E. Lee, D.A. Orringer, O. Sagher, M.A. Philbert, et al., *Methylene blue-conjugated hydrogel nanoparticles and tumor-cell targeted photodynamic therapy.* Macromol Biosci, 2011. **11**(1): p. 90-9.

227. Orringer, D.A., Y.E. Koo, T. Chen, G. Kim, H.J. Hah, H. Xu, et al., *In vitro characterization of a targeted, dye-loaded nanodevice for intraoperative tumor delineation.* Neurosurgery, 2009. **64**(5): p. 965-71; discussion 971-2.

228. Qin, M., H.J. Hah, G. Kim, G. Nie, Y.E.K. Lee, and R. Kopelman, *Methylene blue covalently loaded polyacrylamide nanoparticles for enhanced tumor-targeted photodynamic therapy.* Photochem Photobiol Sci, 2011. **10**(5): p. 832-41.

229. Simmer, K.A., H.J. Hah, Y.E.K. Lee, O. Sagher, D.A. Orringer, M.A. Philbert, et al., *Towards glioma intra-operative photodynamic therapy: Targeted photo-active nanoparticles in a brain tumor window model.* Int J Nanomed Nanosurg, 2015. **1**(2).

230. Tang, W., H. Xu, R. Kopelman, and M.A. Philbert, *Photodynamic characterization and in vitro applications of methylene blue-containing nanoparticle platforms.* Photochem Photobiol, 2005. **81**(2): p. 242-9.

231. Tang, W., H. Xu, E.J. Park, M.A. Philbert, and R. Kopelman, *Encapsulation of methylene blue in polyacrylamide nanoparticle platforms protects its photodynamic effectiveness.* Biochem Biophys Res Commun, 2008. **369**(2): p. 579-83.

232. Yoon, H.K., X. Lou, Y.C. Chen, Y.E. Koo Lee, E. Yoon, and R. Kopelman, *Nano-photosensitizers Engineered to Generate a Tunable Mix of Reactive Oxygen Species, for Optimizing Photodynamic Therapy, Using a Microfluidic Device.* Chem Mater, 2014. **26**(4): p. 1592-1600.

233. Caruthers, S.D., S.A. Wickline, and G.M. Lanza, *Nanotechnological applications in medicine.* Curr Opin Biotechnol, 2007. **18**(1): p. 26-30.

234. Ageitos, J.M., J. Chuah, and K. Numata, *Design considerations for properties of nanocarriers on disposition and efficiency of drug and gene delivery*, in *Nanomedicines:*

Design, Delivery and Detection, M. Braddock, Editor. 2016, Royal Society of Chemistry: Cambridge. p. 1-22.

235. Nikalje, A.P., *Nanotechnology and its applications in medicine.* Med Chem, 2015. **5**(2): p. 81-89.

236. Abhilash, M., *Potential applications of Nanoparticles.* Int J Pharm Bio Sci, 2010. **1**(1): p. 1-12.

237. Palombo, M., M. Deshmukh, D. Myers, J. Gao, Z. Szekely, and P.J. Sinko, *Pharmaceutical and toxicological properties of engineered nanomaterials for drug delivery.* Annu Rev Pharmacol Toxicol, 2014. **54**: p. 581-98.

238. Singh, R. and J.W. Lillard, Jr., *Nanoparticle-based targeted drug delivery.* Exp Mol Pathol, 2009. **86**(3): p. 215-23.

239. Doane, T.L. and C. Burda, *The unique role of nanoparticles in nanomedicine: imaging, drug delivery and therapy.* Chem Soc Rev, 2012. **41**: p. 2885-2911.

240. Gillies, E. and J. Frechet, *Dendrimers and dendritic polymers in drug delivery.* Drug Discovery Today, 2005. **10**(1): p. 35-43.

241. De Jong, W.H. and P.J.A. Borm, *Drug delivery and nanoparticles: Applications and hazards.* Int J Nanomedicine, 2008. **3**(2): p. 133-49.

242. Bozzuto, G. and A. Molinari, *Liposomes as nanomedical devices.* Int J Nanomedicine, 2015. **10**: p. 975-99.

243. Jamieson, T., R. Bakhshi, D. Petrova, R. Pocock, M. Imani, and A.M. Seifalian, *Biological applications of quantum dots.* Biomaterials, 2007. **28**(31): p. 4717-32.

244. Ramteke, K.H., S.A. Joshi, and S.N. Dhole, *Solid lipid nanoparticle: A review.* IOSR J Pharm, 2012. **2**(6): p. 34-44.

245. Muller, R.H., K. Mader, and S. Gohla, *Solid lipid nanoparticles (SLN) for controlled drug delivery - a review of the state of the art.* Eur J Pharm Biopharm, 2000. **50**(1): p. 161-77.

246. Otsuka, H., Y. Nagasaki, and K. Kataoka, *PEGylated nanoparticles for biological and pharmaceutical applications.* Advanced Drug Delivery Reviews, 2012. **64**: p. 246-255.

247. Giner-Casares, J.J., M. Henriksen-Lacey, M. Coronado-Puchau, and L.M. Liz-Marzan, *Inorganic nanoparticles for biomedicine: where materials scientists meet medical research.* Mater Today, 2016. **19**(1): p. 19-28.

248. Liong, M., J. Lu, M. Kovochick, T. Xia, S.G. Ruehm, A.E. Nel, et al., *Multifunctional inorganic nanoparticles for imaging, targeting, and drug delivery.* ACS Nano, 2008. **2**(5): p. 889-96.

249. Fadeel, B. and A.E. Garcia-Bennett, *Better safe than sorry: Understanding the toxicological properties of inorganic nanoparticles manufactured for biomedical applications.* Adv Drug Deliv Rev, 2010. **62**(3): p. 362-74.

250. Tonga, G.Y., D.F. MOyano, C.S. Kim, and V.M. Rotello, *Inorganic nanoparticles for therapeutic delivery: Trials, tribulations and promise.* Curr Opin Colloid Interface Sci, 2014. **19**(2): p. 49-55.

251. Zweers, M.L., G.H. Engbers, D.W. Grijpma, and J. Feijen, *In vitro degradation of nanoparticles prepared from polymers based on DL-lactide, glycolide and poly(ethylene oxide).* J Control Release, 2004. **100**(3): p. 347-56.

252. Soppimath, K.S., T.M. Aminabhavi, A.R. Kulkarni, and W.E. Rudzinski, *Biodegradable polymeric nanoparticles as drug delivery devices.* J Control Release, 2001. **70**(1-2): p. 1-20.

253. Jawahar, N. and S.N. Meyyanathan, *Polymeric nanoparticles for drug delivery and targeting: A comprehensive review.* International Journal of Health & Allied Sciences, 2012. **1**(4): p. 217.

254. Liang, R., L. Dong, R. Deng, J. Wang, K. Wang, M. Sullivan, et al., *Surfactant-free biodegradable polymeric nanoparticles generated from self-organized precipitation route: Cellular uptake and cytotoxicity.* European Polymer Journal, 2014. **57**: p. 187-201.

255. Gradishar, W.J., *Albumin-bound paclitaxel: a next-generation taxane.* Expert Opin Pharmacother, 2006. **7**(8): p. 1041-53.

256. Aggarwal, P., J.B. Hall, C.B. McLeland, M.A. Dobrovolskaia, and S.E. McNeil, *Nanoparticle interaction with plasma proteins as it relates to particle biodistribution, biocompatibility and therapeutic efficacy.* Adv Drug Deliv Rev, 2009. **61**(6): p. 428-37.

257. Torcello-Gómez, A., M.J. Santander-Ortega, J.M. Peula-García, J. Maldonado-Valderrama, M.J. Gálvez-Ruiz, J.L. Ortega-Vinuesa, et al., *Adsorption of antibody onto Pluronic F68-covered nanoparticles: link with surface properties.* Soft Matter, 2011. **7**(18): p. 8450.

258. Kumari, A., S.K. Yadav, and S.C. Yadav, *Biodegradable polymeric nanoparticles based drug delivery systems.* Colloids Surf B Biointerfaces, 2010. **75**(1): p. 1-18.

259. Athanasiou, K.A., G.G. Niederauer, and C.M. Agrawal, *Sterilization, toxicity, biocompatibility and clinical applications of polylactic acid/ polyglycolic acid copolymers.* Biomaterials, 1996. **17**(2): p. 93-102.

260. El-Egakey, M.A., V. Bentele, and J. Kreuter, *Molecular weights of polycyanoacrylate nanoparticles.* Int J Pharm, 1983. **13**(3): p. 349-52.

261. Robello, D.R., T.D. Eldridge, and M.T. Swanson, *Degradation and stabilization of polycyanoacrylates.* J Polym Sci A Polym Chem, 1999. **37**(24): p. 4570-81.

262. Matsumura, S., *Mechanism of biodegradation*, in *Biodegradable polymers for industrial applications*, R. Smith, Editor. 2005, CRC Press, LLC: Boca Raton, Florida. p. 357-410.

263. Pohlmann, A.R., F.N. Fonseca, K. Paese, C.B. Detoni, K. Coradini, R.C.R. Beck, et al., *Poly(ε-caprolactone) microcapsules and nanocapsules in drug delivery.* Expert Opin Drug Deliv, 2013. **10**(5): p. 623-38.

264. Woodruff, M.A. and D.W. Hutmacher, *The return of a forgotten polymer - Polycaprolactone in the 21st century.* Prog Polym Sci, 2010. **35**(10): p. 1217-56.

265. Meng, Z.X., W. Zheng, L. Li, and Y.F. Zheng, *Fabrication and characterization of three-dimensional nanofiber membrance of PCL-MWCNTs by electrospinning.* Mater Sci Eng C Mater Biol Appl, 2010. **30**: p. 1014-21.

266. Dinarvand, R., N. Sepehri, S. Manoochehri, H. Rouhani, and F. Atyabi, *Polylactide-co-glycolide nanoparticles for controlled delivery of anticancer agents.* Int J Nanomedicine, 2011. **6**: p. 877-95.

267. Danhier, F., E. Ansorena, J.M. Silva, R. Coco, A. Le Breton, and V. Preat, *PLGA-based nanoparticles: an overview of biomedical applications.* J Control Release, 2012. **161**(2): p. 505-22.

268. Makadia, H.K. and S.J. Siegel, *Poly Lactic-co-Glycolic Acid (PLGA) as Biodegradable Controlled Drug Delivery Carrier.* Polymers (Basel), 2011. **3**(3): p. 1377-1397.

269. Singh-Joy, S.D. and V.C. McLain, *Safety assessment of poloxamers 101, 105, 108, 122, 123, 124, 181, 182, 183, 184, 185, 188, 212, 215, 217, 231, 234, 235, 237, 238, 282, 284, 288, 331, 333, 334, 335, 338, 401, 402, 403, and 407, poloxamer 105 benzoate, and*

poloxamer 182 dibenzoate as used in cosmetics. Int J Toxicol, 2008. **27 Suppl 2**: p. 93-128.

270. Semete, B., L. Booysen, Y. Lemmer, L. Kalombo, L. Katata, J. Verschoor, et al., *In vivo evaluation of the biodistribution and safety of PLGA nanoparticles as drug delivery systems.* Nanomedicine, 2010. **6**(5): p. 662-71.

271. Sempf, K., T. Arrey, S. Gelperina, T. Schorge, B. Meyer, M. Karas, et al., *Adsorption of plasma proteins on uncoated PLGA nanoparticles.* Eur J Pharm Biopharm, 2013. **85**(1): p. 53-60.

272. Turk, C.T.S., Z.S. Bayindir, and U. Badilli, *Preparation of polymeric nanoparticles using different stabilizing agents.* J Fac Pharm Ankara, 2009. **38**(4): p. 257-68.

273. Santander-Ortega, M.J., A.B. Jodar-Reyes, N. Csaba, D. Bastos-Gonzalez, and J.L. Ortega-Vinuesa, *Colloidal stability of pluronic F68-coated PLGA nanoparticles: a variety of stabilisation mechanisms.* J Colloid Interface Sci, 2006. **302**(2): p. 522-9.

274. Kulkarni, S.A. and S.S. Feng, *Effects of particle size and surface modification on cellular uptake and biodistribution of polymeric nanoparticles for drug delivery.* Pharm Res, 2013. **30**(10): p. 2512-22.

275. Albanese, A., P.S. Tang, and W.C.W. Chan, *The effect of nanoparticle size, shape, and surface chemistry on biological systems.* Annu Rev Biomed Eng, 2012. **14**: p. 1-16.

276. Frohlich, E., *The role of surface charge in cellular uptake and cytotoxicity of medical nanoparticles.* Int J Nanomedicine, 2012. **7**: p. 5577-91.

277. Alexis, F., E.M. Pridgen, L.K. Molnar, and O.C. Farokhzad, *Factors affecting the clearance and biodistribution of polymeric nanoparticles.* Mol Pharm, 2008. **5**(4): p. 505-15.

278. Pamujula, S., S. Hazari, G. Bolden, R.A. Graves, D.D. Chinta, S. Dash, et al., *Cellular delivery of PEGylated PLGA nanoparticles.* J Pharm Pharmacol, 2012. **64**(1): p. 61-7.

279. Knop, K., R. Hoogenboom, D. Fischer, and U.S. Schubert, *Poly(ethylene glycol) in drug delivery: Pros and cons as well as potential alternatives.* Angew Chem Int Ed Engl, 2010. **49**: p. 6288-308.

280. Menon, J.U., S. Kona, A.S. Wadajkar, F. Desai, A. Vadla, and K.T. Nguyen, *Effects of surfactants on the properties of PLGA nanoparticles.* J Biomed Mater Res A, 2012. **100**(8): p. 1998-2005.

281. Sahoo, S.K., J. Panyam, S. Prabhu, and V. Labhasetwar, *Residual polyvinyl alcohol associated with poly(D,L-lactide-co-glycolide) nanoparticles affects their physical properties and cellular uptake.* J Control Release, 2002. **82**(1): p. 105-14.

282. Kabanov, A.V. and V.Y. Alakhov, *Pluronic block copolymers in drug delivery: From micellar nanocontainers to biological response modifiers.* Crit Rev Ther Drug Carrier Syst, 2002. **19**(1): p. 1-72.

283. Kabanov, A.V., E.V. Batrakova, and V.Y. Alakhov, *Pluronic block copolymers for overcoming drug resistance in cancer.* Adv Drug Deliv Rev, 2002. **54**(5): p. 759-79.

284. Yan, F., C. Zhang, Y. Zheng, L. Mei, L. Tang, C. Song, et al., *The effect of poloxamer 188 on nanoparticle morphology, size, cancer cell uptake, and cytotoxicity.* Nanomedicine, 2010. **6**(1): p. 170-8.

285. Parnaud, G., S. Tache, G. Peiffer, and D.E. Corpet, *Pluronic F68 block polymer, very potent suppressor of carcinogenesis in colon of rats and mice.* Br J Cancer, 2001. **84**(1): p. 90-3.

286. Rodeheaver, G.T., L. Kurtz, B.J. Kircher, and R.F. Edlich, *Pluronic F68: A promising new skin wound cleanser.* Am J Surg, 1976. **132**: p. 67.

287. Gosselin, A.M. and G.P. Biro, *The cardiovascular effects of the surfactant pluronic F68 in anesthetized dogs.* Adv Exp Med Biol, 1990. **277**: p. 291-9.

288. Batrakova, E.V., S. Lee, S. Li, A. Venne, V.Y. Alakhov, and A.V. Kabanov, *Fundamental relationships between the composition of pluronic block copolymers and their hypersensitization effect in MDR cancer cells.* Pharm Res, 1999. **16**(9): p. 1373-9.

289. Silk, M. and E. Sigman, *Effect of pluronic F68 on the development of tumor metastasis.* Cancer, 1972. **29**(1): p. 171-2.

290. Batrakova, E.V., S. Li, W.F. Elmquist, D.W. Miller, V.Y. Alakhov, and A.V. Rabanov, *Mechanism of sensitization of MDR cancer cells by Pluronic block copolymers: Selective energy depletion.* Br J Cancer, 2001. **85**(12): p. 1987-97.

291. Miller, D.W., E.V. Batrakova, and A.V. Kabanov, *Inhibition of multidrug resistance-associated protein (MRP) functional activity with pluronic block copolymers.* Pharm Res, 1999. **16**(3): p. 396-401.

292. Vandervoort, J. and A. Ludwig, *Biocompatible stabilizers in the preparation of PLGA nanoparticles: a factorial design study.* Int J Pharm, 2002. **238**: p. 77-92.

293. Zhang, L., J.M. Chan, F.X. Gu, J. Rhee, A.Z. Wang, A.F. Radovic-Moreno, et al., *Self-assembled lipid-polymer hybrid nanoparticles: A robust drug delivery platform.* ACS Nano, 2008. **2**(8): p. 1696-702.

294. Hadinoto, K., A. Sundaresan, and W.S. Cheow, *Lipid-polymer hybrid nanoparticles as a new generation therapeutic delivery platform: A review.* Eur J Pharm Biopharm, 2013. **85**(3 Pt A): p. 427-43.

295. Zhang, L.I. and L. Zhang, *Lipid–Polymer Hybrid Nanoparticles: Synthesis, Characterization and Applications.* Nano LIFE, 2010. **01**(01n02): p. 163-173.

296. Wohlfart, S., S. Gelperina, and J. Kreuter, *Transport of drugs across the blood-brain barrier by nanoparticles.* J Control Release, 2012. **161**(2): p. 264-73.

297. Lockman, P.R., R.J. Mumper, M.A. Khan, and D.D. Allen, *Nanoparticle technology for drug delivery across the blood-brain barrier.* Drug Dev Ind Pharm, 2002. **28**(1): p. 1-12.

298. Masserini, M., *Nanoparticles for brain drug delivery.* ISRN Biochem, 2013. **2013**: p. 238428.

299. Alyautdin, R., I. Khalin, M.I. Nafeeza, M.H. Haron, and D. Kuznetsov, *Nanoscale drug delivery systems and the blood-brain barrier.* Int J Nanomedicine, 2014. **9**: p. 795-811.

300. Dinda, S.C. and G. Pattnaik, *Nanobiotechnology-based drug delivery in brain targeting.* Curr Pharm Biotechnol, 2013. **14**(15): p. 1264-74.

301. Grover, A. and A. Hirani, *Nanoparticle-Based Brain Targeted Delivery Systems.* Journal of Biomolecular Research & Therapeutics, 2013. **02**(02): p. e113.

302. Harpreet, K. and S. Gurpreet, *In vivo methods to study uptake of nanoparticles into the brain.* J Drug Deliv Ther, 2013. **3**(4): p. 173-7.

303. Lahkar, S. and M.K. Das, *Surface modified polymeric nanoparticles for brain targeted drug delivery.* Curr Trends Biotechnol Pharm, 2013. **7**(4): p. 914-31.

304. Pinzon-Daza, M.L., I. Campia, J. Kopecka, R. Garzon, D. Ghigo, and C. Riganti, *Nanoparticle- and liposome-carried drugs: New strategies for active targeting and drug delivery across blood-brain barrier.* Curr Drug Metab, 2013. **14**(6): p. 625-40.

305. McCarthy, D.J., M. Malhotra, A.M. O'Mahony, J.F. Cryan, and C.M. O'Driscoll, *Nanoparticles and the blood-brain barrier: Advancing from in vitro models towards therapeutic significance.* Pharm Res, 2015. **32**(4): p. 1161-85.

306. Cupaioli, F.A., F.A. Zucca, D. Boraschi, and L. Zecca, *Engineered nanoparticles. How brain friendly is this new guest?* Prog Neurobiol, 2014. **119-120**: p. 20-38.

307. Rempe, R., S. Cramer, R. Qiao, and H.J. Galla, *Strategies to overcome the barrier: use of nanoparticles as carriers and modulators of barrier properties.* Cell Tissue Res, 2014. **355**(3): p. 717-26.

308. Voigt, N., P. Henrich-Noack, S. Kockentiedt, W. Hintz, J. Tomas, and B.A. Sabel, *Surfactants, not size or zeta-potential influence blood-brain barrier passage of polymeric nanoparticles.* Eur J Pharm Biopharm, 2014. **87**(1): p. 19-29.

309. Kreuter, J., *Drug delivery to the central nervous system by polymeric nanoparticles: what do we know?* Adv Drug Deliv Rev, 2014. **71**: p. 2-14.

310. Loureiro, J.A., B. Gomes, M.A.N. Coelho, M. do Carmo Pereira, and S. Rocha, *Targeting nanoparticless across the blood-brain barrier with monoclonal antibodies.* Nanomedicine, 2014. **9**(5): p. 709-22.

311. Neha, B., B. Ganesh, and K. Preeti, *Drug delivery to the brain using polymeric nanoparticles: A review.* IJPLS, 2013. **2**(3): p. 107-32.

312. Lu, C., Y. Zhao, H.L. Wong, J. Cai, L. Peng, and X. Tian, *Current approaches to enhance CNS delivery of drugs across the brain barriers.* Int J Nanomed, 2014. **9**: p. 2241-57.

313. Gelperina, S., O. Maksimenko, A. Khalansky, L. Vanchugova, E. Shipulo, K. Abbasova, et al., *Drug delivery to the brain using surfactant-coated poly(lactide-co-glycolide)*

nanoparticles: influence of the formulation parameters. Eur J Pharm Biopharm, 2010. **74**(2): p. 157-63.

314. Kulkarni, S.A. and S.S. Feng, *Effects of surface modification on delivery efficiency of biodegradable nanoparticles across the blood-brain barrier.* Nanomedicine (Lond), 2011. **6**(2): p. 377-94.

315. Kreuter, J., *Mechanism of polymeric nanoparticle-based drug transport across the blood-brain barrier (BBB).* J Microencapsul, 2013. **30**(1): p. 49-54.

316. Saraiva, C., C. Praca, R. Ferreira, T. Santos, L. Ferreira, and L. Bernardino, *Nanoparticle-mediated brain drug delivery: Overcoming blood-brain barrier to treat neurodegenerative diseases.* J Control Release, 2016. **235**: p. 34-47.

317. Michaelis, K., M.M. Hoffmann, S. Dreis, E. Herbert, R.N. Alyautdin, M. Michaelis, et al., *Covalent linkage of apolipoprotein e to albumin nanoparticles strongly enhances drug transport into the brain.* J Pharmacol Exp Ther, 2006. **317**(3): p. 1246-53.

318. Hu, K., Y. Shi, W. Jiang, J. Han, S. Huang, and X. Jiang, *Lactoferrin conjugated PEG-PLGA nanoparticles for brain delivery: preparation, characterization and efficacy in Parkinson's disease.* Int J Pharm, 2011. **415**(1-2): p. 273-83.

319. Hu, K., J. Li, Y. Shen, W. Lu, X. Gao, Q. Zhang, et al., *Lactoferrin-conjugated PEG-PLA nanoparticles with improved brain delivery: In vitro and in vivo evaluations.* J Control Release, 2009. **134**(1): p. 55-61.

320. Ji, B., J. Maeda, and M. Higuchi, *Pharmacokinetics and brain uptake of lactoferrin in rats.* Life Sci, 2006. **78**: p. 851-5.

321. Ulbrich, K., T. Knobloch, and J. Kreuter, *Targeting the insulin receptor: nanoparticles for drug delivery across the blood-brain barrier (BBB).* J Drug Target, 2011. **19**(2): p. 125-32.

322. Marchetti, C., I. Palaia, M. Giorgini, C. De Medici, R. Iadarola, L. Vertechy, et al., *Targeted drug delivery via folate receptors in recurrent ovarian cancer: a review.* Onco Targets Ther, 2014. **7**: p. 1223-36.

323. Wang, C., L. Feng, X. Yang, F. Wang, and W. Lu, *Folic acid-conjugated liposomal vincristine for multidrug resistant cancer therapy.* Asian J Pharm Sci, 2013. **8**: p. 118-27.

324. Vauthier, C., C. Dubernet, C. Chauvierre, I. Brigger, and P. Couvreur, *Drug delivery to resistant tumors: the potential of poly(alkyl cyanoacrylate) nanoparticles.* J Control Release, 2003. **93**(2): p. 151-60.

325. Kreuter, J., D. Shamenkov, V. Petrov, P. Ramge, K. Cychutek, C. Koch-Brandt, et al., *Apolipoprotein-mediated transport of nanoparticle-bound drugs across the blood-brain barrier.* J Drug Target, 2002. **10**(4): p. 317-25.

326. Win, K.Y. and S.S. Feng, *Effects of particle size and surface coating on cellular uptake of polymeric nanoparticles for oral delivery of anticancer drugs.* Biomaterials, 2005. **26**(15): p. 2713-22.

327. Kim, T.Y., D.W. Kim, J.Y. Chung, S.G. Shin, S.C. Kim, D.S. Heo, et al., *Phase I and pharmacokinetic study of Genexol-PM, a cremophor-free, polymeric micelle-formulated paclitaxel, in patients with advanced malignancies.* Clin Cancer Res, 2004. **10**(11): p. 3708-16.

328. Danhier, F., B. Vroman, N. Lecouturier, N. Crokart, V. Pourcelle, H. Freichels, et al., *Targeting of tumor endothelium by RGD-grafted PLGA-nanoparticles loaded with with paclitaxel.* J Control Release, 2009. **140**(2): p. 166-73.

329. Moreno, D., C.T. de Ilarduya, E. Bandres, M. Bunuales, M. Azcona, J. Garcia-Foncillas, et al., *Characterization of cisplatin cytotoxicity delivered from PLGA-systems.* Eur J Pharm Biopharm, 2008. **68**: p. 503-12.

330. Moreno, D., S. Zalba, I. Navarro, C.T. de Ilarduya, and M.J. Garrido, *Pharmacodynamics of cisplatin-loaded PLGA nanoparticles administered to tumor-bearing mice.* Eur J Pharm Biopharm, 2010. **74**: p. 265-74.

331. Jain, A.K., N.K. Swarnakar, C. Godugu, R.P. Singh, and S. Jain, *The effect of the oral administration of polymeric nanoparticles on the efficacy and toxicity of tamoxifen.* Biomaterials, 2011. **32**: p. 503-15.

332. Renoir, J.M., B. Stella, T. Ameller, E. Connault, P. Opolon, and V. Marsaud, *Improved anti-tumoral capacity of mixed and pure anti-oestrogens in breast cancer cell xenografts after their administration by entrapment in colloidal nanosystems.* J Steroid Biochem Mol Biol, 2006. **102**: p. 114-27.

333. Gryparis, E.C., M. Hatziapostolou, E. Papdimitriou, and K. Avgoustakis, *Anticancer activity of cisplatin-loaded PLGA-mPEG nanoparticles on LNCaP prostate cancer cells.* Eur J Pharm Biopharm, 2007. **67**(1): p. 1-8.

334. Mukerjee, A. and J.K. Vishwanatha, *Formulation, characterization and evaluation of curcumin loaded PLGA nanospheres for cancer therapy.* Anticancer Res, 2009. **29**(10): p. 3867-75.

335. Khalil, N.M., T.C. do Nascimento, D.M. Casa, L.F. Dalmolin, A.C. de Mattos, I. Hoss, et al., *Pharmacokinetics of curcumin-loaded PLGA and PLGA-PEG blend nanoparticles after oral administration in rats.* Colloids Surf B Biointerfaces, 2013. **101**: p. 353-60.

336. Cohen, E.M., H. Ding, C.W. Kessinger, C. Khemtong, J. Gao, and B.D. Sumer, *Polymeric micelle nanoparticles for photodynamic treatment of head and neck cancer cells.* Otolaryngol Head Neck Surg, 2010. **143**(1): p. 109-15.

337. Yoo, H.S. and T.G. Park, *Folate receptor targeted biodegradable polymeric doxorubicin micelles.* J Control Release, 2004. **96**(2): p. 273-83.

338. Le Droumaguet, B., J. Nicolas, D. Brambilla, S. Mura, A. Maksimenko, L. De Kimpe, et al., *Versatile and efficient targeting using single nanoparticulate platform: Application to cancer and Alzheimer's disease.* ACS Nano, 2012. **6**(7): p. 5866-79.

339. Sahoo, S.K. and V. Labhasetwar, *Enhanced antiproliferative activity of transferrin-conjugated paclitaxel-loaded nanoparticles is mediated via sustained intracellular drug retentiion.* Mol Pharm, 2005. **2**(5): p. 373-83.

340. Graf, N., D.R. Bielenberg, N. Kolishetti, C. Muus, J. Banyard, O.C. Farokhzad, et al., *α(V)β(3) integrin-targeted PLGA-PEG nanoparticles for enhanced anti-tumor efficacy of a Pt(IV) prodrug.* ACS Nano, 2012. **6**: p. 4530-9.

341. Aggarwal, S., S.C. Yadav, and S. Gupta, *EGFR targeted PLGA nanoparticles using gemcitabine for treatment of pancreatic cancer.* J Biomed Nanotechnol, 2011. **7**: p. 137-8.

342. Punfa, W., S. Yodkeeree, P. Pitchakarn, C. Ampasavate, and P. Limtrakul, *Enhancement of cellular uptake and cytotoxicity of curcumin-loaded PLGA nanoparticles by*

conjugation with anti-P-glycoprotein in drug resistance cancer cells. Acta Pharmacol Sin, 2012. **33**(6): p. 823-31.

343. Farokhzad, O.C., S. Jon, A. Khademhosseini, T.N. Tran, D.A. Lavan, and R. Langer, *Nanoparticle-aptamer bioconjugates: a new approach for targeting prostate cancer cells.* Cancer Res, 2004. **64**(21): p. 7668-72.

344. Hrkach, J., D. Vo Hoff, A.M. Mukkaram, E. Andrianova, J. Auer, T. Campbell, et al., *Preclinical development and clinical translation of a PSMA-targeted docetaxel nanoparticle with a differentiated pharmacological profile.* Sci Transl Med, 2012. **4**(128): p. 128ra39.

345. Dhar, S., F.X. Gu, R. Langer, O.C. Farokhzad, and S.J. Lippard, *Targeted delivery of cisplatin to prostate cancer cells by aptamer functionalized Pt(IV) prodrug-PLGA-PEG nanoparticles.* Proc Natl Acad Sci U S A, 2008. **105**: p. 17356-61.

346. Yang, J., S.X. Xie, Y. Huang, M. Ling, J. Liu, Y. Ran, et al., *Prostate-targeted biodegradable nanoparticles loaded with androgen receptor silencing constructs eradicate xenograft tumors in mice.* Nanomedicine, 2012. **7**: p. 1297-309.

347. Kocbek, P., N. Obermajer, M. Cegnar, J. Kos, and J. Kristl, *Targeting cancer cells using PLGA nanoparticles surface modified with monoclonal antibody.* J Control Release, 2007. **120**(1-2): p. 18-26.

348. Thamake, S.I., S.L. Raut, A.P. Ranjan, Z. Gryczynski, and J.K. Vishwanatha, *Surface functionalization of PLGA nanoparticles by non-covalent insertion of a homo-bifunctional spacer for active targeting in cancer therapy.* Nanotechnology, 2011. **22**(3): p. 035101.

349. Wohlfart, S., A.S. Khalansky, S. Gelperina, O. Maksimenko, C. Bernreuther, M. Glatzel, et al., *Efficient chemotherapy of rat glioblastoma using doxorubicin-loaded PLGA nanoparticles with different stabilizers.* PLoS One, 2011. **6**(5): p. e19121.

350. Petri, B., A. Bootz, A. Khalansky, T. Hekmatara, R.H. Muller, R. Uhl, et al., *Chemotherapy of brain tumour using doxorubicin bound to surfactant-coated poly(butyl cyanoacrylate) nanoparticles: Revisiting the role of surfactants.* J Control Release, 2007. **117**(1): p. 51-8.

351. Wang, C.X., L.S. Huang, L.B. Hou, L. Jiang, Z.T. Yan, and Y.L. Wang, *Anti-tumor effects of polysorbate-80 coated gemcitabine polybutyl-cyanoacrylate nanoparticles in vitro and its pharmacodynamics in vivo on C6 glioma cells of a brain tumor model* Brain Res, 2009. **1261**: p. 91-9.

352. Gulyaev, A.E., S. Gelperina, I.N. Skidan, A.S. Antropov, G.Y. Kivman, and J. Kreuter, *Significant transport of doxorubicin into the brain with polysorbate 80-coated nanoparticles.* Pharm Res, 1999. **16**(10): p. 1564-9.

353. Hekmatara, T., C. Bernreuther, A. Khalansky, A. Theisen, J. Weissenberger, S. Gelperina, et al., *Efficient systemic therapy of rat glioblastoma by nanoparticle-bound doxorubicin is due to antiangiogenic effects.* Clin Neuropathol, 2009. **28**: p. 153-64.

354. Xin, H., L. Chen, J. Gu, X. Ren, Z. Wei, J. Luo, et al., *Enhanced anti-glioblastoma efficacy by PTX-loaded PEGylated poly(ε-caprolactone) nanoparticles: in vitro and in vivo evaluation.* Int J Pharm, 2010. **402**: p. 238-47.

355. Nance, E., C. Zhang, T.Y. Shih, Q. Xu, B.S. Schuster, and J. Hanes, *Brain-penetrating nanoparticles improve paclitaxel efficacy in malignant glioma following local administration.* ACS Nano, 2014. **8**(10): p. 10655-64.

356. Grover, A., A. Hirani, Y. Pathak, and V. Sutariya, *Brain-targeted delivery of docetaxel by glutathione-coated nanoparticles for brain cancer.* AAPS PharmSciTech, 2014. **15**(6): p. 1562-8.

357. Geldenhuys, W., T. Mbimba, T. Bui, K. Harrison, and V. Sutariya, *Brain-targeted delivery of paclitaxel using glutathione-coated nanoparticles for brain cancers.* J Drug Target, 2011. **19**(9): p. 837-45.

358. Cui, Y., Q. Xu, P.K. Chow, D. Wang, and C.H. Wang, *Transferrin-conjugated magnetic silica PLGA nanoparticles loaded with doxorubicin and paclitaxel for brain glioma treatment.* Biomaterials, 2013. **34**(33): p. 8511-20.

359. Gao, H., Y. Xiong, S. Zhang, Z. Yang, S. Cao, and X. Jiang, *RGD and interleukin-13 peptide functionalized nanoparticles for enhanced glioblastoma cells and neovasculature dual targeting delivery and elevated tumor penetration.* Mol Pharm, 2014. **11**(3): p. 1042-52.

360. Gao, H., Z. Yang, S. Cao, Y. Xiong, S. Zhang, Z. Pang, et al., *Tumor cells and neovasculature dual targeting delivery for glioblastoma treatment.* Biomaterials, 2014. **35**(7): p. 2374-82.

361. Kang, T., X. Gao, Q. Hu, D. Jiang, X. Feng, X. Zhang, et al., *iNGR-modified PEG-PLGA nanoparticles that recognize tumor vasculature and penetrate gliomas.* Biomaterials, 2014. **35**(14): p. 4319-32.

362. Herrmann, K., Y.E.L. Koo, D.A. Orringer, O. Sagher, M.A. Philbert, and R. Kopelman, *Photodynamic characterization and optimization using multifunctional nanoparticles for brain cancer treatment.* SPIE BiOS, 2013. **8568**(1): p. 856801.

363. *Cancer facts and figures 2015*. 2015, American Cancer Society: Atlanta, Georgia.

364. Feun, L.G., N. Savaraj, and H.J. Landy, *Drug resistance in brain tumors.* J Neurooncol, 1994. **20**(2): p. 165-176.

365. Robert, M.C. and M. Wastie, *Glioblastoma multiforme: a rare manifestation of extensive liver and bone metastases.* Biomed Imaging Interv J, 2008. **4**(1): p. e3.

366. Mischel, P.S., R. Shai, T. Shi, S. Horvath, K.V. Lu, G. Choe, et al., *Identification of molecular subtypes of glioblastoma by gene expression profiling.* Oncogene, 2003. **22**(15): p. 2361-73.

367. Shai, R., T. Shi, T.J. Kremen, S. Horvath, L.M. Liau, T.F. Cloughesy, et al., *Gene expression profiling identifies molecular subtypes of gliomas.* Oncogene, 2003. **22**(31): p. 4918-23.

368. Phillips, H.S., S. Kharbanda, R. Chen, W.F. Forrest, R.H. Soriano, T.D. Wu, et al., *Molecular subclasses of high-grade glioma predict prognosis, delineate a pattern of disease progression, and resemble stages in neurogenesis.* Cancer Cell, 2006. **9**(3): p. 157-73.

369. Verhaak, R.G., K.A. Hoadley, E. Purdom, V. Wang, Y. Qi, M.D. Wilkerson, et al., *Integrated genomic analysis identifies clinically relevant subtypes of glioblastoma characterized by abnormalities in PDGFRA, IDH1, EGFR, and NF1.* Cancer Cell, 2010. **17**(1): p. 98-110.

370. Poteet, E., G.R. Choudhury, A. Winters, W. Li, M.G. Ryou, R. Liu, et al., *Reversing the Warburg effect as a treatment for glioblastoma.* J Biol Chem, 2013. **288**(13): p. 9153-64.

371. Peter, C., D. Hongwan, A. Kupfer, and B.H. Lauterburg, *Pharmacokinetics and organ distribution of intravenous and oral methylene blue.* Eur J Clin Pharmacol, 2000. **56**(3): p. 247-50.

372. Ranjan, A.P., A. Mukerjee, L. Helson, and J.K. Vishwanatha, *Scale up, optimization and stability analysis of curcumin C3 complex-loaded nanoparticles for cancer therapy.* J Nanobiotechnology, 2012. **10**: p. 38.

373. Thamake, S.I., S.L. Raut, Z. Gryczynski, A.P. Ranjan, and J.K. Vishwanatha, *Alendronate coated poly-lactic-co-glycolic acid (PLGA) nanoparticles for active targeting of metastatic breast cancer.* Biomaterials, 2012. **33**(29): p. 7164-73.

374. Braden, A.R., M.T. Kafka, L. Cunningham, H. Jones, and J.K. Vishwanatha, *Polymeric nanoparticles for sustained down-regulation of annexin A2 inhibit prostate tumor growth.* J Nanosci Nanotech, 2009. **9**(5): p. 907-11.

375. Chiu, S.S., E. Lui, M. Majeed, J.K. Vishwanatha, A.P. Ranjan, A. Maitra, et al., *Differential distribution of intravenous curcumin formulations in the rat brain.* Anticancer Res, 2011. **31**(3): p. 907-11.

376. Yan, F., Y. Zhang, K.S. Kim, H. Yuan, and T. Vo-Dinh, *Cellular uptake and photodynamic activity of protein nanocages containing methylene blue photosensitizing drug.* Photochem Photobiol, 2010. **86**(3): p. 662-6.

377. Jinwal, U.K., A. Groshev, J. Zhang, A. Grover, and V.B. Sutariya, *Preparation and characterization of methylene blue nanoparticles for Alzheimer's disease and other tauopathies.* Curr Drug Deliv, 2014. **11**(4): p. 541-50.

378. Khanal, A., M.P. Bui, and S.S. Seo, *Microgel-encapsulated methylene blue for the treatment of breast cancer cells by photodynamic therapy.* J Breast Cancer, 2014. **17**(1): p. 18-24.

379. Khdair, A., D. Chen, Y. Patil, L. Ma, Q.P. Dou, M.P. Shekhar, et al., *Nanoparticle-mediated combination chemotherapy and photodynamic therapy overcomes tumor drug resistance.* J Control Release, 2010. **141**(2): p. 137-44.

380. Khdair, A., B. Gerard, H. Handa, G. Mao, M.P. Shekhar, and J. Panyam, *Surfactant-polymer nanoparticles enhance the effectiveness of anticancer photodynamic therapy*. Mol Pharm, 2008. **5**(5): p. 795-807.

381. Patel, N.B., *Targeted methylene blue-containing polymeric nanoparticle formulations for oral antimicrobial photodynamic therapy*, in *Department of Pharmaceutical Sciences*. 2009, Northeastern University: Boston, Massachusetts. p. 33.

382. Planas, O., R. Bresoli-Obach, J. Nos, T. Gallavardin, R. Ruiz-Gonzalez, M. Agut, et al., *Synthesis, photophysical characterization, and photoinduced antibacterial activity of methylene blue-loaded amino- and mannose-targeted mesoporous silica nanoparticles.* Molecules, 2015. **20**(4): p. 6284-98.

383. Sahu, A., W.I. Choi, J.H. Lee, and G. Tae, *Graphene oxide mediated delivery of methylene blue for combined photodynamic and photothermal therapy.* Biomaterials, 2013. **34**(26): p. 6239-48.

384. Seong, D.Y. and Y.J. Kim, *Enhanced photodynamic therapy efficacy of methylene blue-loaded calcium phosphate nanoparticles.* J Photochem Photobiol B, 2015. **146**: p. 34-43.

385. Simon, T., S. Boca-Farcau, A.M. Gabudean, P. Baldeck, and S. Astilean, *LED-activated methylene blue-loaded Pluronic-nanogold hybrids for in vitro photodynamic therapy.* J Biophotonics, 2013. **6**(11-12): p. 950-9.

386. Tang, W., H. Xu, R. Kopelman, and M.A. Philbert, *Photodynamic characterization and in vitro application of methylene blue-containing nanoparticle platforms.* Photochem Photobiol, 2005. **81**(2): p. 242-9.

387. Yu, J., C. Hsu, C. Huang, and P. Chang, *Development of therapeutic Au-methylene blue nanoparticles for targeted photodynamic therapy of cervical cancer cells.* ACS Appl Mater Interfaces, 2015. **7**(1): p. 432-441.

388. Warburg, O., *Uber den Stoffwechsel der Carcinomzelle.* J Mol Med, 1925. **4**(12): p. 534-6.

389. Warburg, O., *On the origin of cancer cells.* Science, 1956. **123**(3191): p. 309-14.

390. Kroemer, G., *Mitochondria in cancer.* Oncogene, 2006. **25**(34): p. 4630-2.

391. Mischel, P.S., *HOT models in flux: mitochondrial glucose oxidation fuels glioblastoma growth.* Cell Metab, 2012. **15**(6): p. 789-90.

392. Modica-Napolitano, J.S. and K.K. Singh, *Mitochondrial dysfunction in cancer.* Mitochondrion, 2004. **4**(5-6): p. 755-62.

393. König, K., V. Bockhorn, W. Dietel, and H. Schubert, *Photochemotherapy of animal tumors with the photosensitizer methylene blue using a krypton laser.* J Cancer Res Clin Oncol, 1987. **113**(3): p. 301-3.

394. Guttmann, P. and P. Ehrlich, *Ueber die Wirkung des Methylenblau bei Malaria (On the effect of methylene blue on malaria).* Berliner Klinische Wochenschrift, 1891. **28**: p. 953-6.

395. Ohlow, M.J. and B. Moosmann, *Phenothiazine: the seven lives of pharmacology's first lead structure.* Drug Discov Today, 2011. **16**(3-4): p. 119-31.

396. Wen, Y., W. Li, E.C. Poteet, L. Xie, C. Tan, L.J. Yan, et al., *Alternative mitochondrial electron transfer as a novel strategy for neuroprotection.* J Biol Chem, 2011. **286**(18): p. 16504-15.

397. Weinstein, J., A. Scott, and F.E. Hunter, Jr., *The action of gramicidin D on isolated liver mitochondria.* J Biol Chem, 1964. **239**: p. 3031-7.

398. Baloyannis, S.J., *Alterations of Mitochondria and Golgi Apparatus Are Related to Synaptic Pathology in Alzheimer's Disease*, in *Neurodegenerative Diseases*, U. Kishore, Editor. 2013, InTech. p. 102-24.

399. Atamna, H., J. Mackey, and J.M. Dhahbi, *Mitochondrial pharmacology: electron transport chain bypass as strategies to treat mitochondrial dysfunction.* Biofactors, 2012. **38**(2): p. 158-66.

400. Eckert, G.P., K. Renner, S.H. Eckert, J. Eckmann, S. Hagl, R.M. Abdel-Kader, et al., *Mitochondrial dysfunction--a pharmacological target in Alzheimer's disease.* Mol Neurobiol, 2012. **46**(1): p. 136-50.

401. Gabrielli, D.B., E.; Severino, D.; Kowaltowski, A.J.; Baptista, M.S., *Binding, aggregation, and photochemical properties of methylene blue in mitochondrial suspensions.* Photochemistry and Photobiology, 2004. **79**(3): p. 227-32.

402. Lee, K.K. and U.A. Boelsterli, *Bypassing the compromised mitochondrial electron transport with methylene blue alleviates efavirenz/isoniazid-induced oxidant stress and mitochondria-mediated cell death in mouse hepatocytes.* Redox Biol, 2014. **2C**: p. 599-609.

403. Pardridge, W.M., *Blood-brain barrier delivery.* Drug Discov Today, 2007. **12**(1-2): p. 54-61.

404. Khawli, L.A. and S. Prabhu, *Drug delivery across the blood-brain barrier.* Mol Pharm, 2013. **10**(5): p. 1471-2.

405. Siegal, T., *Which drug or drug delivery system can change clinical practice for brain tumor therapy?* Neuro Oncol, 2013. **15**(6): p. 656-69.

406. Hernandez-Pedro, N.Y., E. Rangel-Lopez, R. Magana-Maldonado, V.P. de la Cruz, A.S. del Angel, B. Pineda, et al., *Application of nanoparticles on diagnosis and therapy in gliomas.* Biomed Res Int, 2013. **2013**: p. 351031.

407. Cheng, Y., R.A. Morshed, B. Auffinger, A.L. Tobias, and M.S. Lesniak, *Multifunctional nanoparticles for brain tumor imaging and therapy.* Adv Drug Deliv Rev, 2014. **66**: p. 42-57.

408. Uhrich, K.E., S.M. Cannizzaro, R.S. Langer, and K.M. Shakesheff, *Polymeric systems for controlled drug release.* Chem Rev, 1999. **99**(11): p. 3181-98.

409. Nair, L.S. and C.T. Laurencin, *Biodegradable polymers as biomaterials.* Prog Polym Sci, 2007. **32**(8-9): p. 762-98.

410. Shive, M.S. and J.M. Anderson, *Biodegradation and biocompatibility of PLA and PLGA microspheres.* Adv Drug Deliv Rev, 1997. **28**(1): p. 5-24.

411. Li, J. and C. Sabliov, *PLA/PLGA nanoparticles for delivery of drugs across the blood-brain barrier.* Nanotechnology Reviews, 2013. **2**(3).

412. Kwon, Y., *Handbook of Essential Pharmacokinetics, Pharmacodynamics, and Drug Metabolism for Industrial Scientists*. 2001, New York, New York: Kluwer Academic /Plenum Publishers. 291.

413. Klepac-Ceraj, V., N. Patel, X. Song, C. Holewa, C. Patel, R. Kent, et al., *Photodynamic effects of methylene blue-loaded polymeric nanoparticles on dental plaque bacteria.* Lasers Surg Med, 2011. **43**(7): p. 600-6.